IST-4-027756 WINNER II

D6.13.10 V1.0

Final CG "wide area" description for integration into overall System Concept and assessment of key technologies

Contractual Date of Delivery to the CEC:	*31. October 2007*
Actual Date of Delivery to the CEC:	**30. November 2007**
Author(s):	Ralf Irmer, Martin Döttling, Simone Redana, Tobias Frank, Thorsten Wild, David Falconer, Tommy Svensson, Eric Hardouin, Antonio Cipriano, Yi Yuan, Mugdim Bublin, Alexander Tyrrell, Ralf Pabst, Roberta Fraccia, Alfonso Tierno, Magnus Olsson, Thierry Lestable
Participant(s):	**ALU, CTH, CU, DoCoMo, EAB, FTR&D, MOT, NSN, RWTH, SAGO, SEUK, TID, VOD**
Workpackage:	*Work Package 6*
Estimated person months:	**11**
Security:	**PU**
Nature:	**R**
Version:	1.0
Total number of pages:	127

Abstract: This document describes the concept proposal for the WINNER wide area deployment scenario and performance assessment of key building blocks and end-to-end performance assessment of key scenarios.

Keyword list: Mobile communications, wide area deployment, performance evaluation, system concept

Executive Summary

This deliverable addresses the Wide Area scenario and presents the performance assessment of the WINNER system concept derived for wide area use.

It is shown that WINNER building blocks outperform methods used in legacy systems both using very specific metrics such as BER performance or SNR degradation as well as end-2-end metrics such as spectral efficiency measured in bit/s/Hz/sector. It was also shown, that some methods used today are already close to achievable limits – very valuable input to target further research in the right direction, and to have confidence to base standards in development on the right methods.

The key performance results in terms of spectral efficiency for the Wide Area deployments are the following:

- Spectral efficiency results are obtained at an operating point, where 95% of users in a particular area are provided with a data rate of 2 Mbit/s in the downlink, and 1.3 Mbit/s in the uplink ("satisfied user criterion"). Results are obtained using the WINNER channel models developed for wide area situations, which also include links to fixed and mobile relay stations.
- The spectral efficiency targets set by WINNER in [WIN2D6114] (R38) are reached and outperformed significantly in the downlink for a 4x2 configuration, and almost for a 2x2 full buffer configuration but with a smaller number of supported users per sector. The spectral efficiency requirement for the uplink is also reached. More particularly:
    - In a 4x2 MIMO configuration, a downlink spectral efficiency of 2.9 bits/s/Hz/sector can be achieved using Grid of Beams (GoB), SDMA and interference rejection combining (IRC) at the receiver.
    - For uplink, a spectral efficiency of more than 3 bits/s/Hz/sector has been demonstrated by implementing SDMA based on a BS receiver with IRC and successive interference cancellation (SIC).
- Relaying can in certain scenarios increase the spectral efficiency by 60 %. Relaying is even more important in the uplink than in the downlink. This improvement can however only be realized by the usage of intelligent and dynamic resource partitioning and reuse schemes to adapt the available capacity on the relay and the access links to the actual distribution of the offered traffic within the relay-enhanced cell.

The following key insights can be obtained regarding the performance of the WINNER building blocks in the context of end-2-end system design and performance:

- B-IFDMA is one WINNER multiple access scheme, where its parameterization is a major issue. Evaluations resulted in a proposal for dimensioning of blocks for non-frequency adaptive transmission in the SISO case. A basic block size of 4 subcarriers x 3 symbols is recommended for low data rates and sufficient frequency diversity is achieved with 16 blocks each separated by 4 chunks in SISO case; if spatial diversity is used 8 or 4 blocks are sufficient. For larger data rates several basic blocks can be combined into larger blocks, as described in [WIN2D61314].
- For spatial processing it has been demonstrated that SDMA implemented with a GoB as basis is a simple but very efficient downlink scheme. The gains of spatial multiplexing for wide area scenarios are limited, even if beamforming is applied and additionally adaptive switching to single stream schemes is allowed. These schemes hardly outperform the GoB based schemes.
- Relaying can improve spectral efficiency for MBMS transmission significantly, especially if outdoor-to-indoor coverage is required.
- Intercell interference is a major challenge in wide area deployments. A range of techniques were developed and investigated with different complexity-performance trade-offs. The most suitable techniques are:
    - Downlink: The use of spatial processing schemes such as transmit beamforming (GoB) in conjunction with receivers with interference suppression capabilities (e.g. IRC).

  - Common Control Channels: Resource partitioning such as FFR is recommended for user throughput improvements at the cell edge if the associated possible sector throughput degradation can be afforded, since beamforming can typically not be applied.
  - Uplink: Receivers with interference suppression capabilities, e.g. IRC.

- In contrast to most beyond 3G standardization activities (such as LTE and mobile WiMAX), WINNER has not only evaluated full-buffer traffic scenarios, but also the impact of realistic traffic models such as constant bit rate (CBR) on key performance metrics, e.g. the spectral efficiency, supported number of users per cell and SINR distribution. Full buffer simulations overestimate the spectral efficiency by ~20-30%. The application of the satisfied user criterion (2 Mbits/s) for full buffer simulations (where each user offers infinite load) and proportional fair scheduling leads to a significant underestimation of the number of supported users, since for realistic services only a finite offered load per user is present. Packet-delay-aware scheduling further improves performance under QoS constraints.
- WINNER includes a concept of handovers within modes (intramode) and between modes (intermode). At the example of local area to wide area handover it is shown, that both wireless connectivity and throughput triggers are essential to maintain undisrupted high throughput.
- The WINNER Spectrum Resource Management concept governs, how sharing is accomplished to access spectrum resources and how to optimize the usage of spectrum.
- WINNER can share the FSS frequency band using adjacent channels or exclusion distances. Exclusion distances depend on the pathloss criterion, the consideration of co-channel or adjacent channel interference, and of the antenna configuration of the BSs. They range from 3 km to 74 km. This has been calculated for flat terrain profiles. When taking into account the terrain profiles in a concrete deployment the exclusion distances are much shorter.
- The performance degradation of non-iterative channel estimation compared to perfect channel knowledge is between 1.5 and 4.3 dB considering SISO links, but can be reduced to 0.2-3.0 dB, if iterative channel estimation is applied.
- SDMA and MIMO impose interference from in-cell co-channel users, which is especially significant for channel estimation with a low-overhead pilot design. Iterative channel estimators can reduce the SNR degradation significantly – being an enabler for low-overhead pilot designs.
- It is shown that inter-block interference due to timing and synchronization errors is negligible.
- Phase noise is no major issue for high-quality hardware components. However, it was shown that low-cost oscillators can be used for WINNER as well, where phase noise compensation algorithms can limit the SNR degradation to tolerable amounts.
- B-IFDMA and DFT-precoded OFDMA have 1.5-2dB lower required power backoff than OFDM or B-EFDMA.
- A self-organized network synchronization procedure developed within WINNER is able to achieve the required accuracy. The maximum misalignment of 1 µs is below the cyclic prefix of 3.2 µs.

These highlighted conclusions, and further ones described in this document are based on extensive simulation results of the WINNER reference design in wide area deployments. Performance results for local and metropolitan areas can be found in [WIN2D61311] and [WIN2D61312], respectively. The WINNER reference design is described in more detail in [WIN2D61314].

Authors

Partner	Name	Phone / Fax / e-mail
Alcatel-Lucent (ALU)		
	Thorsten Wild	Phone: +49 711 821 35762 Fax: +49 711 821 32185 e-mail: thorsten.wild@alcatel-lucent.de
Carleton University (CU)		
	David Falconer	Phone: +1 613 520 5722 Fax: +1 613 520 5727 e-mail: ddf@sce.carleton.ca
Chalmers University of Technology (CTH)		
	Tommy Svensson	Phone: +46 31 772 1823 Fax: +46 31 772 1782 e-mail: tommy.svensson@chalmers.se
DoCoMo		
	Alexander Tyrrell	Phone: +49 89 5682 4235 Fax: +49 89 5682 4301 e-mail: tyrrell@docomolab-euro.com
Ericsson AB (EAB)		
	Magnus Olsson	Phone: +46 8 585 30774 Fax: +46 8 585 31480 e-mail: magnus.a.olsson@ericsson.com
France Telecom (FTR&D)		
	Eric Hardouin	Phone: +33 1 45 29 44 16 Fax: +33 1 45 29 41 94 e-mail: eric.hardouin@orange-ftgroup.com
	Antonio Cipriano	Phone: +33 1 45 29 65 49 Fax: +33 1 45 29 41 94 e-mail: antonio.cipriano@orange-ftgroup.com
	Yi Yuan	Phone: +33 1 45 29 41 96 Fax: +33 1 45 29 41 94 e-mail: yi.yuan@orange-ftgroup.com
Motorola (MOT)		
	Roberta Fracchia	Phone: +33 1 69354846 Fax: +33 1 69354801 e-mail: roberta.fracchia@motorola.com

Nokia Siemens Networks (NSN)		
	Martin Döttling	Phone: +49 89 636 73331 Fax: +49 89 636 73331 e-mail: Martin.Doettling@nsn.com
	Simone Redana	Phone: +39 02 2437 7973 Fax: + 49 02 2437 7989 e-mail: Simone.Redana@nsn.com

Nokia Siemens Networks / TU Darmstadt		
	Tobias Frank	Phone: +49 61 51 16 37 69 Fax: +49 61 51 16 53 94 e-mail: t.frank@nt.tu-darmstadt.de

RWTH Aachen University		
	Ralf Pabst	Phone: +49 241 80 25828 Fax: +49 241 80 22242 e-mail: pab@comnets.rwth-aachen.de

Siemens AG Austria (SAGO)		
	Mugdim Bublin	Phone: +43 51707 21724 Fax: +43 51707 51933 e-mail: mugdim.bublin@siemens.com

Samsung Electronics (UK) Ltd (SEUK)		
	Thierry Lestable	Phone: +44.1784.428600 (Ext.720) Fax: +44.1784.428624 e-mail: thierry.lestable@samsung.com

Telefonica I+D (TID)		
	Alfonso Tierno	Phone: +34 91 3374863 Fax: +34 91 3374212 e-mail: atierno@tid.es

Vodafone (VOD)		
	Ralf Irmer	Phone: +44 7717 275461 Fax: +44 1635 676147 e-mail: ralf.irmer@vodafone.com

Table of Contents

List of Acronyms and Abbreviations

ARQ	Automatic Repeat reQuest
APP	A posteriori probability
AWGN	Additive White Gaussian Noise
BCH	Broadcast channel
BER	Bit Error Rate
B-EFDMA	Block Equidistant Frequency Division Multiple Access
B-IFDMA	Block Interleaved Frequency Division Multiple Access
BLER	BLock Error Rate
BS	Base Station
CBR	Constant Bit Rate
CC	Convolutional Codes or Chase Combining
CCB	Chunk-by-Chunk Balancing of the relay and access link
CCDF	Complementary Cumulative Distribution Function
CDF	Cumulative Distribution Function
CQI	Channel Quality Indicator
DFE	Decision Feedback Equalizer
DFT	Discrete Fourier Transform
DRS	Dynamic Resource Sharing
EESM	Exponential Effective SINR Mapping
EV-DO	Evolution Data Only
FDD	Frequency Division Duplex
FDMA	Frequency Division Multiple Access
FEC	Forward Error Correction
FRN	Fixed Relay Node
FSS ES	Fix Satellite Service Earth Station
FSU	Flexible Spectrum Use
GoB	Grid of Beams
GI	Guard Interval
HARQ	Hybrid Automatic Repeat Request
HSPA	High Speed Packet Access
HPA	High Power Amplifier
HwC/ HwoC	Horizontal Sharing with/without Coordination
IFDMA	Interleaved Frequency Division Multiple Access
IR	Incremental Redundancy
IRC	Interference Rejection Combining
ISI	Inter-Symbol Interference
L2S	Link to System interface
LA	Link Adaptation
LDPC	Low-Density Parity-Check Codes
LFDMA	Localized FDMA
LNA	Logical Node Architecture
LUT	Look-Up-Table
LTE	Long Term Evolution
MAP	Maximum A-Posteriori
MC-CDMA	Multi-Carrier Code Division Multiple Access
MCS	Modulation and Coding Scheme
MAC	Media Access Control
MIMO	Multiple Input Multiple Output
MISO	Multiple Input Single Output

MRC	Maximum Ratio Combining
MRN	Mobile Relay Node
MMSE	Minimum Mean Square Error
MIESM	Mutual Information Effective SINR Mapping
OFDM	Orthogonal Frequency Division Multiplexing
OFDMA	Orthogonal Frequency Division Multiple Access
PAPR	Peak to Average Power Ratio
RCM	Raw Cubic Metric
PER	Packet Error Rate
PIC	Parallel Interference Cancellation
QAM	Quadrature Amplitude Modulation
QPSK	Quadrature Phase Shift Keying
RACH	Random Access Channel
RTU	ReTransmission Unit
RV	Redundancy Version
SDMA	Space Division Multiple Access
SINR	Signal to Interference and Noise Ratio
SNR	Signal to Noise Ratio
SISO	Single-Input Single-Output
SRM	Spectrum Resource Management
SSC	Spectrum Sharing and Coexistence
STC	Space Time Coding
TDD	Time Division Duplex
TDMA	Time Division Multiple Access
TD-SCDMA	Time-Division Code Division Multiple Access
UMB	Ultra Mobile Broadband
UMTS	Universal Mobile Telecommunications System
UT	User Terminal
VT	Vertical Sharing

1. Introduction

Concept groups coordinate the definition of a proof of concept among the various expert tasks in the WINNER project. A proof of concept is a WINNER system tuned to a specific deployment scenario. Three scenarios have been defined: Local Area (LA), Metropolitan Area (MA), Wide Area (WA), corresponding to different environments, traffic patterns, bandwidth, etc. Concept groups are also a vehicle to investigate innovative techniques as key differentiators compared to existing or forthcoming systems. For example, a key differentiator of WINNER is its flexibility and its ability to adapt to any kind of environment.

This deliverable addresses the Wide Area scenario and presents the performance assessment of the WINNER system concept derived for wide area use. Due to the complexity of each technique, the document does not aim at providing an exhaustive description and evaluation but rather provides an overview with links to other WINNER deliverables for further reading.

In Chapter 2, we introduce Wide Area deployment scenarios. In Chapter 3, a condensed overview of the Wide Area Reference design is given, which is described in more detail in [WIN2D61314] and other deliverables. Chapter 4 looks at the performance of WINNER building blocks –including benchmarks between different legacy and new approaches and the performance in the context of end-2-end metrics such as spectral efficiency, overhead or delay.

Section 4.1 lists the channel models used in this document. Accurate channel modelling based on field measurements is key for algorithm development and assessment of the system in scenarios which are as close as possible to reality.

Section 4.2 highlights the key features of coding, modulation and link adaptation. Since coding and modulation is unified for all WINNER deployment scenarios, a more detailed overview is captured therefore in [WIN2D61312].

The multiple access is a central part of the WINNER system, interfacing with spatial processing, link adaptation, RRM, and relaying. Section 4.3 describes the principles of multiple access without going too much into details. Further recommendations on configuration and use of the multiple access schemes can be found in [WIN2D61314]. The performance of both frequency-adaptive as well as frequency-non-adaptive transmission is evaluated in the appendix of this deliverable.

Spatial processing provides the largest spectral efficiency gains both for the uplink and downlink. Section 4.4 highlights performance evaluation results.

Relaying is a key feature of the WINNER system. Section 4.5 compares the performance of relay enhanced cells (RECs) and conventional single hop deployments in the uplink and downlink under consideration of advanced antenna technologies.

One major challenge in wide area deployments is inter-cell interference. Mitigation schemes are evaluated in Section 4.6

Section 4.8 describes the WINNER Radio Resource Management and indicates handover performance.

Spectrum technologies are an enabler of WINNER – and an important innovation compared to legacy systems. Section 4.9 gives an overview of spectrum technologies in a wide area deployment context.

In most evaluations, certain assumptions were made, such as ideal channel estimation. The degradation of the end-2-end performance due to “real world effects” of link level procedures are covered in Section 4.10.

Chapter 5 summarizes the key results of WINNER in Wide Area Deployments.

1.1. Technology Evaluation in the end-to-end context

It would be very desirable to measure directly the impact of any innovation in a specific technical area to the user perceived quality of service. However, mobile communications systems are very complex, with many interworking effects. The ultimate answer could only be given by trials and test deployments – which is far too costly and time consuming. Simulations are a good compromise – where certain elements of the whole system can be simplified or replaced by a model, like the link-to-system interface or a channel model. Another challenge is to find a metric which is simple at the one hand and reflects the user experience and operator requirements at the other hand.

WINNER has agreed a set of metrics and evaluation scenarios in [WIN2D6137], [WIN2D6133], [WIN2D6134], and [WIN2D6135], which is used throughout this document. The main advantage of the approach taken in WINNER is that individual results are set into relation to the end-to-end performance. This approach is very difficult to take for small research groups, and is otherwise only taken to some extend by standardisation groups.

1.2. Evaluation methodology in technical standardisation

In the process of standardisation of wide area systems, evaluation of end-2-end performance plays a significant role. Existing and currently developed standards are analysed in [WIN2D6139]:

- The requirements and evaluation methodology for 3GPP LTE is specified in [3GPP06a] and [3GPP06b]. The evaluation methodology was refined by the group of NGMN operators in [NGMN07a]. End-2-End evaluation results were published for this methodology by several 3GPP member companies in April 2007. They are summarized in [3GPP07]. The results differ significantly between companies for some scenarios (e.g. HSDPA baseline or LTE uplink or VoIP user capacity), but are much more aligned for other scenarios (e.g. LTE downlink). This shows that end-2-end simulations are very complex and provide room for a spread of results, since it is not possible to specify exactly all system and environment parameters. The performance evaluation of a standard, which is not yet complete is a further challenge LTE is facing, as it is the case even more for WINNER. Therefore, LTE had to make assumptions, e.g. on the overhead, CQI feedback errors, etc.
- 3GPP2 has established a very detailed performance evaluation methodology defined in [3GPP204].
- The IEEE 802.20 evaluation methodology is also very advanced [IEEE05]. Performance evaluation is especially important for the selection of different proposals within this standardisation group.
- IEEE 802.16 (“mobile WiMAX”) is discussing performance evaluation, which includes relaying within the sub-group IEEE 802.16j [ST06]. The IEEE 802.16m performance evaluation methodology is currently developed [SZ078]. It is substantially influenced by the WINNER project.
- The ITU is currently specifying the evaluation methodology for IMT-Advanced. This activity is significantly influenced by WINNER.
- The NGMN group of operators has published a technology agnostic performance evaluation methodology to unify metrics across several standardisation bodies [NGMN07b].

The conclusion is that performance evaluation is very complex, and true apples-to-apples comparisons between different complete standards and technology building blocks are very difficult. Within WINNER, a common evaluation methodology is used which allows us to compare the impact of approaches at different layers on the end-to-end performance.

1.3. Spectral Efficiency under QoS constraints

Although several key performance indicators will be discussed in this document, particular focus will be on spectral efficiency evaluation under QoS constraint. The complex matter of QoS is modelled in a way suitable for MAC and PHY-oriented system-level simulations by a so-called satisfied user criterion (SUC). For full buffer simulations the SUC is modelled by an requirement on the 5%-ile of the average user throughput. In wide area this requirement is set to 2 Mbps in downlink and to 1.3 Mbps in uplink, i.e. satisfactory service provision is assumed if 95% of the users have an average user throughput greater than these values. This 5%-ile of average user throughput is also referred to as cell edge user throughput in standardisation.

User throughput is defined as the number of correctly received information bits including all effects of packet loss and retransmissions, and taking into account the overhead due to guard bands, guard times, preambles, pilots, headers, and control signaling. The impact of functions related to header compression, encryption, ciphering, and transport delays between base station and gateway is however not considered.

In simulations the number of users per sector is increased up to a load, where this SUC is still met. At this maximum number of supported user, the cell spectral efficiency is determined, as illustrated in Figure 1-1. In this example technique would provide higher spectral efficiency and the maximum number of supported user (32 in this example) is another key performance indicator, which is closely related to economics of a network operator.

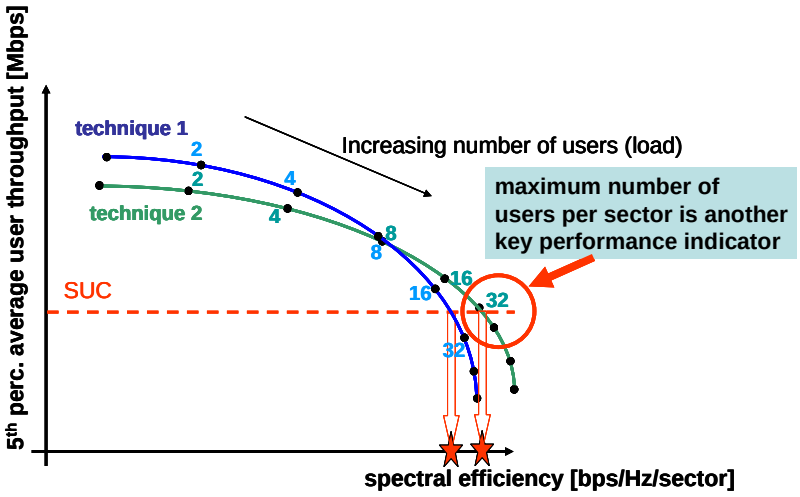

Figure 1-1 Evaluation methodology for spectral efficiency under QoS constraints modelled by a satisfied user criteria

Many results presented later, will show results following this methodology. In Section 4.7.2 this concept is extended for simulations using traffic models. In this case user satisfaction is only assumed if a requirement on average user throughput and user packet delay statistics are concurrently fulfilled. The user packet delay is defined as a one-way transit time between a time instance when a packet is available at the IP layer in the transmitter and the moment when it becomes available at the IP layer of the receiver. Thus, user plane packet delay includes delay introduced by associated protocols and control signaling assuming the user terminal is in the active state. The impact of functions related to header compression, encryption, ciphering, and transport delays between base station and a gateway is not considered.

The CDF of the user plane packet delay is calculated for each user (and called user packet delay CDF). The system packet delay CDF is calculated by extracting the 95%-iles of all users packet delay CDFs. The packet delay SUC is then defined based on the value of the system packet delay CDF that is only exceeded by 5% of the users. The actual values of the SUC are different for different services and the values chosen here are simply examples for a particular service.

2. Wide Area Deployment Scenarios

The **deployment scenarios** describe the relevant characteristics of a selection of environments where a WINNER system might be deployed. “Environment” means here that the description is independent from the technical solution WINNER provides, but refers only to the external characteristics that cannot be changed by WINNER.

The key identifier of the **wide area concept group** is the provision of **ubiquitous coverage**; that is, providing a seamless level of service across a coverage area similar to that achieved by GERAN systems deployed today. This covers not just rural areas but also a contiguous coverage layer in towns and cities, where it will overlap with metropolitan and local area deployments. Another important target is to support the full range of mobility scenarios up to high speed trains. One requirement of WINNER is that that the ubiquitous radio system has to be self-contained, allowing WINNER to target the chosen requirements without the need for inter-working with other systems.

Wide area systems have to allow for both cost-efficient network deployments and shall enable low-cost terminals. This is especially important to achieve a high population and area coverage with reasonable expenditure. For many countries, overcoming the Digital Divide is an essential goal as highlighted by several UN organizations like FAO (Food and Agriculture Organization of the United Nations) or UNESCO [FAO07]. Providing mobile internet services for rural communities could be one key element to achieve this.

The benchmark technologies for the wide area system concept are deployed cellular systems such as GSM/GPRS, cdma2000, UMTS, TD-CDMA, HSPA and EV-DO. Furthermore, systems about to be standardised or deployed during the course of WINNER II are evolved 3G ("HSPA+"), 3GPP Long Term Evolution (LTE), Ultra Mobile Broadband (UMB), IEEE 802.16e and m ("Mobile WiMax"), and proprietary systems like Flash-OFDM. Research results from WINNER have had direct and indirect impact on the development of some of these technologies (e.g. 3GPP LTE or IEEE 802.16m). An overview of state-of-the-art technologies can be found in [WIN2D6139].

The main objective of the concept groups to provide a proof of the WINNER concept is achieved by detailing the common end-to-end (e2e) concept to a design which can be implemented, e.g. in simulators. For that, the concept group defines a **reference design** that provides the reference for simulations and that was iterated during the course of WINNER phase I and II by exchanging particular building blocks by new ones which have proven to perform better. The current status of the reference design is summarized in Chapter 3 and evaluated in the following chapter. A full description of the WINNER system concept and reference design can be found in [WIN2D61314].

The **baseline** system implementation forms a minimal configuration of the WINNER system which is supported by the majority of the simulators. Its purpose is to ensure integrity of the assumptions throughout the project, and to allow a relative comparison of innovative features. The baseline system implementation is defined in [WIN2D6137] and is based on the outcome of WINNER phase I [WIN1D210].

2.1. Base Coverage Urban and Rural

A key aspect of mobile cellular systems is the ability to make a call, access content, send an e-mail and so on from anywhere. Particularly in Europe GERAN coverage is ubiquitous and there is the expectation of being able to be contactable in any geographic location (including in-building coverage). WINNER needs to provide this same ubiquitous coverage layer. This base layer will cover rural, suburban and urban areas, providing the umbrella coverage; whilst there will be other deployments (as considered in the Metropolitan and Local Area concept groups [WIN2D61311],[WIN2D61312]), providing more targeted, higher data rate coverage.

The wide area evaluation scenario is to reflect the ubiquitous coverage deployment of WINNER in towns and cities, where it will overlap with deployments considered by the Metropolitan and Local Area concept groups. This is foreseen as similar to today's macro-cell deployments.

2.2. Service Provision to Transport Links

Still following the principle of ubiquitous coverage users expect to be able to use mobile communication services whilst on the move. At present only aircraft are exempt from this expectation, therefore WINNER needs to be able to provide service to cars, buses, trains and so on. The most challenging of these transportation types are high speed trains, which may reach speeds of up to 350 km/h. The WINNER system accommodates this scenario, but graceful performance degradation has to be taken into account.

2.3. Evaluation Assumptions

Evaluation assumptions and physical deployment assumptions are summarized in Table 2.3-1 and Table 2.4-1, respectively. To limit the simulation parameter space, performance results are mainly provided for the base coverage urban scenario at 3.7/3.95 GHz as defined in [WIN2D6137]. However, this does not mean that the other scenarios are less relevant; i.e., they will be very likely play a major role to provide *ubiquitous coverage*. The 3.5/3.9 GHz scenario is the most challenging with respect to propagation conditions.

Parameter	Base Coverage Urban @ 3.7/3.95 GHz	Base Coverage Urban @ 2.6 GHz	Base Coverage Rural	Service Provision to Transport Links
Frequency	FDD DL: 3.95, UL: 3.7GHz	FDD 2.6GHz	FDD 2GHz	FDD 2GHz

Bandwidth	2x50MHz	2 x 20MHz	2 x 10MHz	2 x 10MHz
Deployment	Cellular, hexagonal layout			
Traffic model(s)	Conversation voice Internet/browsing			Conversational voice File transfer
User mobility model	3km/h 50km/h 120km/h			350km/h

Table 2.3-1: Evaluation Assumptions of Wide Area Deployment Scenarios

Channel models for wide area investigations are specified in [WIN2D6137]. [WIN2D111] provides details on the channel measurements, the modelling approach, parameters, and implementation. The final status of the WINNER channel models, partially with updates not included in the simulation campaigns of this report can be found in [WIN2D112].

2.4. Physical Deployment Assumptions

Table 2.4-1 provided an overview on the deployment assumptions. Due to limited efforts focus has been on the base coverage urban scenario at 3.7/3.95 GHz, which is described in more detail in [WIN2D6137].

Parameter	Base Coverage Urban @ 3.7/3.95 GHz	Base Coverage Urban @ 2.6 GHz	Base Coverage Rural	Service Provision to Transport Links
BS location	Above rooftop, 25m		Masts, 30m	Masts, 25m
Base station, site-to-site	1km		5km	3km (tbc)
Base station, number of sectors	3		3	2
Relay node location	5m, below rooftop	Above rooftop	25m	On train
BS antennas	4 (opt. 8)	8	4	4
RN antennas	2	8	4	4
UT antennas	2 (assumes handheld)		2	4 (assumes laptop)
BS transmit power	46dBm		46dBm	46dBm
RN transmit power	37dBm (optional 24 dBm) .	24 dBm	40dBm	40dBm (cross-check to LA)
UT transmit power	24dBm		24dBm	24dBm
Relaying	Optional in relay Enhanced Cells (REC)			
Relaying	flexible hop-number with			

Hops	optimisations for 2 hops.	
Number of RNs per sector	1	
Minimum BS-RN distance	RN placed at 2/3 of the distance to the REC cell border	

Table 2.4-1: Physical Deployment Assumptions of Wide Area Deployment Scenarios.

3. Reference Wide Area Design Overview

The WINNER II baseline system implementation used for evaluations in the test scenarios is defined in [WIN2D6137]. The WINNER reference design is described in [WIN2D61314], based on intermediate versions in [WIN2D6133], [WIN2D6134], and [WIN2D6135]. In this chapter, a short overview of the WINNER reference design for wide area deployments is given. It should be noted that insight gained during the simulations reported in this document has lead to subsequent updates in the reference design assumptions, i.e. simulations may have been performed using different assumptions, in particular based on [WIN2D6137].

Wide area deployments require **design flexibility,** to adapt to frequency bands, bandwidth, and different antenna deployments, etc**.** The following tables contain therefore a column commenting primarily on flexibility. The WINNER concept development was guided by the following principles. On the one hand, the number of unnecessary options (i.e. alternatives with similar focus and performance) was kept small; on the other hand, flexibility was introduced where necessary to adapt either to the user application requirements or environmental circumstances (channel, frequency band, etc).

Table 2.4-1 provides a synopsis of OFDM parameters and frame design. Basic OFDM parameters, like subcarrier spacing, symbol duration and guard interval are adapted to specific environments, i.e. a design for local area differs from the wide area design, as physical channel characteristics are different and a common design would yield unacceptable overhead. Nevertheless the parameters are chosen such that they can be derived from a common clock. Due to the massive increase in system complexity, flexible guard interval within one physical layer mode was not pursued further. Equal frame duration in FDD and TDD mode facilitates implementation additionally.

The basic resource unit, called chunk, spans 12 x 8 symbols, i.e. 0.3456 ms x 312.5 kHz. This dimension provides the required granularity to support low rate services efficiently. It is also smaller than coherence time and bandwidth, which is a prerequisite for link adaptation. Short frame and slot length allow fast control loops supporting all kind of services even in the case of relaying.

Pilot-aided channel estimation using scattered pilots is used and dependent on the spatial processing schemes different types of common and dedicated pilots may be configured, see [WIN2D61314]. In the wide area design, the downlink uses common pilots per antenna/beam, while on the uplink dedicated pilots per antenna are used. For chunks associated to high velocity users additional pilots may be configured.

As WINNER supports operational scenarios ranging from a few users with very large resource allocations to many users with small allocations, control channel design must scale accordingly. This is achieved by a multi-part flexible-length control channel design which adapts the format in a semi-static fashion according to the long-term statistics of the number of active users and their resource allocation, see [WIN2D61314][1].

Entity	Reference Design	Comment, e.g. on design flexibility
Subcarrier spacing	39062.5 Hz	Fixed subcarrier spacing within wide area deployments. Different subcarrier spacing for MA/LA design
Useful symbol duration	25.6 us	
Guard interval length	3.2 us	Fixed guard interval for whole deployment. Flexible GI not included in reference design
Total symbol duration	28.8 us	
Used subcarriers	[576:576], subcarrier 0 unused	Number of subcarriers can be flexibly adapted to the available spectrum.
Overall frame length	0.6912 ms	Short frame and slot length allows fast control loops and enables support of relaying without

[1] Overhead included in most simulation results herein is based on [WIN2D6137], which assumed in downlink per chunk: 4 pilot symbols per antenna/beam and 12 control symbols for frequency adaptive transmission, and 8 pilot symbols per antenna and 18 control symbols in the non-frequency-adaptive case (larger overhead due to potential higher velocity and lower SINR).

		negative overall delay
Chunks dimension in symbols x subcarriers	12 x 8 = 96	Provides required granularity to efficiently support low rate as well as high rate services and ensures block fading within one chunk
Number of chunks per frame in time and frequency direction	2 x 144	
Pilot Design	Scattered pilots, common pilots per antenna/beam in DL, dedicated pilots per antenna in UL	Pilot pattern is configurable according to link direction, number of antennas, spatial scheme, and user velocity, Exact pilot definition, see [WIN2D223, WIN2D61314]
Control Channel Design	Common control channel design with different parameterization for frequency-adaptive and frequency-non-adaptive transmission, Multi-part control information, flexible length	Parameterisation allows low overhead up to a large number of users by flexibly adapting format to operational scenario (dedicated vs. common signalling) Exact control channel design, see [WIN2D61314]

Table 2.4-1: WINNER II Wide Area Reference Design: OFDM, Generalized Multicarrier and Frame Parameters

Table 2.4-2 summarises the WINNER system configuration in the wide area test scenario. Based on the quality of the channel state information at the transmitter, either frequency-adaptive or frequency-non-adaptive transmission is used. The former performs channel-aware assignment of resources using OFDMA, TDMA and SDMA per slot and explicit link adaptation per chunk. The latter allows supporting users without or only long-term CQI information and improves robustness using frequency diversity. Design of the B-E/IFDMA subblocks considers granularity of the FEC blocks, micro sleep time, and further aspects.

Owing to the low angular spread of typical wide area channels, beamforming techniques including SDMA (in particular in case of many users per cell) have proven to provide high performance at low complexity. In uplink interference rejection combining (IRC) and successive interference cancellation (SIC) enable the use of SDMA. The design supports different number of antennas at transmitter and receiver, as well as different beamforming algorithms. It has proven that these spatial processing schemes are also the most suitable means for interference mitigation [WIN2D473].

While LDPC codes are used for block sizes greater than 200 bit, convolutional codes with tailbiting are used for smaller blocks and control signalling. In order to efficiently support large cell sizes in WA and low minimum SINR, a mother code rate of ¼ is available. The use of HARQ retransmissions and or repetition coding further improves low SINR support for data and control channels, respectively.

For frequency-adaptive transmission the MI-ACM link adaptation scheme has been developed within WINNER. Each codeword extends over multiple chunks in order to obtain coding gain. Modulation is adapted for each chunk, whereas a common weighted-average code rate is applied. This scheme achieves near-optimum performance with significantly less complexity and overhead than ideal bit and power loading. Non-frequency-adaptive transmission is based on the adaptation of modulation and code rate to the average SINR. Therefore proper link adaptation is ensured for users with bad CQI quality, such as high-speed users in WA.

HARQ is based on an *N*-channel Stop-And-Wait protocol using Incremental Redundancy (including Chase Combining as special case). The possibility to use different transport format for retransmission ensures full flexibility of the scheduler.

In-band relaying with stationary and synchronised relay nodes is considered, where the resource partitioning between BS and RN can be updated on a superframe basis. Adaptive resource partitioning is an enabler for capacity gains due to relaying. Evaluation assumptions in [WIN2D6137] have set stringent

constraints on cost, complexity, and form factor of RN in order to facilitate rapid and flexible deployment, e.g. on lampposts.

Entity	Reference Design	Comment, e.g. on design flexibility
Multiple Access with frequency-adaptive resource allocation	DL and UL: OFDMA-TDMA, with optional additional SDMA component [WIN2D461]	Resource partitioning (chunk allocation to different RAP) is determined per super-frame, scheduling is done on slot basis
Multiple Access with non-frequency adaptive resource allocation	DL: B-EFDMA [WIN2D461] (Block-Equally spaced FDMA) UL: B-IFDMA [WIN2D461] (Block-Interleaved FDMA)	Supports large as well as small FEC blocks. Design of chunk sub-blocks can be adjusted to balance terminal hibernation/micro sleep time within chunks against other aspects.
Decision procedure between frequency adaptive/non-frequency adaptive resource allocation	See Section 5.2 of [WIN2D461] and Section 5.1.2 of [WIN2D6135], [WIN2D61314]	Based on quality of the channel state information at the transmitter (influenced e.g. by user velocity)
Spatial Processing and Interference Mitigation	DL: GoB + SDMA (see [WIN2D341] and [WIN2D61314]) at transmitter IRC at receiver UL: SDMA based on IRC+SIC at receiver	Design flexibility in number of BS and UT antennas
Coding	LDPC coding, mother code rate 1/3 [WIN2D61314] Convolutional codes (memory 8, R=1/3 and 1/4) [WIN2D61314] References for performance comparisons: [WIN2D221], [WIN2D222].	LDPC used for data channels and larger packet size, convolutional codes with tailbiting used for control signalling and packet size < 200 bits.
Interleaving	Random	
Modulation	M-QAM with Gray Mapping, M=2,4,16,64	Fast adaptation of modulation and code rate, innovative feature of MI-ACM (mutual information based adaptive coding and modulation used for frequency-adaptive transmissions)
Link Adaptation	MI-ACM for frequency adaptive transmission, Adaptation to average SINR for non-frequency-adaptive transmission See Section 5 of [WIN2D6135] and [WIN2D61314]	
H-ARQ	Chase combining or incremental redundancy, see chapter 5 of see [WIN2D6135] *N*-Channel Stop-And-Wait Protocol	Fast retransmission enabled by tight control loop (H-ARQ feedback), retransmission can use different transport format [WIN2D223]
Scheduling	Proportional Fair / Score-Based	Used as a standard scheduler to evaluate performance, as it is simple and contains

		a reasonable trade-off between fairness and exploitation of the channel. Several contributions provide a direct comparison of different schedulers (e.g. Round Robin, and Max SINR in order to span the range of achievable performance)
Relaying Concept	BS and RN are synchronized, stationary RNs Optimised for 2 hops, but *n* hops possible, Resource partitioning with chunk granularity, update interval max. once per super-frame	Small relays suitable for lamppost mounting enable fast roll-out and flexible deployment Adaptive resource partitioning between BS and RN

Table 2.4-2: Wide Area Reference System Configuration

Table 2.4-3 provides an overview of receiver algorithms, procedures and concepts for wide area. For further detail references are provided to the interested reader.

Entity	Reference Design	Comment, e.g. on design flexibility
BS receiver baseband spatial processing	IRC+SIC	More complex processing in BS
UT receiver baseband spatial processing	IRC	
Decoding	LDPC decoding	See [WIN2D221] section 2.3
Reference Channel estimation	Pilot-based data-assisted decision feedback	See section 4.10
Reference Synchronisation	Preamble-based link synchronisation Self-organised network synchronisation based on so-called Firefly synchronisation algorithm, including timing advance for large cells	See [WIN2D61314], Maximum misalignment of 1 µs
Fast paging procedure	Idle mode mobility based on paging groups,	See [WIN2D61314]
Cell search, association procedure and random access	Association procedure based on frequency-multiplexed RACH channels from different RAPs	Described in [WIN2D61311]
RRM	Intra- and intermode handover	See section 4.8 and [WIN2D61311]
Power saving concept	In-chunk micro-sleep/hibernation enabled frame and channel design Dormant RRC state	Discussed in [WIN2D6134] and in Section 2.7 of [WIN2D461].
Flexible spectrum use concept	Spectrum sharing with other RAT Flexible spectrum use between WINNER RATs	See section 4.9 and [WIN2D61314]

Table 2.4-3: Wide Area Reference Receiver Algorithms, Procedures and Concepts

4. Performance of key WINNER Building Blocks in the Wide Area Scenarios

4.1. Channel models and propagation scenarios

Especially for future radio systems with enhanced spatial processing capabilities propagation effects have major impact on design choices and applied algorithms in different environments. Therefore it is very important to model the wireless channel as accurate as possible to capture all relevant propagation effects on the one hand and to have a simplified model for fast simulations on the other hand. The WINNER spatial channel model development is based on measurements within WINNER and extensive literature evaluation. The WINNER channel models have had a wide-spread impact on standardisation bodies such as 3GPP and IEEE. The channel models are explained in detail in [WIN2D112]. Models are available for the user links and also for links to fixed relay nodes (FRN) and mobile relay nodes (MRN); all models are valid in the frequency range of 2 GHz to 6 GHz. In most models, line-of-sight (LOS), obstructed line-of-sight (OLOS), and non-line-of-sight (NLOS) are distinguished, as blockage and shadowing has major impact on channel signatures. The relevant channel models for wide area include:

- User link BS → UT: typical urban macro-cell (model C2), bad urban macro cell (C3), suburban (C1), rural macro cell (D1)
- Feeder link BS → FRN at approximately rooftop level (B5f), above rooftop (C1)
- User link FRN → UT (B1)
- Moving networks in rural area, BS → MRN and MRN → UT link (D2).

In the base coverage urban scenario used predominantly in the evaluations, the C2, C1, and B1 channel models are used for BS → UT, BS → FRN, and FRN → UT links, respectively, see [WIN2D6137]. Outdoor-to-indoor channel models are also available, however, with primary focus on microcellular deployments. Therefore, alternatively a wall penetration loss of 20 dB has been assumed for investigations of outdoor-to-indoor coverage in wide area, e.g. in [WIN2D353].

There are models for each of the scenarios with two levels of complexity: the generic model and the cluster delay line models. The following channel models have been updated for D1.1.2: C2, C3 and D2. This means that simulations performed for these scenarios have used an earlier channel model than [WIN2D112]. For a detailed description of the channel models the reader is referred to [WIN2D112, WIN2D111].

One of the most important characteristic of the channel in wide area is the low amount of scattering (i.e. small angular spread). This leads to low-rank channels and limits the possibilities for spatial multiplexing, unless cross-polarised antennas are used. On the other hand, this correlation promotes the use of beamforming, which is also a technique to counteract the severe range problems for large cells at higher carrier frequencies in the 4 GHz range. High path loss and penetration loss lead to challenges in indoor coverage by outdoor base stations. In [WIN2D353] it has been shown that in the base coverage urban scenario noise limitation starts to become relevant already at a penetration loss of 10 dB. For 20 dB penetration loss the 5%-ile of the SINR distribution is reduced by 8 dB and spectral efficiency is decreased by 35% if all users are assumed to be indoors. These harsh propagation conditions require technical solutions to improve coverage and cell edge user performance, such as relaying. [WIN2D353] shows that already the use of one relay node per sector can improve the 5%-ile of SINR by 3 dB and spectral efficiency by 10% for indoor users.

4.2. Modulation and coding

Modulation and coding is unified for all deployment scenarios, and described in detail in [WIN2D61312].

Modulation and coding determine the overall performance of the WINNER system to a large extend. They both have an impact on:

- The necessary SINR to achieve a certain QoS (e.g. CWER) and through this indirectly on the **average** and **cell edge throughput**, **spectral efficiency** and **coverage**.

- The **delay** which is caused by retransmissions and the trade-off between tolerable delay and throughput.
- The **complexity** of the receiver and transmitter in terms of the **computational effort**, **power consumption** and hence **cost**.

In *state-of-the art* (SoA) systems, the impact of coding and modulation on the overall performance has increased. Adaptive coding and modulation with fine granularity (in time, frequency and spatial dimension), advanced HARQ and advanced spatial processing schemes provide a larger degree of freedom, but the large achievable data rates also impose challenges on decoding/encoding complexity.

The WINNER coding and modulation reference design defined in [WIN2D61312] defines the following building blocks based on a thorough analysis:

- Modulation alphabet
- Forward error correction techniques
- Link adaptation for frequency adaptive and non-adaptive transmission
- Hybrid ARQ

Analysis is made on the performance of the coding and modulation schemes. Additionally, gains of power-loading and non-square modulation formats are investigated.

4.3. Multiple access

In this chapter we give a brief overview of the approach for Multiple Access in the current WINNER system concept. The reference design of the WINNER multiple access remains to a large degree as described in [WIN2D6133]. Further investigations have been carried out in Appendix A2 to complement the studies in [WIN2D461], and we introduce them along with the main findings below. They support the final reference design of the Multiple Access solution described in [WIN2D61314].

4.3.1. Frequency-adaptive transmission

The multiple access scheme for frequency-adaptive uplink and downlink is based on chunk-wise frequency-adaptive **TDMA/OFDMA** in both the FDD and the TDD modes. The same scheme is used for both uplinks and downlinks.

Chunk-based TDMA/OFDMA means that flows are mapped onto individual chunk layers[2]. The mapping is exclusive within the cells, i.e. each chunk layer carries data from only one flow. Individual link adaptation is used within each chunk layer, based on predicted SINR that will be perceived within that particular chunk layer for that particular user, at the time instance when the transmission will occur. One set of link adaptation parameters is used within the whole chunk.

Fast control loops for FDD and TDD enable reliable prediction up to vehicular speeds. The uplink control is based on a request for transmission in frame *j-2*. If granted, the transmission is scheduled and prepared during frame *j-1* and is then performed in the uplink slot of frame *j*. The downlink transmission in frame *j*, is prepared by using a small amount of downlink control signalling during frame *j-1*. The main downlink control signalling then follows during frame *j*. It is performed simultaneously with the payload transmission to reduce delays.

Note that strong FEC coding will span multiple chunks with individually calculated link adaptation parameters, see [WIN2D223] for further details of the final FEC schemes.

4.3.2. Non-frequency-adaptive transmission

The multiple access schemes for non-frequency adaptive uplinks and downlinks were introduced in [WIN2D461]. They are called Block Interleaved Frequency Division Multiple Access (B-IFDMA) and Block Equidistant Frequency Division Multiple Access (B-EFDMA) respectively. The resource allocation

[2] A chunk comprises a certain time-frequency resource consisting of a few OFDM subcarriers in a few consecutive OFDM symbols. A chunk can be spatially reused, and the spatial reuse dimension is denoted a chunk layer.

for B-IFDMA and B-EFDMA are the same and is illustrated in Figure 4-1 below. The difference between the schemes is that in B-IFDMA a common DFT precoding step is performed over the allocated blocks[3].

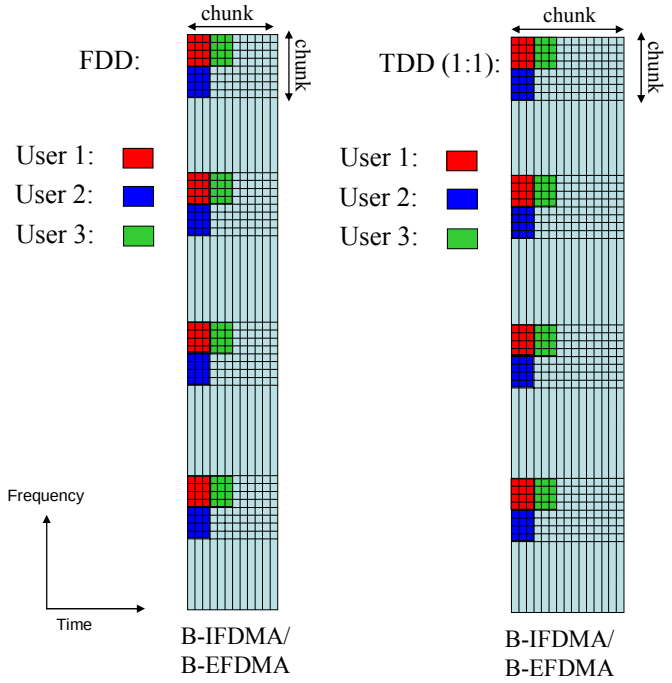

Figure 4-1: Illustration of B-IFDMA and B-EFDMA resource allocation in FDD and TDD.

These schemes aim to maximise frequency diversity, to enable micro-sleep within chunks, support high speed trains, keep low addressing overhead and to simultaneously enable low envelope variations of transmitted uplink signals. The similarity of the uplinks and downlinks further simplify the system.

A default parameterisation of B-IFDMA and B-EFDMA has been a basic block size of 4 subcarriers x 3 OFDM symbols in both FDD and TDD. This block size fits the chunk size in both FDD and the TDD chunk size defined in [WIN2D6137]. These smallest blocks are of use for small packets, encoded by convolutional coding. For larger code block sizes, it is advantageous to combine the 4x3 blocks into larger units. The appropriate block size(s) for the different scenarios is under investigation and is presented in [WIN2D61314]. One common link adaptation is used for all the allocated resources in a chunk layer for the duration of the chunk, and the CQI is based on moving average SINR, averaged over the small-scale (fast) fading of the channel.

4.3.3. Co-existence of multiple access schemes

Both frequency-adaptive and non-frequency-adaptive transmission benefit from a large resource pool with independent fading statistics. Non-frequency adaptive transmission needs the independent resources to combat the small-scale fading by diversity combining techniques. Frequency adaptive transmission benefit from independent resources to minimize the service outage probability for semi-static users and to enable large multi-user diversity gains. The default assumption is to do frequency multiplexing of the resources for frequency adaptive and non-frequency adaptive transmission, but for deployment with low system bandwidth and low carrier frequency, time multiplexing of resources for frequency adaptive and non-frequency adaptive transmission could be preferred.

[3] In the downlink, the B-EFDMA scheme does not apply a DFT precoding step. The reason to disregard the envelope properties of the downlink signal is that the RAP does not benefit from a low PAPR of each users signals, since multiple downlink signals are multiplexed including also signals for frequency-adaptive transmission.

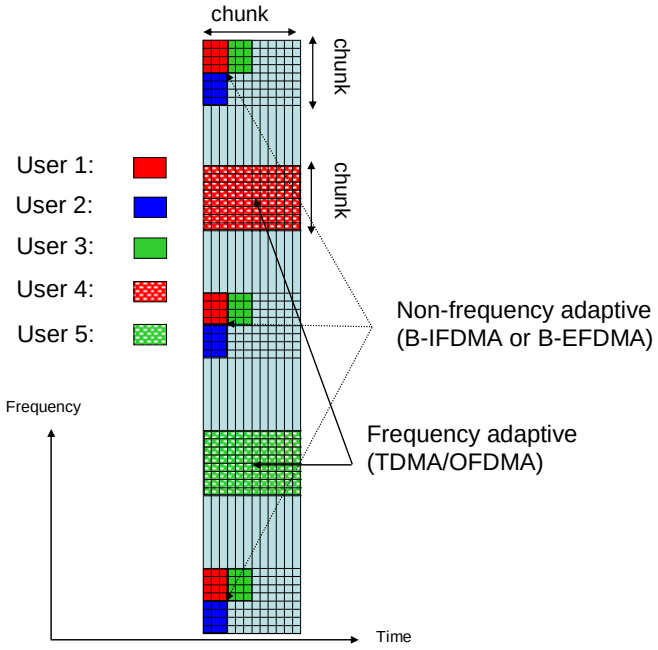

Figure 4-2: Frequency multiplexing of resources for frequency-adaptive and non-frequency-adaptive transmission.

4.3.4. Performance investigations of the multiple access schemes

4.3.4.1. Parameterization of the non-frequency-adaptive multiple access scheme B-IFDMA in the wide-area scenario

The appropriate parameterization of the non-frequency adaptive multiple access schemes, B-IFDMA for the uplink and B-EFDMA for the downlink, in the wide-area scenario depends on the performance w.r.t. e.g. frequency and spatial diversity gains, channel estimation performance, power backoff in the power amplifier (uplink), sleep mode gains, addressing efficiency and link performance due to channel coding gains over the allocated resources. In Appendix A2.1 and A2.2, further investigations towards appropriate parameterizations are provided.

In Appendix A.2.1, B-IFDMA is investigated w.r.t. pilot overhead, envelope fluctuations for different block sizes and signal bandwidths under the metrics PAPR distribution, Raw Cubic Metric and backoff required to meet the WINNER spectral requirements mask. Furthermore, diversity gains depending on block size and signal bandwidth, with and without transmit and receive diversity are investigated. Based on the considered aspects in the investigations, the findings could be summarized as follows, more than 4 subcarriers per block is not recommended. Furthermore, 16 blocks with 4 chunks separation per frame in the frequency direction seems to be appropriate for SISO transmission, whereas with 1x2 or 2x2 spatial diversity, 8 or even 4 blocks in the frequency direction per frame could be sufficient with the assumed convolutional code.

In Appendix A2.2, B-IFDMA is investigated w.r.t. performance with different receiver equalizers to mitigate the ISI introduced by the DFT precoding[4]. Furthermore, resource allocation in B-IFDMA to accommodate stronger FEC coding using larger information block sizes is investigated. It is shown that

[4] In this study, the B-IFDMA signal is generated as a sum of a few frequency-adjacent IFDMA signals. In [WIN2D461] it is shown that generating the B-IFDMA signal as a sum of frequency-adjacent IFDMA signals results in larger envelope fluctuations, implying a larger requirement on power amplifier backoff to meet the spectral requirement mask. For this reason, the preferred way to generate the B-IFDMA signal is to use one common DFT precoding matrix. However, the overall conclusions on performance in this chapter should be similar also for receivers adapted to B-IFDMA signals generated with a common DFT.

allocating more blocks in the frequency domain within a frame is as efficient as coding over two consecutive frames, which is promising in order to maintain a low latency in the MAC. An interesting result is also, that compared to the baseline assumption in [WIN2D6137], there is no penalty (actually a small gain) by allocating the blocks with two chunks separation in the frequency direction instead of four, as assumed in [WIN2D6137]. This result is useful for narrowband deployment, or in general for scenarios where no resources for frequency-adaptive transmission need to be frequency multiplexed with the resources for non-frequency-adaptive transmission. Finally, investigations are provided regarding the interplay with receive diversity, and it is shown that receive diversity is useful and can actually help to utilize the frequency-diversity better, since the residual ISI after the equalizer becomes smaller when the fading among the blocks used by the FEC code is less.

Please see also recent results on channel estimation performance for B-IFDMA and B-EFDMA in [WIN2D233],], and summarized in Chapter **Fehler! Verweisquelle konnte nicht gefunden werden.**. The parameterization of the non-frequency adaptive multiple access schemes is described in [WIN2D61314].

4.3.4.2. Throughput for Frequency-adaptive WA DL using the L2S for HARQ

In Appendix A2.3, a Link-to-system (L2S) interface for Hybrid-ARQ (HARQ) is proposed and calibrated. This L2S is used in throughput investigations for the frequency-adaptive TDMA/OFDMA downlink in a wide-area multi-cell scenario, and these simulation results are included in Appendix A2.4.

Even though there are some deviating and simplifying simulation assumptions compared to the reference design of the final WINNER system concept [WIN2D61314], the results show that HARQ helps to mitigate the uncertainty on CQI used for multi-user scheduling and link adaptation in frequency-adaptive transmission. Specifically, the investigation shows that even without the use of a channel prediction (i.e. only using the outdated channel estimates), two HARQ retransmissions with Chase combining is enough to mitigate the CQI uncertainty due to channel variability and intercell interference at the considered mobile speed of 50 km/h.

A small persistence for the HARQ scheme in frequency-adaptive transmission is very useful to meet the WINNER targets on low delays in the system.

4.3.5. Conclusions

In this chapter, we gave a brief overview of the multiple access solution in the WINNER system concept along with recent findings of the properties of these schemes. A large part of these investigations, detailed in Appendix A.2, targeted performance of B-IFDMA w.r.t. its parameterization.

For B-IFDMA, the main conclusions are that more than 4 subcarriers per block is not recommended. Furthermore, 16 blocks with 4 chunks separation per frame in the frequency direction seems to be appropriate for SISO transmission, whereas with 1x2 or 2x2 spatial diversity, 8 or even 4 blocks in the frequency direction per frame could be sufficient assuming convolutional coding. Despite the DFT precoding, stronger FEC coding can be supported by allocating more blocks per frame, which is important in order to maintain a low latency in the MAC. It is also shown that receive diversity is useful and can actually help to utilize the frequency-diversity better, since the residual ISI after the equalizer becomes smaller when the fading among the blocks used by the FEC code is less.

Finally, a link to system interface for HARQ was derived and calibrated to be used for system level simulations of adaptive TDMA/OFDMA. These simulations showed that two HARQ retransmissions with Chase combining is enough to mitigate the CQI uncertainty due to channel variability and intercell interference at the considered mobile speed of 50 km/h.

Final description of the Multiple Access solution included in [WIN2D61314] considers the above findings as well as recent findings related especially to channel estimation based on an appropriate pilot design as described in [WIN2D233] and summarized in Chapter 4.10.

4.4. Spatio-temporal processing

The wide area baseline scheme is using a grid of beams (GoB) and is described in [WIN2D6133]. The wide area results in [WIN2D6133] and [WIN2D341] have shown that the extension of the GoB baseline scheme with SDMA is the promising approach for the WINNER spatial processing reference scheme.

This conclusion is again affirmed (see Section 4.4.1, 4.4.2 and 4.4.3) throughout the new results contained in this section based on system level results using the WINNER satisfied user criterion.

In addition to that, the results in this section investigate spatial scheme switching (Section 4.4.1 and 4.4.3) and spatial multiplexing (Section 4.4.1, 4.4.3 and 4.4.4). Besides the default ULA antenna configuration with small antenna spacing, an antenna configuration with two separated sub-arrays also has shown a promising potential. The results below (Section 4.4.3 and 4.4.4) contain spatial schemes which are proposed to be used in this alternative antenna configuration.

Further aspects of spatial schemes can be found in Appendix A.1.

4.4.1. Downlink: Adaptive Switching between Single Stream and Multi Stream GoB

In [WIN2D341] we investigated the throughput achievable by adaptive switching of the spatial transmission mode in a link-level environment for a single user. We now present results that take benefit of the multi-user diversity gains on link- as well as on system-level.

The link-level results show that increasing the number of user in the system as well as providing additional beams in the GoB improves the selection probability of the SDMA mode, which then becomes the most favoured mode even at low SNR. The selection probability of the SU-MUX mode decreases by increasing the number of users, while it increases if additional transmit diversity is utilized. We further studied the effect of the antenna spacing at the BS, revealing that in a system where the BS is equipped with 2 transmit antennas, a higher throughput can be achieved with the multi stream GoB mode at high SNR if a larger antenna spacing is considered. The same relation is observed if only two beams are served in parallel if the BS has 4 antennas. However, if we increase the number of beams served in parallel here, the achievable throughput is significantly larger for smaller antenna spacing, which comes due to significantly larger SDMA gains. For systems where the BS is equipped with 4 antennas with SDMA support, a small antenna spacing thus is recommended. We further investigate the influence of the time variant channel on the adaptive multi-user transceiver concept, showing that the system can be regarded robust if a time period no longer than 1/10 of the channel's coherence time elapses between evaluation of the user channels at the terminals and the application in the succeeding time slot. If support for higher mobility is desired, switching to the Alamouti transmission mode is recommended.

On system level, we applied the score-based scheduler, which has been adapted to our system requirements, to ensure fairness in resource allocation. We investigate the so called satisfied user criterion (SUC), which is defined in [WIN2D6137] (Figure 6-1). While increasing the number of served users, the system capacity is characterized by calculating the 5-percentile user throughput and plotting it against the average sector throughput. The system capacity is determined at the point where the 5-percentile of the user throughput falls below 2 Mbit/s. In this context, high user outage has a critical impact, i.e. the SUC cannot be met. This is the case for SISO transmission as well as for MIMO transmission where the mode is fixed to multiple stream transmission (SU-MUX, SDMA). By using the single stream GoB mode with diversity reception (MRC) exclusively, the average sector throughput is less than 2.2 bps/Hz and up to 13 users can be served (MIMO 2x2 MRC in the figure). The SIMO system with receive diversity (MRC) and the baseline MCS may support almost 10 users with an average sector throughput of 1.92 bps/Hz. With the reference design MCS, the SIMO system is capable to serve 10 users, too, but with a higher average sector throughput of 2.1 bps/Hz. By adaptive switching between MRC, SU-MUX and SDMA (while considering the intra-cell interference at the receiver only), the average sector throughput is increased to 2.97 bps/Hz and 13 users can be served at the same time for the reference MCS. If we use IRC considering full knowledge of the inter-cell interference at the receiver instead, the average sector throughput is further enhanced to 3.29 bps/Hz and almost 15 users may be served.

Summarizing the system-level results, we observe that it is of major importance to introduce a fair scheduling strategy in order to reduce the outage events while achieving a high sector throughput at the same time. In the case of employing multiple antennas the outage may be substantially reduced by including the diversity oriented transmission and interference aware receiver schemes which both improve the conditions of cell-edge users. A higher average throughput can be achieved and more satisfied users may be served if multiple stream transmission techniques are further allowed. The combination of the best schemes, studied here for the 2x2 MIMO case, results in an average sector throughput of 3.29 bps/Hz taking the SUC into account.

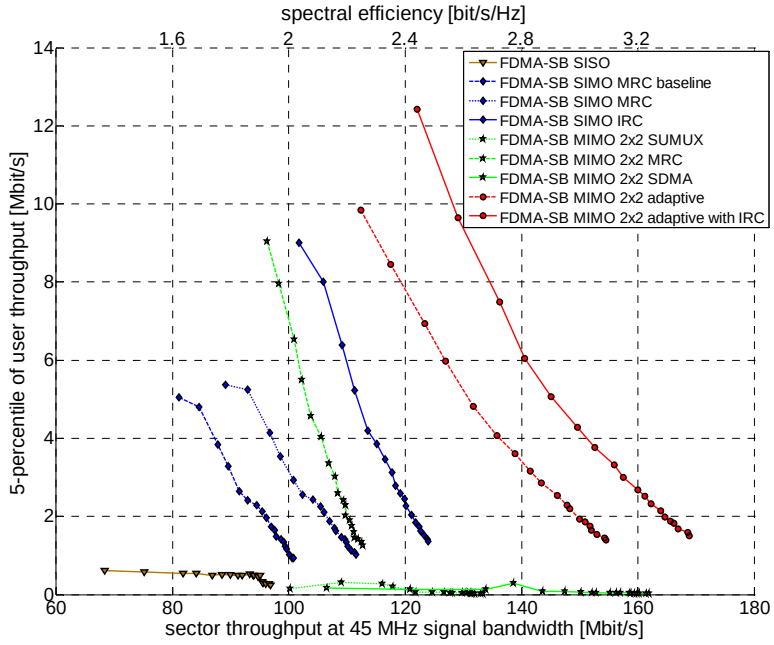

Figure 4-3: Satisfied user criterion (SUC) for different transmission schemes. Overhead is already included, i.e. according to [WIN2D6137] control overhead is set to (4+12)/96=1/6 per chunk and preamble overhead is set to 6%. Signal and system bandwidth are set to 45 MHz and 50 MHz, respectively.

No. of Tx and Rx antennas	Tx Scheme(s) & Receiver algorithm	Supported users meeting the SUC (2 Mbit/s)	Spectral efficiency (bit/s/Hz/sector)
Pure single stream techniques			
1 x 1	**SISO**	0	-
1 x 2	**MRC baseline MCS**	10	1.92
1 x 2	**MRC reference MCS**	10	2.12
1 x 2	**IRC reference MCS**	14	2.42
2 x 2	**GoB** (Grid of Beams) & **MRC** & **ref. MCS**	13	2.17
Pure SU-MIMO dual stream techniques			
2 x 2	**SU-MUX – MMSE**	0	-
Pure MU-MIMO scheme			
2 x 2	**SDMA – MMSE**	0	-
MU-MIMO adaptive scheme switching between single stream and multiple stream			
2 x 2	**GoB, SU-MUX, SDMA, MRC/MMSE**	13	2.97
2 x 2	**GoB, SU-MUX, SDMA, IRC**	15	3.29

Table 4.4-1: Spectral Efficiency and number of satisfied users for different system technologies.

4.4.2. Downlink: Performance Comparison of Different MIMO schemes, Schedulers and the Impact of the MI-ACM-based Link Adaptation

Based on a dynamic system-level simulator, the maximum number of supported users and the spectral efficiency have been evaluated and compared to SISO performance for the following MIMO schemes:

- per-user switching between STBC and S-PARC based on average SINR using 2 antennas at the UT and at the BS (2x2 adaptive MIMO), either
  - vertically polarized with 2λ element spacing , or
  - cross-polarized.
- GoB baseline design, i.e. 4 elements, vertically polarized at λ/2 element spacing, generating 8 beams,
- using SDMA based on the above GoB set-up (GoB+SDMA).

For the GoB each sector 8 fixed beam directions are defined. SINR from each beam is measured and upon this information the optimal beam for a given user is selected. For GoB+SDMA it was assumed that in one sector the same resources can be used at most by two spatially separated users with a minimum of 2 beams separation in between in order to control inter-beam interference even in the baseline NLOS case, which will be used in all subsequent results. No coordination of the used beams between sectors is assumed. Further simulation assumptions were compliant to the baseline design in [WIN2D6137], but exceeding them in the following main aspects:

- additional and also adaptive spatial schemes were investigated,
- the impact of chunk-wise adaptive modulation within one codeword was studied, i.e. the additional gain when using *identical chunks* but either adapted all of them to the average SINR (denoted basic link adaptation, BLA, in the following) or using the reference algorithm for frequency-adaptive transmission MI-ACM [WIN2D222],
- different schedulers, i.e. Proportional Fair (PF), Round Robin (RR), and Maximum C/I (MaxCoI) were compared,
- an explicit modelling of a 4-channel Stop-and-Wait Protocol and Chase Combining for HARQ was used.

4.4.2.1. MI-ACM gains for different spatial processing schemes

A comparison of different MIMO schemes and different frequency-domain link adaptation algorithms is provided in Figure 4-4 (left). Proportional fair scheduling is used and the following overhead is taken into account: 12 symbols per chunk for general control information [WIN2D6137]. In case of MI-ACM an additional symbol per chunk is assumed to be used to transmit the additional modulation information. Four common pilot symbols per antenna and chunk are assumed in order to allow fair comparison of different antenna configurations. The 2x2 MIMO results are based on cross-polarized antennas at the BS and the UT.

The additional gain of MI-ACM compared to state-of-the art adaptation to average SINR decreases with the increasing number of users, as in this case the number of chunks allocated to one user diminishes and hence less variability of SINR exists within the chunks of one codeword.

It can also be observed that the relative gain is different for different MIMO schemes. For 16 users, around 10% gain is observed for GoB+SDMA, 40% for the 2x2 adaptive MIMO, and 25% in the SISO case. However, almost no improvement is obtained for the GoB processing. The reason for this behaviour is that in particular GoB results in relatively high received SINR. The usage probability of different MCS is depicted in the right picture of Figure 4-4. The GoB scheme very often reaches the upper limits of the MCS scheme currently defined (64-QAM, $R = ¾$). A proper adaptation of the individual chunks is then no longer possible and the gain of MI-ACM is small.

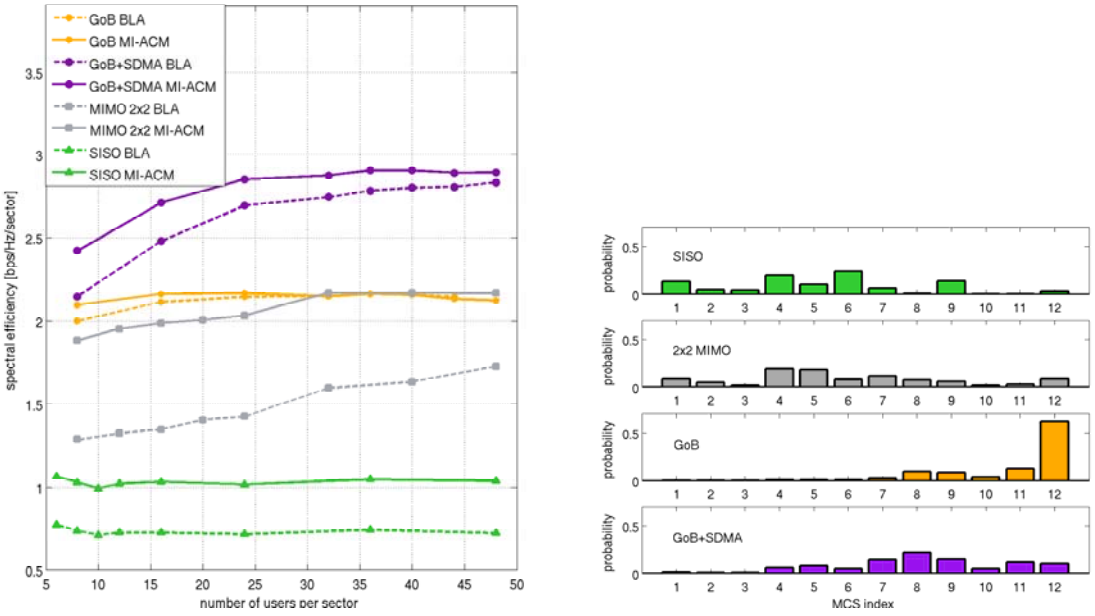

Figure 4-4: Impact of chunk-wise adaptive modulation within a codeword (MI-ACM) on spectral efficiency (left) and MCS distribution (right) for different MIMO schemes.

4.4.2.2. MI-ACM gains for different schedulers

For the 2x2 adaptive MIMO scheme the interrelation of MI-ACM gains with different scheduling strategies is further investigated in Figure 4-5. For 16 users per sector, the MI-ACM gain is around 40% for proportional fair and MaxCoI scheduling, and even 100% gain is achieved in case of Round Robin scheduling.

PF scheduling using MI-ACM even outperforms the Max CoI scheduler adapting to average SINR for up to 12 users per sector. It needs to be noted, that details of the implemented frequency-dependent scheduling strategy impacts significantly the observed gains from chunk-wise adaptive modulation, as both techniques basically exploit frequency selectivity. In particular for large bandwidth and few high-rate users, chunk-wise adaptive modulation will be of major interest. Moreover, under real-world operation conditions, it can be assumed that the scheduler would have several additional constraints (e.g. from QoS per flow, interference coordination, etc.). Therefore, the relevance to perform an advanced link adaptation per chunk will become even more important.

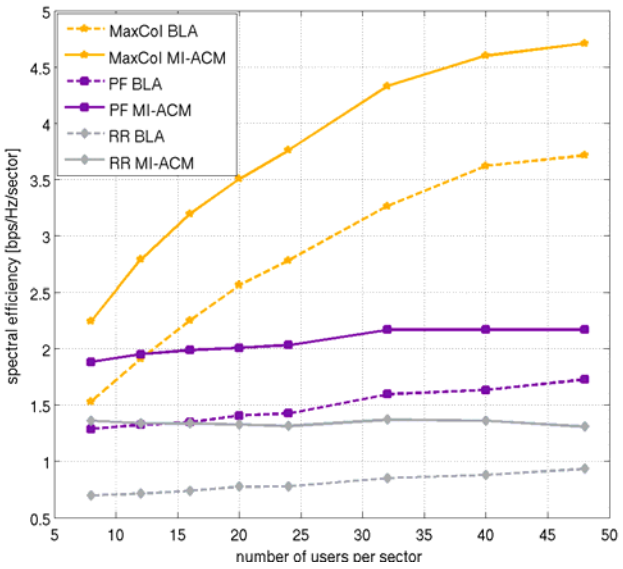

Figure 4-5: Interrelation between gain of chunk-wise adaptive modulation and scheduling strategy.

4.4.2.3. Spectral efficiency and maximum number of users under QoS constraints

Key system-level performance indicators are spectral efficiency and the maximum number of users supported under QoS constraints. For full buffer simulations, the QoS constraint is modelled as a satisfied user criterion, requiring that 95% of users have at least 2 Mbps average user throughput. Figure 4-6 shows the 5%-ile of the average user throughput vs. spectral efficiency. The figures along the curves indicate the associated load in terms of the number of users per sector.

It can be seen that the 4x2 GoB-based schemes in particular boost the maximum number of satisfied users: from 7 users per sector for SISO, to 9 users for 2x2 adaptive MIMO, to 28 users for GoB, and to 30 users for GoB+SDMA. The spectral efficiency achieved for this maximum supported load is 1.0 bps/Hz/sector, 1.9 bps/Hz/sector, 2.2 bps/Hz/sector, and 2.9 bps/Hz/sector for SISO, 2x2 MIMO, 4x2 GoB, and 4x2 GoB+SDMA, respectively.

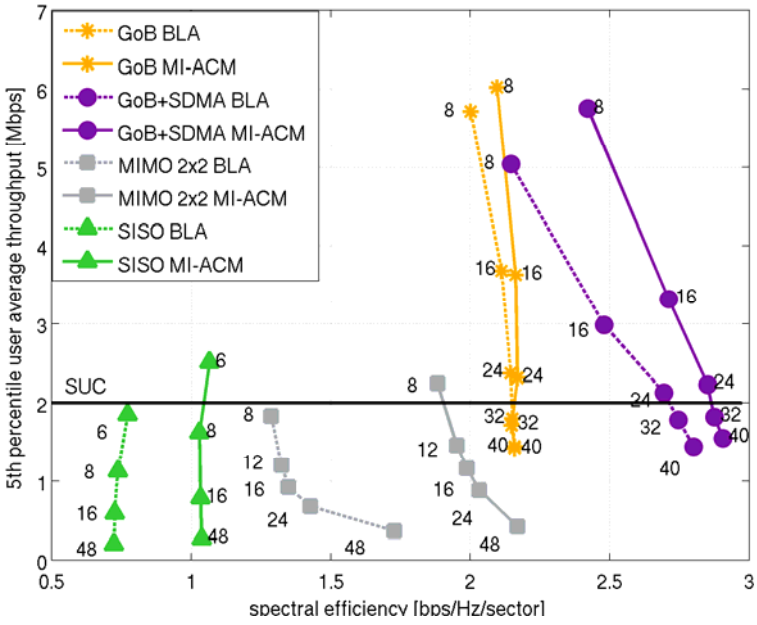

Figure 4-6: 5th percentile average user throughput vs. spectral efficiency for different spatial processing schemes

The relative gains compared to SISO for these schemes are summarised in Table 4.4-2. While the 2x2 MIMO already improves spectral efficiency by 90%, there is only a small increase (30%) in the supported number of users, since the considered schemes do not improve the performance for low SINR users, which determine the number of supported users under the satisfied user criterion. However, the number of supported satisfied users is the most relevant end-to-end performance criterion, since it directly relates to potential revenues of an operator. The 4x2 GoB-based schemes show impressive performance advantages in this respect due to improved cell-edge performance (300% increase of satisfied users), cf. also [WIN2D473].

A complete overview of spectral efficiency under satisfied user criterion constraints and the associated maximum number of supported users per sector is given in Table 4.4-3.

Table 4.4-2 – Relative gains of spectral efficiency and satisfied users for different spatial processing schemes using MI-ACM and PF scheduler compared to SISO

MIMO Config	Scheme	Spectral efficiency increase compared to SISO	Increase of satisfied users compared to SISO
2x2	Adaptation between STBC, S-PARC, x-pol Tx	+90%	+30%
4x2	GoB	+120%	+300%

4x2	GoB+SDMA	+190%	+330%

Table 4.4-3 – Spectral efficiency and supported number of users based on 2 Mbps satisfied user criterion for different spatial processing schemes

MIMO Config.	Scheme	Link Adaptation	Scheduler	Receiver	Spectral efficiency in bit/s/Hz/sector	Max. number of satisfied users
1x1	SISO	BLA	PF	MRC	0.8	5
1x1	SISO	MI-ACM	PF	MRC	1.0	7
2x2	Adaptation between STBC, S-PARC, v-pol Tx, 2λ	BLA	PF	MRC/MMSE	1.0	6
2x2	Adaptation between STBC, S-PARC, v-pol Tx, 2λ	MI-ACM	PF	MRC/MMSE	1.4	8
2x2	Adaptation between STBC, S-PARC, x-pol Tx	BLA	PF	MMSE	1.3	7
2x2	Adaptation between STBC, S-PARC, x-pol Tx	MI-ACM	PF	MMSE	1.9	9
2x2	Adaptation between STBC, S-PARC, x-pol Tx	BLA	MaxCoI	MMSE	1.2	3
2x2	Adaptation between STBC, S-PARC, x-pol Tx	MI-ACM	MaxCoI	MMSE	1.5	3
2x2	Adaptation between STBC, S-PARC, x-pol Tx	BLA	RR	MMSE	1.1	3
2x2	Adaptation between STBC, S-PARC, x-pol Tx	MI-ACM	RR	MMSE	1.4	4
4x2	GoB	BLA	PF	MMSE	2.2	28
4x2	GoB	MI-ACM	PF	MMSE	2.2	28
4x2	GoB+SDMA	BLA	PF	MMSE	2.7	25
4x2	GoB+SDMA	MI-ACM	PF	MMSE	2.9	30

4.4.3. Downlink: SU-MIMO scheme switching compared to GoB-based MU-MIMO

A class III system level simulator is used to study the performance of SU- and MU-MIMO schemes. SU-MIMO is further improved by switching between different schemes with either single- or dual-stream transmission. The single user MIMO schemes (4x2 SU-MIMO switching) are based on a combination of beamforming with either single- or dual-stream transmission. The GoB scheme is described in [WIND341] Appendix D1.1. The GoB SDMA with tapering is done according to Section 3.2.3.2 in [WIND341] and uses a proportional fair scheduling with a pure frequency domain window for determining the priority score based on estimated capacity.

Figure 4-7 and Table 4.4-4 are showing results regarding the satisfied user criterion.

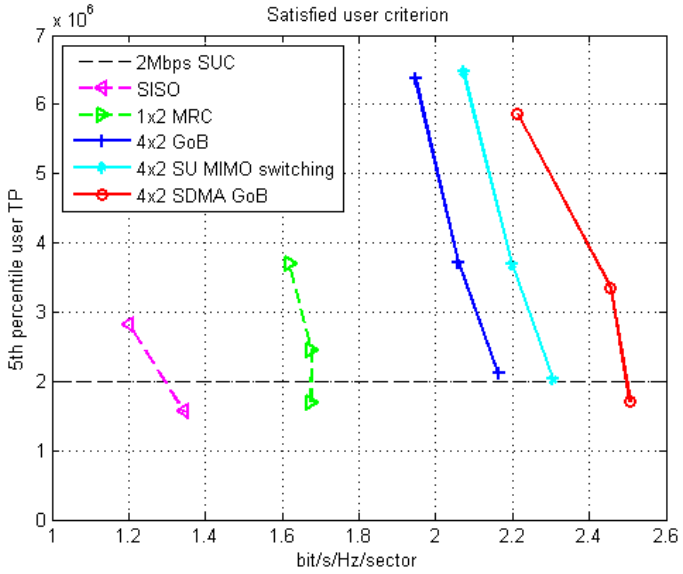

Figure 4-7 Satisfied user criterion system level results. With 4x2 antennas, for 5, 10 and 20 users, the baseline GoB is compared to SU-MIMO scheme switching and MU-MIMO based on SDMA GoB. As a comparison case SISO with 5 and 10 users and SIMO with 5, 10 and 15 users is shown

No. of Tx and Rx antennas	Scheme	Receiver	Spectral efficiency in bit/s/Hz/sector	Supported satisfied users
1x1	Single Tx antenna	MRC	1.29	8
1x2	Single Tx antenna	MRC	1.67	13
4x2	GoB = single stream baseline scheme	MRC	2.17	20
4x2	SU-MIMO switching (single stream and dual stream)	MRC / ZF	2.30	20
4x2	SDMA GoB	MRC	2.50	18

Table 4.4-4 – Spectral efficiency based on 2 Mbps satisfied user criterion for different 4x2 antenna schemes. The overhead is already included (control overhead is 12.5%, pilot overhead is 16.7%).

The Table 4.4-5 below shows the normalized sector throughput and cell border user throughput (5th percentile) for different spatial schemes with 10 users per sector on average and 2, 4 and 8 Tx antennas. The antenna configuration is always chosen in an advantageous way for the each corresponding scheme.

No. of Tx and Rx antennas	Tx Scheme(s) & Receiver algorithm	Tx antenna configuration	Normalised total throughput in bit/s/Hz/sector	5th percentile user throughput in Mbit/s
Pure single stream techniques				
1 x 2	**MRC**	-	1.68	2.45
2 x 2	**CL-TxDiv** (Closed-loop Tx-Diversity) & MRC	10 λ spacing	1.69	2.68
2 x 2	**GoB** (Grid of Beams) & MRC	λ/2 spacing	1.89	3.10
4 x 2	**GoSB+CLTxDiv** (= Grid of subarray	2 x λ/2 spacing with	1.98	3.66

	beams + closed-loop diversity) & MRC	10 λ distance		
4 x 2	**GoB** & MRC	λ/2 – ULA	2.06	3.72
Pure SU-MIMO dual stream techniques				
2 x 2	**PARC** (Per antenna rate control) & MMSE	10 λ spacing	1.52	1.33
4 x 2	**DPARC** & ZF ("Directional" PARC = PARC + sub-array GoB)	2 x λ/2 spacing with 10 λ distance	1.89	1.68
8 x 2	**DPARC** & ZF	2 x λ/2-ULA with 10 λ distance	2.15	2.45
SU-MIMO scheme switching between single stream and dual stream				
2 x 2	Single stream: **CL-TxDiv** & MRC Dual stream: **PARC** & MMSE	10 λ spacing	1.78	2.64
4 x 2	Single stream: **GoSB+CLTxDiv** & MRC Dual stream: **DPARC** & ZF	2 x λ/2 spacing with 10 λ distance	2.20	3.68
MU-MIMO (maximum of 3 streams)				
4 x 2	**GoB+SDMA** & MRC	λ/2 – ULA	2.46	3.35
8 x 2	**GoB+SDMA** & MRC	λ/2 – ULA	2.84	3.91

Table 4.4-5 – For 10 users on average per sector: Normalised sector throughput and cell border throughput for different SU- and MU-MIMO schemes. The overhead is already included (control overhead is 12.5%, pilot overhead is 16.7%).

Conclusion:

The SU-MIMO schemes strongly benefit from switching between rank 1 and rank 2 transmission. Without switching, the dual stream techniques (like 2x2 PARC) perform very poor due to their lack of robustness. Most users have a low SINR and thus can not make use of two data streams. These users experience a strong improvement when they can switch back to single stream transmission.

Despite this SU-MIMO improvement by switching we can see that MU-MIMO outperforms all SU-MIMO schemes and achieves a spectral efficiency of 2.5 bit/s/Hz/sector based on the 2 Mbps satisfied user criterion.

4.4.4. Downlink: Clustered Transmit beamforming

We will compare different options for using 4 transmit antennas by the network at the various BS to 1x2 SIMO. The investigated cases are:

- 1x2 SIMO, i.e. 1 antenna at the BS and 2 antennas at the UT using IRC
- 4 antennas are placed widely apart with 4x2 PARC-SIC
- 4 antennas are placed in two clusters with four fixed beams and 2x2 PARC-SIC

It is further assumed that the BS only knows the long-term statistics of the downlink channels. The 5 percentile user throughput of 1x2 SIMO, 4x2 PARC with successive interference cancellation and 4x2 Clustered Transmit Beamforming (CTB) are shown in Figure 4-8 for both proportional fair and round robin scheduler, respectively. It can be deduced that CTB provides 47% and 55% spectral efficiency gain at a user bit rate of 2Mbps for PF and RR scheduler, respectively. PARC-SIC yields negligible gain compared to SIMO.

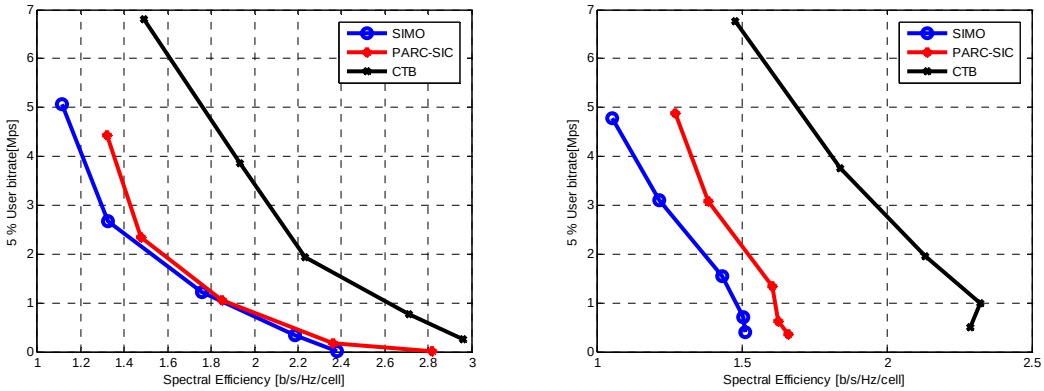

Figure 4-8 The 5% user bit rate versus the spectral efficiency per cell for proportional fair and round robin scheduler. The control overheard was not taken into account.

The satisfied user criterion for the various investigated techniques is shown in table Table 4.4-6 for proportional fair and round robin scheduler.

Technique\ Scheduler	PF	RR
1x2 SIMO	1.52	1.37
4x2 PARC-SIC	1.58	1.52
4x2 CTB	2.22	2.12

Table 4.4-6: The spectral efficiency in bits/s/Hz for the SUC (i.e. 5% user bit rate at 2Mbps). The control overhead was not taken into account.

4.4.5. Uplink: SU & MU MIMO

In this section different SU-MIMO and MU-MIMO configurations are evaluated for different offered traffic loads (average number of users per cell) in the base coverage urban scenario. A base station deployment with 1000 m inter-site distance is considered and the base station receivers are equipped with four antennas spaced ten wavelengths. MMSE combining and successive interference cancellation (SIC) after channel decoding are employed at the receiver side. A 5 MHz transmission bandwidth is used and the user terminal output power equals 24 dBm. If only a sub-band (e.g. 5 MHz) of the available bandwidth is allocated to a user in the UL, the transmit power can be increased. In interference-limited environment, the findings from looking at a subband should be very similar to looking at the full band. The traffic modeling assumes full (infinite) transmit buffers. One, two or four SDMA users are scheduled for simultaneous transmission (SDMA-1, SDMA-2, and SDMA-4, respectively) and each user terminal transmits one or two streams (single stream and dual stream PARC). The total number of transmitted streams per cell is however always limited to four. Note that SDMA-1 is a reference case that corresponds to receive diversity. Round robin scheduling is employed and a scheduled user is assigned the entire transmission bandwidth. Ideal link adaptation is used to adapt the transmissions (modulation mode and channel code rate) to the channel conditions.

In Figure 4-9, the 5th percentile (left) and the 95th percentile (right) user throughput are plotted versus the average cell throughput. At high loads the cell edge users, here represented by the 5th percentile value, benefit slightly from the use of SDMA (in comparison to multi-stream transmission). High SINR users, on the other hand, represented by the 95th percentile user throughput (depicted in the right plot of Figure 4-9), benefit highly from dual stream transmission, in particular at low network load levels. With dual stream transmission, the 95th percentile user data rate may increase significantly in comparison to single stream transmission (with and without SDMA).

Table 4.4-7 provides the uplink spectral efficiency estimates for the studied techniques. In the uplink, the SUC is defined as a user throughput of 1.3 Mbps and the spectral efficiency is measured, from the left plot in Figure 4-9, at the highest load for which the user data rates for 95 % of the users exceed the SUC.

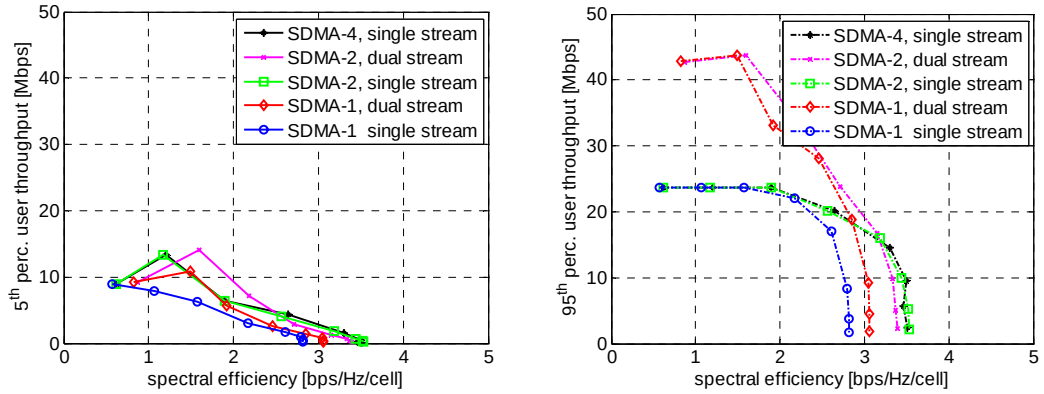

Figure 4-9 4-10 5th percentile user throughput versus sector (i.e. cell) throughput (left) and 95th percentile user throughput versus sector throughput (right). The control overhead signaling is not included.

Uplink scheme	Spectral efficiency [bps/Hz/cell]
SDMA-1, single stream	2.8
SDMA-1, dual stream	2.9
SDMA-2, single stream	3.3
SDMA-2, dual stream	3.1
SDMA-4, single stream	3.4

Table 4.4-7: Uplink spectral efficiency accounting for the SUC (user data rates of 1.3Mbps for at least 95 % of the users)

4.4.6. Conclusions

In [WIN2D341] it was concluded that the described WA baseline GoB scheme already performs well and can be improved with SDMA on top of it.
The new results contained in this section 4.4 re-emphasize this conclusion, showing a spectral efficiency of about 2.2 bit/s/Hz for GoB, which can be improved with SDMA to 2.5-2.9 bit/s/Hz, depending on a receiver type and granularity of modulation order.
Additionally combinations of spatial multiplexing (SMUX) with beamforming were investigated (either called clustered transmit beamforming (CTB) or SU-MIMO scheme switching). Here it was shown that pure spatial multiplexing performs poor, can be improved with beamforming and with switching to single stream schemes. Nevertheless in the wide area context these combinations hardly exceed the performance of the baseline GoB by achieving up to 2.3 bit/s/Hz.

Spatial scheme	Spectral efficiency based on SUC
4x2 baseline GoB	≈2.2 bit/s/Hz/sector
4x2 GoB + SDMA	≈2.5 – 2.9 bit/s/Hz/sector
4x2 SMUX + BF	≈2.3 bit/s/Hz/sector

Table 4.4-8: Average Downlink Spectral Efficiency of Spatial Processing Approaches with Satisfied User Criterion (SUC)

For the uplink it has be shown that the system performance with a SIC receiver saturates for SDMA with two simultaneous users, each with one spatial stream. So additional spatial multiplexing is not needed on top of SDMA. The gains for four simultaneous users are negligible compared to 2 users.

Further detail conclusions are:

When switching between SDMA GoB and SMUX for 2 transmit antennas, the selection probability of the SDMA mode increases with the increasing number of users.

For SDMA it was found preferable in terms of spectral efficiency to have small antenna spacings. SU-MIMO can be largely improved by switching between different schemes. A promising antenna configuration is in this case two uncorrelated subarrays consisting of two correlated antenna elements. With the same number of antennas, MU-MIMO outperforms SU-MIMO.

4.5. Relaying

In [WIN2D353] we have shown how the relaying solution can outperform the BS only deployment, however if appropriate protocol functions are not employed the possible gain can be lost. In this section we show how flexible radio resource partitioning schemes can significantly increase performance of relaying solution in the wide area test case.

Section 4.5.1 presents performance results of dynamic resource partitioning in combination with GoB-based interference mitigation, and shows that relay-based deployment outperforms a BS only deployment in terms of overall spectral efficiency. In Section 4.5.2, uplink performance results for static load-based resource partitioning in combination with SDMA show the importance of RNs when it comes to providing area-wide cell coverage.

4.5.1. Dynamic Resource Partitioning - Frequency-Adaptive Scheduling

In this section we provide more insight of performance evaluation for relay based deployment in a wide area test case of a dynamic approach for the resource partitioning. In particular, the Dynamic Resource Sharing (DRS) is illustrated in Sections 4.5.1.1 and its performance evaluation in Section 4.5.1.2. Parameters used in the simulations follow the assumptions proposed in [WIN2D6137].

Results are obtained considering only the cell in the centre and 18 cells around, C2 NLOS channel model for BS-UT links, C1 NLOS for BS-RN links and B1 NLOS for RN-UT links. We have assumed an ideal approach for packet retransmissions due to errors: if a packet is received by destination with errors, it will be en-queued in the source. This assumption consists of having an ideal feedback that is not affected by transmission errors. We have assumed larger packet size segmented into segments of 1200 bytes. Users are considered fixed in position. The full buffer model and Round Robin resource scheduling have been adopted.

4.5.1.1. Dynamic Resource Sharing (DRS)

Details can be found in [CoFrRe+07][FrReCo+07] and [WIN2D352] Section B.1.

The idea behind the resource partitioning scheme consists of grouping users served by a single RAP and which are unable to share the same resources, according to their mutual spatial correlation. In the following each group of users is called beam.

Beams that might be grouped together and share the same resources can be selected using a simplified estimate of the transmission rate of each beam. The computation of this term makes use of estimates of the average inter-beam interference, i.e. a measure the interference experienced by the users of a beam when a transmission is occurring in another one.

In [WIN2D352] Sections B.1.3.1 the CCB (Chunk-by-Chunk Balancing of the relay and access link) resource partitioning scheme is illustrated. The CCB algorithm tries to achieve the maximum possible cell throughput by always allocating the groups of beams having the highest total rate. It further keeps the balance between the first and second hop allocation by making sure that enough resources are assigned for the first hop for each allocation on the last hop.

The chosen approach consists of having a stepwise alternating allocation between the two links of the same connection. At each step, a chunk is assigned on the access link to the group of beams which achieves the highest average throughput. The allocation on the relay links is then checked to see whether it is sufficient to forward all the data which is scheduled to be transmitted on the access link, and

resources are assigned to them when needed. When one of the beams belonging to the selected group has been completely served, a new beams group is calculated and the whole procedure repeats.

The main advantage of this algorithm is that at each step to every allocation on the second hop corresponds at least an equivalent allocation on the first one in order to guarantee enough resources for the end-to-end connection. The resulting resource partitioning would consequently cause lower losses due to unbalanced allocations with respect to a fixed resource partitioning case.

4.5.1.2. Simulations results

Results in [WIN2D352] were obtained by means of a snapshot simulator which estimates the average cell throughput according to the expected SINRs of the users only. Therefore the short term scheduling (or equivalently resource scheduling), retransmissions, segmentation and reassembly, etc. were out of scope of that work.

In Figure 4-11 we show the spectral efficiency versus the number of users for BS only and BS+RNs deployments using Dynamic Resource Sharing (DRS) resource partitioning illustrated in Section 4.5.1.1. The Baseline Fixed Partitioning, as proposed in [WIN2D6137] is also plotted for comparison purpose.

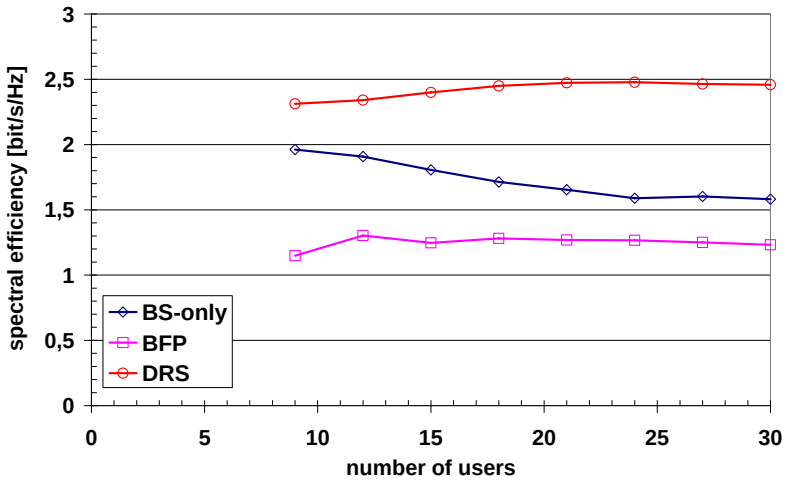

Figure 4-11: Spectral efficiency versus number of users for BS only and BS+RNs deployments using dynamic resource partitioning scheme called Dynamic Resource Sharing (DRS). The Baseline Fixed Partitioning (BFP) is also plotted for comparison purpose.

In Figure 4-11 we can observe that the spectral efficiency decreases with an increasing number of users due to the overhead introduced by user plan packet processing, which increases with the number of users. This effect is compensated by the more flexibility in the resource allocation provided by DRS approach.

The relaying solution provides 60% increase in spectral efficiency compared to BS only deployment for high number of users. However, if appropriate protocol functions are not employed the possible gain can be lost as shown by the Baseline Fixed Partitioning (BFP).

4.5.2. Static Resource Partitioning - Non-Frequency-Adaptive Scheduling

4.5.2.1. Load-based resource partitioning

The target of the proposed static partitioning is to provide a low-cost solution with low hard-ware requirements put to the relay nodes. The envisaged deployment is characterized by: (a) Single (Omni directional) Antenna Relay Nodes, (b) Single Transceiver Relay Nodes (Relaying/Forwarding is performed in the time domain) (c) Smart Antenna Technology at the BS only, to keep RN equipment cost low.

We investigate a regular, hexagonal deployment covered by two-hop RECs. Each REC consists of one BS and three RNs. Both BSs and RNs are referred to as Radio Access Points (RAPs). From the perspective of the user terminal, there is no difference in being connected to either or the other of the two RAP types. As a worst-case assumption this work considers a reuse factor of one between adjacent RECs. This means the possibility of full inter-cell collision is inherent to all investigated schemes.

The system's available time-frequency resources are assigned to the so-called groups of RAPs, where - in the extreme case - each RAP node belongs to a distinct group while - in the other extreme - all RAPs could belong to the same group. The groups are used for intracell frequency planning by the partitioning scheme – RAPs belonging to the same group may reuse the same resources. In order to exploit the resources within a REC as efficiently as possible, one can try to identify RAPs within the REC that are sufficiently well separated from each other (in terms of path loss/shadowing) to enable re-using the same resources. In the case of centralized resource partitioning schemes, the groups may also be used for intercell frequency planning (see [WIN2D353], Section 3.2.3).

The optimal fragmentation of resources within a REC also highly depends on the distribution of the users, i.e. of the distribution of the offered traffic load within the REC. As a starting point, this work assumes a relatively homogeneous traffic distribution and therefore an even distribution of resources.

The overall spectral efficiency of a relay based deployment is expected to highly benefit from a spatial reuse of the resources, not only between different relay subcells as outlined above but also on the relay link. It is therefore envisaged that the BS uses SDMA based on beam forming to feed the RNs and the User Terminals (UTs) on the first hop. In addition a careful placement of the RNs with respect to the BS is considered and thus yields maximum spectral efficiency on the relay links.

4.5.2.2. Simulation Results

The goal of the simulations is to provide an estimation of the performance of the WINNER protocol in Wide-Area mode under the following assumptions:

- Varying Cell size (BS-BS distances investigated: 800m, 1000m, 1200m)
- different static resource partitioning settings ("NoReuse" and "FullReuse"), see [WIND353])
- non-full buffer traffic and finite buffer-capacity at all nodes
- SDMA group scheduling at the BS

Detailed Simulation Parameters can be found in [WIN2D353], Section 3.2.2.

Figure 4-12 shows the DL sustained REC throughput vs. the total offered DL traffic. Only the relay

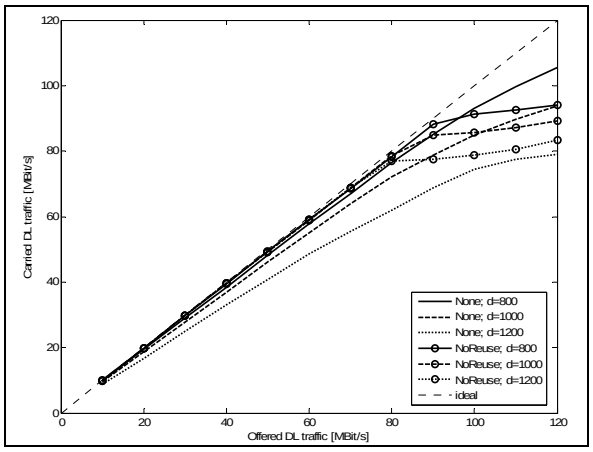

Figure 4-12: DL Cell Throughput in the center cell vs. offered DL traffic

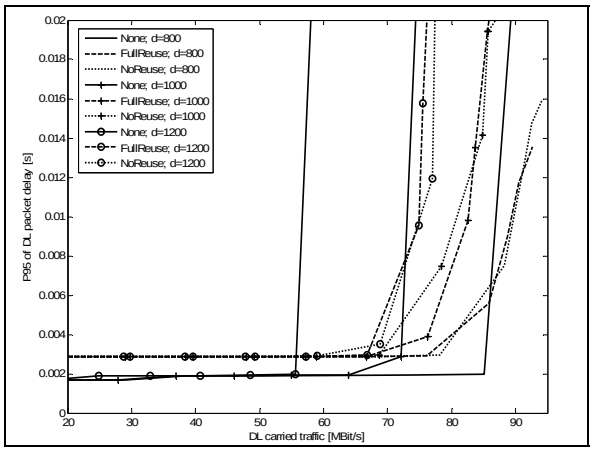

Figure 4-13: 95th Percentile of DL packet delay vs. center cell throughput

deployment "NoReuse" is shown for simplicity and because it performed slightly better than "FullReuse". The latter one .improves coverage as the performance at low traffic loads. With increasing cell size, the BS can not serve all users, leading to a discrepancy between offered and sustained traffic already at low loads. On the contrary, the relaying deployment delivers stable coverage and - in the case of larger cells - higher saturation and peak throughput than the single-hop solution. At 1200m inter-site distance, a cell throughput of about 80Mbit/s is achieved.

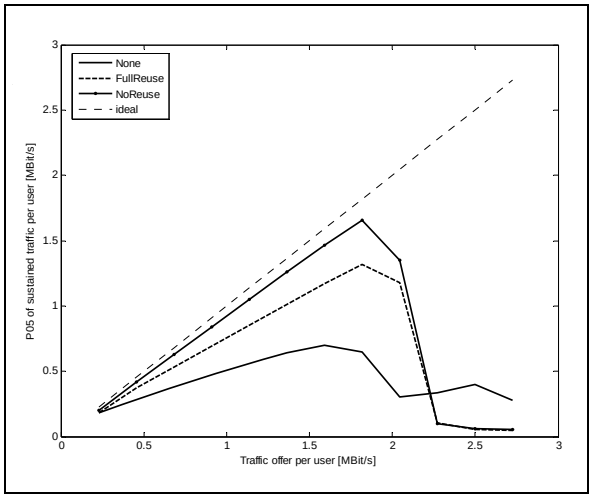

Figure 4-14: 5th Percentile of DL individual user throughput vs. offered DL traffic per user

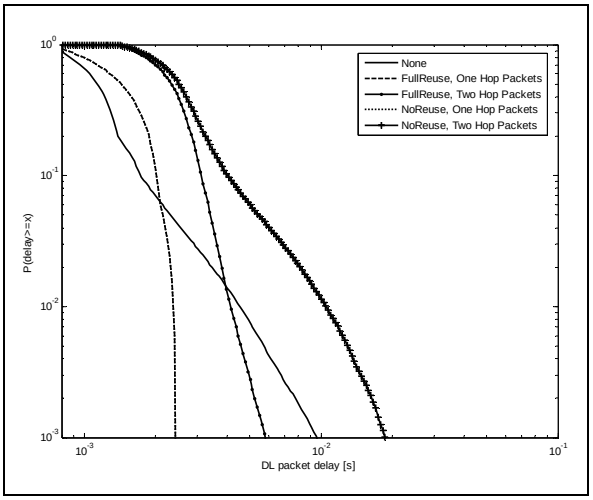

Figure 4-15: CCDF of DL Delay for One- and Two-Hop data packets at a DL traffic offer of 80Mbit/s and a site-separation of 1000m

Figure 4-13 indicates the achieved Quality of Service. It plots the 95th percentile of the DL Packet Delay versus the sustained DL traffic. Naturally, in low load cases the BS-only deployment exhibits ca. 30% shorter delays than the relay-based deployment. However, all relay-based cases show a less harsh saturation behavior and overall higher saturation throughput than the respective single-hop cases. At e.g. 1200m site separation, the relay deployment improves the saturation throughput from 55Mbit/s to more than 70Mbit/s, i.e. by more than 25%.

Figure 4-14 and Figure 4-15 illustrate the individual user experience. Figure 4-14 shows the 5th percentile of the individual user's received DL throughput vs. the offered traffic per user. This means that 95% of all users achieve a DL data rate higher than the given figures. It can be seen that the introduction of relay nodes improves user satisfaction and inter-user fairness substantially. The "NoReuse" partitioning seems to perform best in this discipline. Figure 4-15 plots the Complementary Cumulative Distribution Function (CCDF) of the DL packet delay at an exemplary traffic offer of 80MBit/s. Where applicable, the figure distinguishes between users which are immediately connected to the BS (One-hop) and those which are connected to RNs (Two-hop). The smaller amount of resources available on the second hop notably increases the delay for two-hop users. It also shows that the two partitioning patterns compared do not differ in terms of delay on the first hop, since the first-hop resources are the same in both cases (see [WIN2D353]).

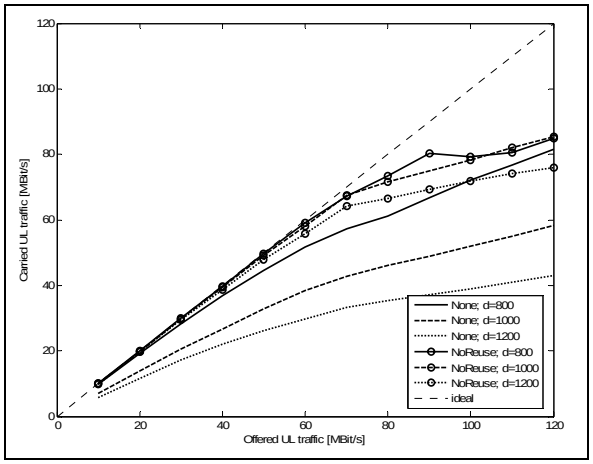

Figure 4-16: UL Cell Throughput vs. offered UL traffic

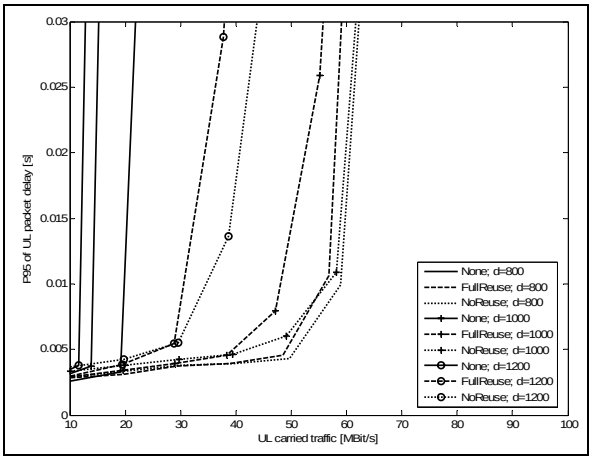

Figure 4-17: 95th Percentile of UL packet delay vs. center cell throughput

Figure 4-16 and Figure 4-17 show the same information as Figure 4-12 and Figure 4-13, only for the uplink. It becomes apparent that a substantial lack of UL coverage is observed in the single-hop comparison case, especially at 1000m and 1200m inter-site-distance. The reason for this is the low output power of the user terminals and the resulting imbalance of the link budget, which can only partly be remedied by the combined UL power control and resource allocation scheme from [WIN2D352] which was applied in the shown simulations.

4.5.3. Conclusion

Section 4.5.1 indicates that relay-based deployments can outperform a BS-only deployment in terms of overall spectral efficiency. The observed improvements are about 60 percent for a high number of users. The contribution also shows that the relaying gains can only be attained under the assumption of a dynamic resource partitioning scheme. This property becomes even more visible when switching from full-buffer traffic models to more realistic packet arrival processes, which leads to an inhomogeneous distribution of traffic in the REC. Section 4.5.2 gives simulation results based on a simple Poisson packet arrival model. The attainable spectral efficiency figures are slightly (between 1.7 and 1.9 Bits/s/Hz) lower than the ones given in Section 4.5.1 (up to 2.5 Bits/s/Hz), which can be explained by the following differences: (a) 4.5.1 makes a full-buffer assumption, which leads to an overestimate of the performance (b) 4.5.1 looks at frequency-adaptive scheduling while 4.5.2 investigates non-frequency-adaptive transmission, (c) in the simulations for 4.5.2, a fixed code-rate of ½ was assumed, leading to a more coarse link adaptation and less efficiency (minus 33%) in the highest MCS (64-QAM ½ instead of 64-QAM ¾).

Both results underline the necessity of a dynamic adaptation of the partitioning. Furthermore, uplink performance results from Section 4.5.2 show the importance of RNs when it comes to providing area-wide cell coverage. Owing to the limited output power assumed for the WINNER user terminals (24dBm), the uplink range is limited such that in the single-hop case, not the entire cell area can be covered and a large percentage of users (>20 percent) remain in outage.

The resource partitioning schemes investigated and the performance results presented can be condensed into the following statement:

In the Wide-Area CG scenario, the deployment of relay nodes has shown the potential to improve the level of coverage - especially to overcome uplink power limitations - while achieving similar or even better spectral efficiency figures as single-hop deployments with comparable BS density. The latter improvement can however only be realized by the usage of intelligent and dynamic resource partitioning and reuse schemes to adapt the available capacity on the relay and the access links to the actual distribution of the offered traffic within the relay-enhanced cell.

4.6. Inter-cell interference mitigation

To handle inter-cell interference is a major challenge in WINNER, and in particular in the wide area deployment scenario. For this purpose, a number of different interference mitigation methods have been investigated within WINNER, these include interference averaging techniques [WIN2D471], interference avoidance techniques [WIN2D472], and smart antenna based interference mitigation methods [WIN2D473].

Table 4.6-1 below gives an overview of the investigated techniques and summarises the results in terms of cost/performance tradeoffs. The table contains for each of the investigated technique: Gain (in mean SINR, sector throughput, cell edge user throughput, etc.), required signalisation and measurements, algorithms complexity (like O(n!) or relative to some basic algorithms) and re-use factor (amount of spectrum available in each cell). The simulations that the table is based on are done for the base coverage urban scenario, specified in Chapter 2. Most of the techniques consider downlink; in case uplink is considered it is clearly stated in the table.

Table 4.6-1: Interference mitigation techniques.

Technique	Gain	Signalisation and Measurements	Complexity	re-use factor
Uplink Frequency Hopping	Almost no gain over simple OFDMA with receive diversity	No special measurements and signalisation needed	Minor – FH patterns as look up table in mobiles	1
Interference Cancellation at UT	2-3 dB in SINR. High sector throughput (+ 25-40 %) and cell-edge user	Synchronisation among the neighbour cells Pilot design need to allow for	significant additional complexity at the UT, see [WIN2D471]	1

	throughput gains (x3-5)	reliable channel estimates of dominant interferers Control signaling for MCS of dominant interferers are required		
Random DCA	Basis for comparison	No special measurements and signalisation needed	Simplest of all resource allocation algorithms	1
Min Interference DCA	0.1 – 0.5 dB	Interference on the chunks	Linear in number of chunks	1
Grid of Beams (GoB)	Tremendous sector throughput (+ >50 %) and cell-edge user throughput gains (x8) SINR gain of 4.5 dB w.r.t. single Tx antenna	Feedback of the best beam's index	Measurement of the power received from each beam at the UT	1
Tapered GoB in combination with SDMA	Significant additional gain of 24% in sector throughput compared to pure GoB leading to increased spectral efficiency from approx. 2.0 to 2.5 b/s/Hz/sector but slight degradation of cell edge user throughput of 14%	Additional CQI feedback per chunk for the best beam	Additional algorithms for beam tapering as well as selection and scheduling of the users	<1 (SDMA)
Interference Rejection Combining (IRC) at UT	Significant gain in cell-edge user throughput (x 1.5) and sector throughput (+15 %) SINR gain of 1 dB w.r.t. MRC	Estimation of the received signal correlation matrix	Higher than MRC: need to estimate and invert the correlation matrix	1
Uplink IRC (at BS)	Gain in cell-edge user throughput (15-20 %) and sector throughput (+10 %) SINR gain of 0.5-1 dB w.r.t. MRC	Estimation of the received signal correlation matrix	Higher than MRC: need to estimate and invert the correlation matrix	1
Cost Function based scheduler	The same gain as the proportional fair or score based	The same as for proportional fair or score based. No	Linearly proportional to the number of users multiplied by number	1

	scheduler with the optimal parameter settings for a given load and QoS requirements. The difference to the other scheduling algorithms is that parameters are adjusted to load and service requirements self-adaptively.	special measurements and signalisation needed	of free resources.	
Token Bank Fair Queuing (TBFQ) scheduler	Gain over SB in terms of queuing delay and number of packets dropped. Throughput gain for cell edge users (x 1.5)	Short term CQI is required at the BS for every UT in every chunk	No additional complexity required at UT. Minor - in the scheduler implementation at BS side	1
Macro diversity for MBMS : Single Frequency Network (SFN)	Gain at the cell border	Quite accurate time/frequency synchronization	No extra complexity at the UT	1
Macro diversity for MBMS: Cellular Cyclic Delay Diversity (C-CDD)	Gain only directly at cell border (i.e. gain if no influence of macro diversity)	Synchronisation and communication among the neighbour cells	No complexity at UT Minor - in the scheduler implementation at BS side	1
Macro diversity for MBMS: Cellular Alamouti Technique (CAT)	Gain over whole cell border area	Synchronisation and communication among the neighbour cells	Increased signal processing and higher channel estimation process at UT Minor - in the scheduler implementation at BS side	1
Fractional Frequency Re-use (FFR)	Significant gain in cell-edge user throughput (x2.5), but loss in sector throughput (-15%) compared to re-use 1	average SINR measured over the whole bandwidth	Minor – in the scheduler implementation at BS side	1 in the inner part of the cell, 3 at the cell border

Techniques identified suitable for wide area deployments include transmit beamforming, e.g. GoB, and UTs with interference suppression capabilities, e.g. IRC. Also the use of interference aware schedulers, e.g. the cost function based one, is important to achieve good performance in interference limited conditions. For uplink, BS receivers with interference suppression capabilities, e.g. IRC, has been identified as an efficient method. In some cases, e.g. for common control channels, transmit beamforming is typically not applicable, hence some resource partitioning scheme, e.g. FFR, may be needed for these cases.

It should also be noted that the techniques can be employed in different combinations. Some of the techniques combine well, e.g. GoB at BS and IRC at UT, while others do not combine that well, e.g. GoB at BS and FFR.

4.6.1. Combination of Grid of Beams and IRC

One of the recommended inter-cell interference mitigation schemes for downlink data channels in wide area deployments combines Grid of Beams (GoB) at the base station transmitter and Interference Rejection Combining (IRC) at the UT receiver [WIN2D473], see also Section 4.4. In the following, we investigate the end-to-end system performance achieved using this scheme. We investigate the maximum spectral efficiency and average user throughput enabled by the combination of GoB and IRC in the downlink under the WINNER2 satisfied user criterion (95 % of the users have an average throughput greater than or equal to 2 Mbit/s), as well as the maximum number of users supported in these conditions. In addition, the user throughput cumulative distribution function (CDF), the fairness curve and the CDF of the SINR on the allocated resources are given for the conditions where the highest spectral efficiency is reached.

4.6.1.1. Simulation scenario and assumptions

The considered scenario almost matches the WINNER2 Base coverage urban scenario, whose parameters are summarised in Chapter 2 above, and more detailed in [WIN2D6137], except the following deviations:

- in frequency non-adaptive mode, chunk-based resource allocation is used instead of the B-EFDMA. However, like in the B-EFDMA, the allocated resources are regularly spaced apart within the whole system bandwidth;
- the link adaptation is performed based on the average channel quality on all the allocated chunks, i.e. there is no chunk-wise modulation adaptation;
- receive diversity at the UT is obtained through a linear antenna array instead of cross-polarized antennas;
- the duo-binary turbo codes are used instead of the LDPC codes;
- variable FEC block sizes (max size in the order of 5100 bits) are used instead of fixed ones, without modulation adaptation within a FEC block.

The main simulation parameters are summarised in Table 4.6-2 below.

Table 4.6-2: Summary of the simulation assumptions

Channel model	C2
Number of sectors	57
Number of UTs per sector	Variable parameter
Inter-site distance	1000 m
Multi-cell simulation method	Central cell
System bandwidth	50 MHz
Relaying	No
Indoor users	No
Interference modelling	The channels of the 7 dominant interferers on a long term basis are modelled accurately The remaining ones are modelled as single-path SISO channels All the interfering BSs transmit at full power with full load
BS antenna configuration	4-element ULA with antenna element separation 0.5λ
BS spatial processing	GoB with 4 antennas
UT antenna configuration	2-element ULA, antenna element separation 0.5λ

UT spatial processing	IRC
UT velocity	3 km/h in frequency-adaptive mode 50 km/h in non-adaptive mode 120km/h in non-adaptive mode
Modulation and coding schemes	10 MCS BPSK, QPSK, 16QAM, 64QAM Duo binary turbo code with rates 1/2 , 2/3, 3/4
Link adaptation	simulated with CQI feedback delayed from one frame
Retransmission / HARQ	4 / Chase combining simulated with explicit feedback of ACK/NACK messages
Multiple access	Chunk-wise OFDMA; regularly spaced apart within the whole system bandwidth in non-adaptive mode
Scheduling	Score based (window size: 30) in frequency-adaptive mode Round Robin in non-adaptive mode
Traffic model	Full buffer
Channel and interference parameters estimation	Perfect
Feedback messages transmission	Perfect

For 9 UTs per sector or more:

- 9 UTs are scheduled simultaneously in the 45 MHz bandwidth, which leads to 16 chunks per UT which are not necessarily co-localized;
- one retransmission unit contains a single FEC block only.

For less than 9 UTs per sector:

- 3 UTs are scheduled simultaneously, which leads to 48 chunks per UT;
- one retransmission unit contains 2 FEC blocks.

The interfering cells whose contribution to the interference is accurately modelled also use the GoB, whereas the cells simulated in a simplified manner are assumed to transmit using a single transmit antenna. The beam allocation in the interfering cells is drawn randomly in a uniform and independent manner for each chunk, and changes at each time slot.

4.6.1.2. Results

Table 4.6-3 summarises the maximum number of supported users per sector (i.e. such that the cell-edge throughput is greater or equal to 2 Mb/s), as well as the sector spectral efficiency, average user throughput and cell-edge user throughput obtained with this maximum number of users.

Table 4.6-3: Summary of results

Conditions	Frequency-adaptive 3km/h	Frequency-adaptive 50 km/h	Frequency non adaptive 50 km/h	Frequency non adaptive 120 km/h
Maximum number of	20	12	12	10

supported users per sector				
Sector spectral efficiency (b/s/Hz/sector)	2.0	1.7	1.6	1.6
Average user throughput (Mb/s/sector)	5.0	7.2	6.7	6.3
Cell-edge user throughput (Mb/s/sector)	2.15	2.10	2.05	2.32

4.6.1.3. Discussion

These results are obtained with perfect channel estimation but without chunk wise modulation adaptation, which may compensate each other. In addition, possible estimation errors on the interference correlation matrix involved in the IRC weights computation may lower the results; however, the significance of the degradation is not known. If only outdoor UTs are considered; for indoor users' coverage, the sector throughput (and thus the spectral efficiency) may decrease significantly. Adding relays may increase the sector throughput. At last, note that the basis for these results is the baseline design; all the enhancements brought by the reference design are consequently not reflected in these results, and should lead to increased performance. In particular, SDMA is expected to bring significant throughput improvements, as discussed in Section 4.4.

Besides, we can remark that the maximum number of supported users is almost divided by 2 between user velocities of 3 km/h and 50 km/h, essentially due to the reduced efficiency (in frequency-adaptive mode) or deactivation (in non-adaptive mode) of functions exploiting accurate channel predictions (opportunistic scheduling in time and frequency, fast link adaptation, etc.). However, increasing the user velocity from 50 km/h to 120 km/h only marginally affects this number, which shows the robustness of the frequency non-adaptive mode to medium vehicular speeds. Note that at 50 km/h, the frequency-adaptive mode still provides a small gain (7 %) in spectral efficiency w.r.t. the non-adaptive mode.

4.6.1.4. Additional performance indicators

For the reader's information, we give in the following the CDF of the user throughput, the fairness curve (CDF of the user throughput normalized by the average user throughput), and the CDF of the average SINR over the scheduled resources. In particular, the significant shift of the fairness curves to the right of the y=x curve indicates that the system is clearly fair in the investigated conditions.

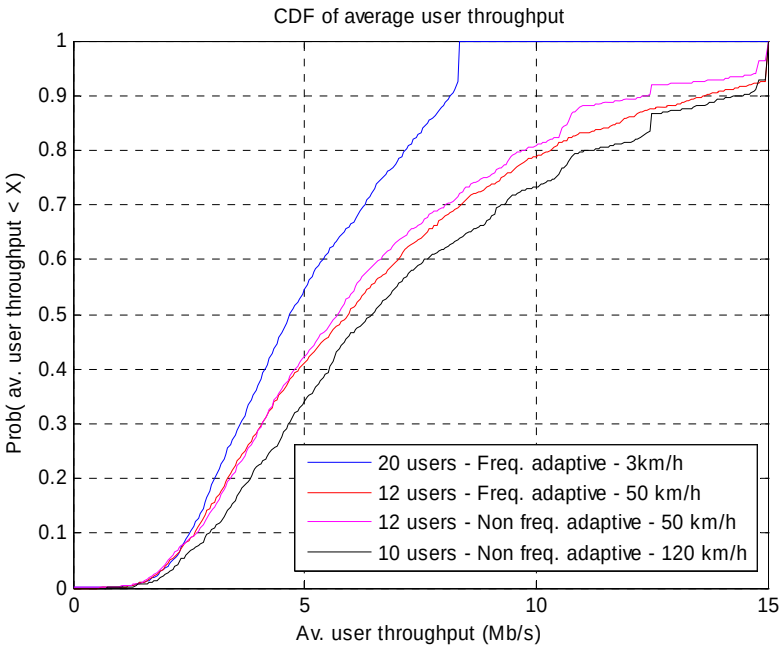

Figure 4-18: CDF of average user throughput for GoB + IRC

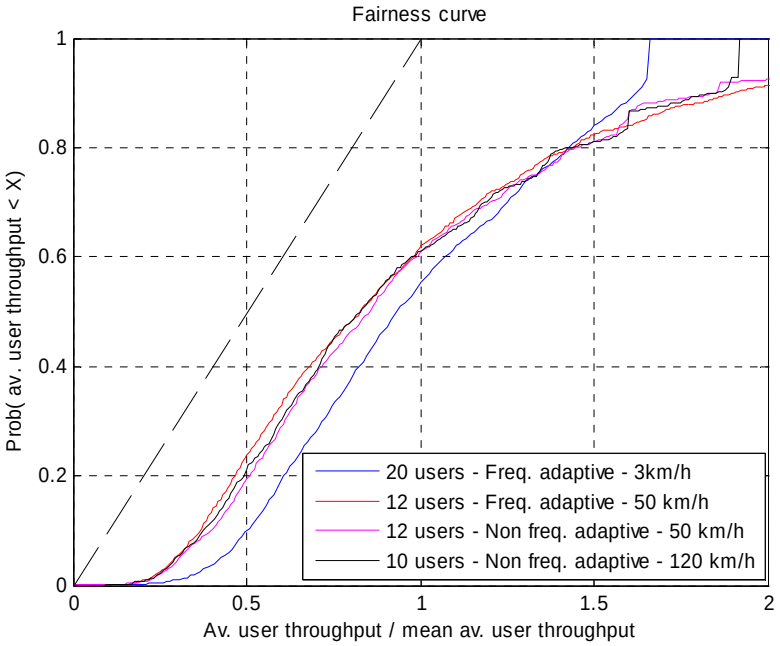

Figure 4-19: Fairness curve for GoB + IRC

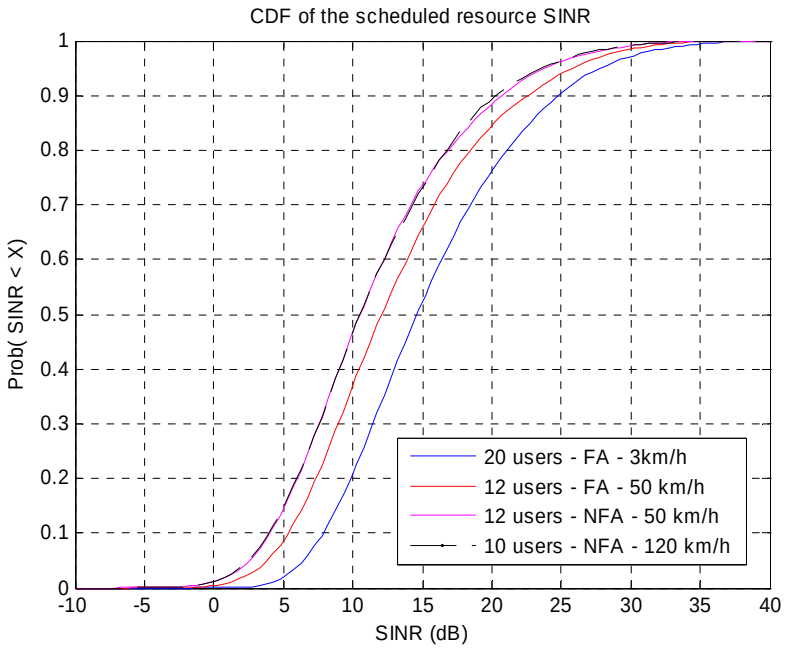

Figure 4-20: CDF of the average SINR over the allocated resources for GoB + IRC (FA: Frequency Adaptive; NFA: Non Frequency Adaptive)

4.7. Impact of User Data Traffic on E2E Performance

In most simulations, a full buffer is assumed. This simplifies simulations substantially and allows also a relatively easy comparison of results obtained by different sources. This approach is very common in research and standardization, but has some deficiencies. User traffic is usually very bursty, involves small and large packets, and has packets with different delay and QoS requirements. All this has to be taken into account by the scheduler, which is also in charge of exploiting multiuser diversity.

For that reason, it is essential to assess a system with real traffic models. WINNER has defined generic traffic models [WIN2D6137], which are commonly applied in standardization bodies.

There are two different approaches to generate user data traffic:

1. Separate Traffic and Mobility Generation

- Input: Desired distribution for the traffic type
- Output: File containing for each mobile a time stamp with packet size and reading time

2. Traffic Generator implemented in dynamical simulator

- Input: Traffic model with distribution parameters
- Output: Packets dynamically created during simulation

Since many simulators use full-buffer, it is interesting question what difference does it make on simulation results in comparison to realistic traffic models. In following we investigate differences between full-buffer and realistic traffic models like VoIP, WWW and CBR in respect to receive SINR distribution and spectrum efficiency.

4.7.1. SINR Distribution Difference between Realistic Traffic Models and Full Buffer Simulation

Downlink

Figure 4-21 shows the SINR distribution comparison between WWW traffic and a full buffer traffic model in DL. For the both schedulers (BestCQI and Proportional Fair (PropFair)), the realistic WWW

traffic has a much lower SINR than the full buffer one, i.e. for about 16 dB in the case of BestCQI and 7.5 dB in the Case of PropFair. Whereas the BestCQI outperforms the PropFair scheduler in a full buffer evaluation; their performance difference is marginal if WWW traffic is prevalent. Without GoB, the difference between full buffer and WWW is much smaller.

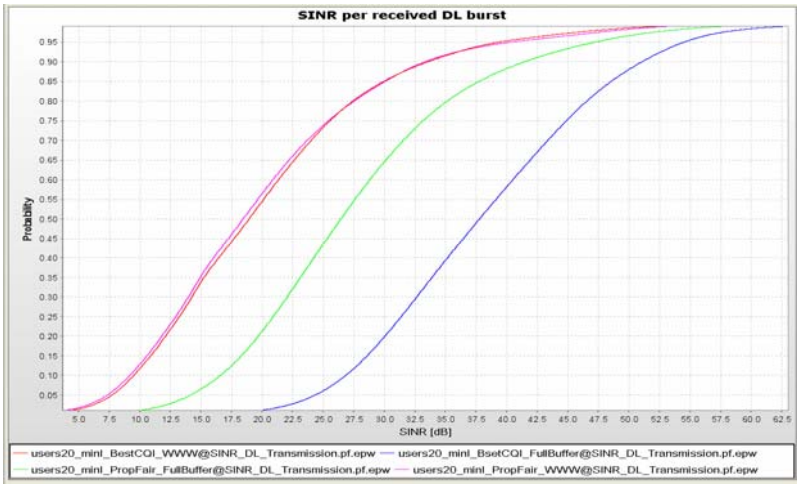

Figure 4-21: SINR Distribution for WWW Traffic Model and Full Buffer in DL for Proportional fair and Best SQI Schedulers. 20 Users, with GoB

From Figure 4-22 can be seen that the difference between full-buffer and realistic traffic models in DL is about 7.5 dB for Proportional Fair Scheduler almost independently of traffic type (VoIP or Web-browsing) , load (20 or 40 users per cell) and Proportional Fair Scheduler implementation (giving more or less weight to the data rate achieved so far by a user).

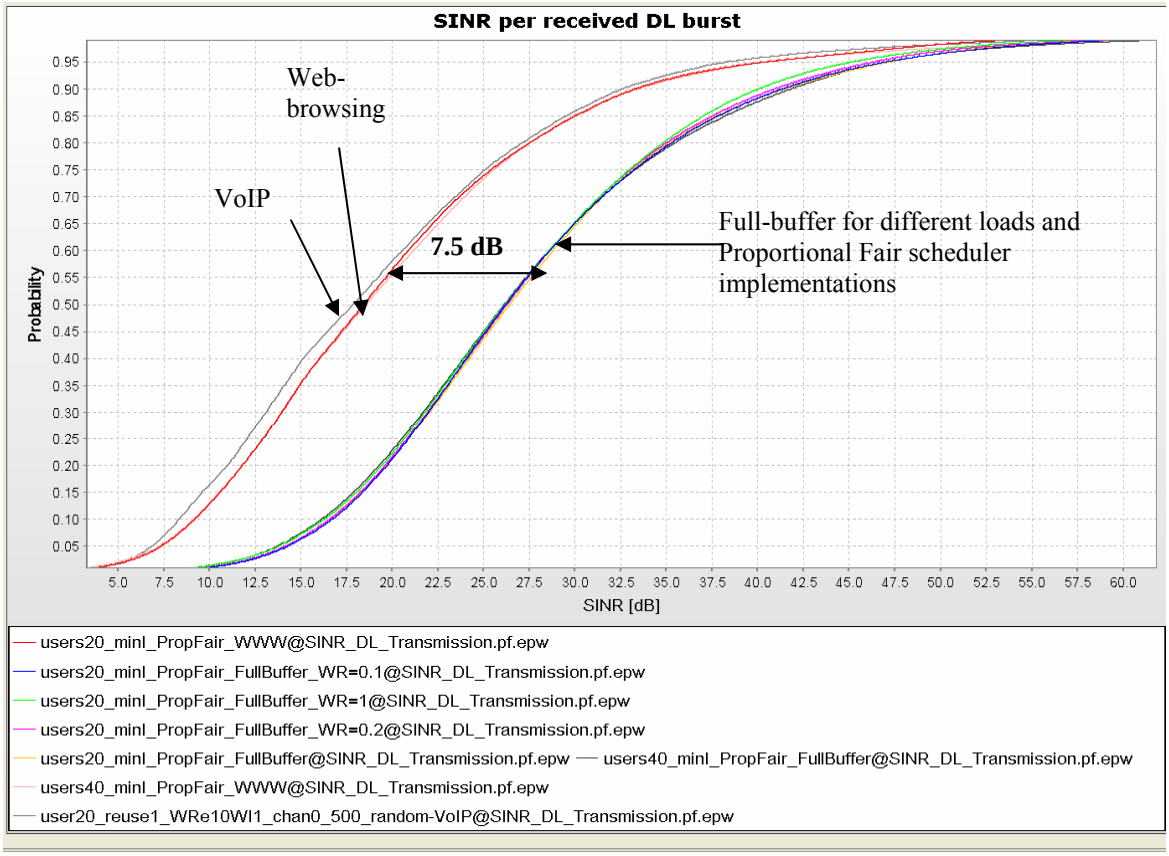

Figure 4-22: SINR Distribution for WWW and VoIP Traffic Model and Full Buffer for different loads and different version of Proportional fair Schedulers

Uplink

From Figure 4-23 can be seen that difference in SINR-distributions in UL between full-buffer and WWW traffic is quite different than the difference in DL (compare with Figure 4-21). Whereas in DL the difference between mean SINR with full-buffer and realistic traffic models is about 7.5 dB, in UL is the mean SINR with WWW traffic even higher (for about 1 dB) than with full-buffer.

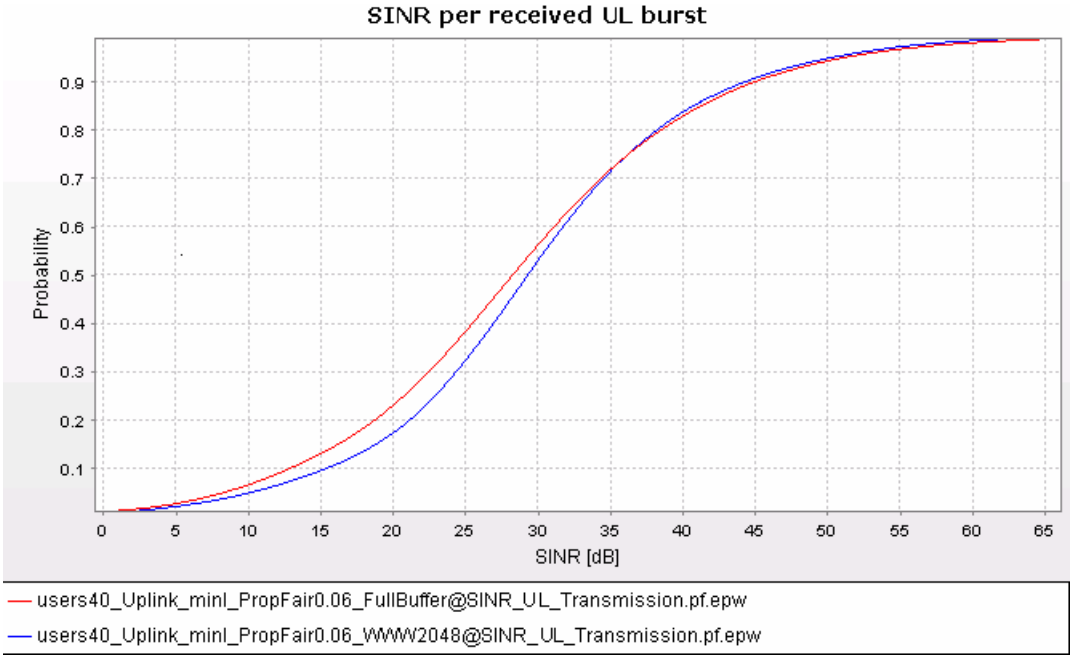

Figure 4-23: SINR Distribution for Full Buffer and WWW Traffic Model in UL for Proportional fair Scheduler, 40 Users, with GoB

The reason for much lower SINR difference between full-buffer and WWW traffic is that the difference interference with full-buffer traffic in UL (about 28 dB) is much higher than in DL (about 5 dB), as can be seen from Figure 4-24. In UL we have much more interferer (mobiles) than in DL (base stations). Furthermore, interference in UL (variance 8 dB) is much more difficult to predict than in DL (variance 4 dB), since the number and positions of interferers change over time. So scheduler decisions in UL are less reliable than in DL and the scheduled users experience much more interference.

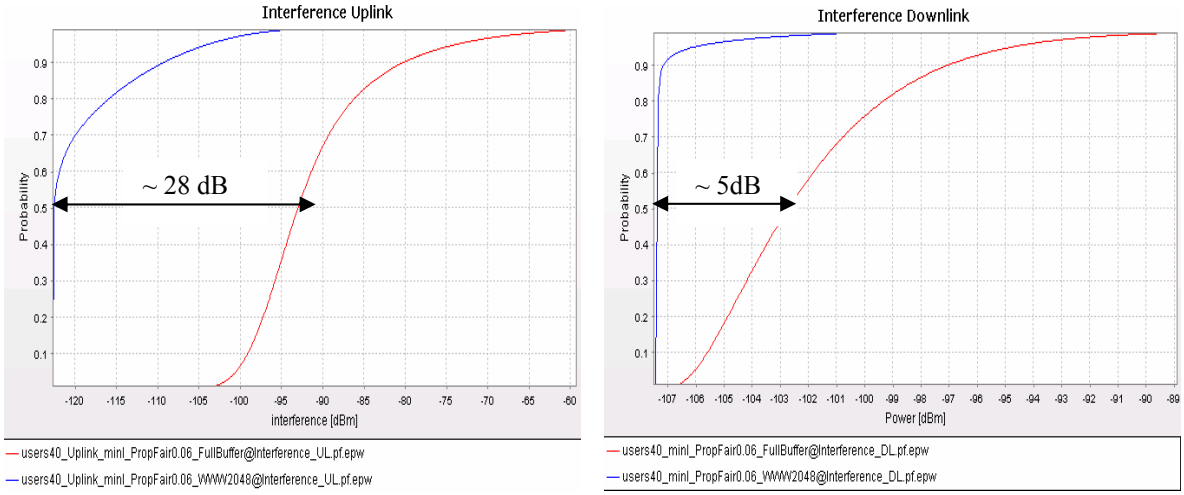

Figure 4-24: Comparison between Interference Distribution for Full Buffer and WWW Traffic Model in UL (left) and DL (right), Proportional Fair Scheduler, 40 Users, with GoB

The simulations are done for the WINNER2 Base coverage urban downlink scenario, whose parameters are described in [WIN2D6137].

4.7.2. Impact of Traffic and Packet Modeling on Spectral Efficiency

Full buffer simulations provide optimistic results, since neither the impact of the traffic model (reduced queue length, reduced multi-user diversity, reduced link adaptation accuracy, etc.) nor the impact of packet handling, such as segmentation, padding loss, etc., are considered. In order to understand the resulting degradation dynamic system-level simulations are performed comparing full buffer simulations with a constant bit rate model (CBR). A CBR traffic model with constant packet size was used in order to eliminate effects due to varying packet size and reading times. The CBR traffic parameters are comparable to a low resolution live streaming service class according to the service classification of ITU-R to be used for IMT-Advanced evaluations [8F0568]. The traffic load is 2.06 Mbps assuming one packet (of 712 information bits) arrival per slot per user. The service-class-related satisfied user criterion (SUC) requires that

- 95% of the users have an average user throughput greater or equal than 2 Mbps (i.e. a maximum of 3% packet loss is allowed on average), and at the same time
- 95% of the packets arrive with a delay of less than T_{SUC} =100 ms.

Packets are discarded if they are older than 110 ms in order to prevent congestion in the transmit queue.

Simulations are performed for the downlink of a frequency-adaptive transmission in the base coverage urban test scenario. Simulation assumptions are according to [W2D6137]. Results are shown from dynamic system-level simulations using dedicated modeling of a *N*-Channel-Stop-And-Wait Protocol with Chase Combining of packets. Overhead is considered (13 symbols for control signaling and four pilot symbols per antenna, i.e. a total overhead of 29 out of 96 symbols). Besides a standard Proportional Fair scheduler simple packet-aware schedulers are used, where the standard metric *m* is multiplied by a factor M_d that considers packet delay. Two different factors are investigated:

$$M_{d,lin} = \frac{T_{SUC}}{T_{SUC} - \min\left(t_{HOL}, T_{SUC} - 1\right)}, \text{ and} \tag{4.1}$$

$$M_{d,ex} = e^{\left(\frac{w \cdot T_{SUC}}{T_{SUC} - \min\left(t_{HOL}, T_{SUC} - 1\right)}\right)}. \tag{4.2}$$

where T_{SUC} =100 ms is the delay-related satisfied user criterion of the service, and t_{HOL} is the age of the head-of-line packet (oldest packet) in the transmit queues of the particular user. In the subsequent figures, a scheduler using the additional factor according to Eq. (4.1) is denoted DS (delay-sensitive), DSexp indicates a scheduler according to Eq. (4.2).

The CDFs of user packet delay and user packet throughput are depicted in Figure 4-25 for a load of 40 users and the baseline spatial processing technique of a fixed grid of eight beams (4x2 MIMO). Both figures contain a zoom-in for the area of the SUC requirements on delay, and throughput, respectively.

It can be seen that all scheduler variants still fulfill the packet delay requirement. However, the standard PF scheduler cannot meet the average throughput requirement, whereas the DS and certain parameterisations of the DSexp scheduler (w=3, 0.3) can. For a load of 44 users all investigated scheduler already infringe upon the throughput requirement. It can therefore be concluded that the maximum load using a delay-aware scheduler and GoB is around 40 users.

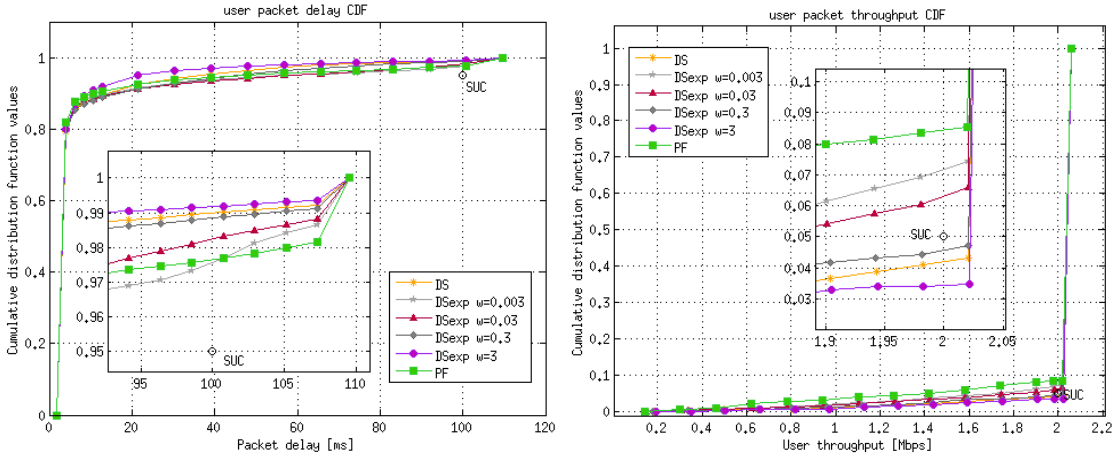

Figure 4-25: CDFs of user packet delay (left) and user packet throughput (right) for a 4x2 Grid-of-Beams configuration and different scheduler variants (40 users per sector)

The same investigation has been performed for GoB with SDMA. Comparing both schemes at equal load of 40 users per sector (i.e. Figure 4-25 against Figure 4-26) it is clearly visible that GoB+SDMA improves user throughput and packet delay compared to GoB. For GoB+SDMA and delay-aware scheduling the load can be even further increased up to 56 users, as shown in Figure 4-27.

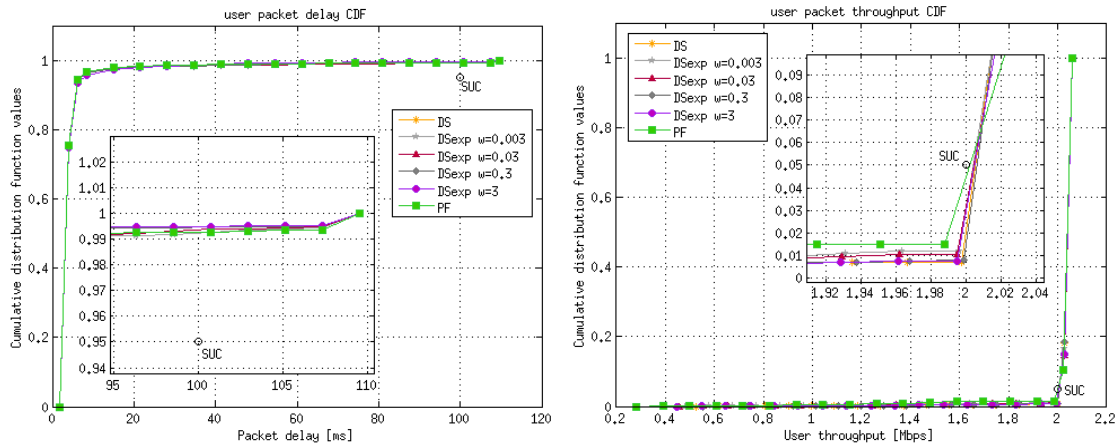

Figure 4-26: CDFs of user packet delay (left) and user packet throughput (right) for a 4x2 Grid-of-Beams + SDMA configuration and different scheduler variants (40 users per sector)

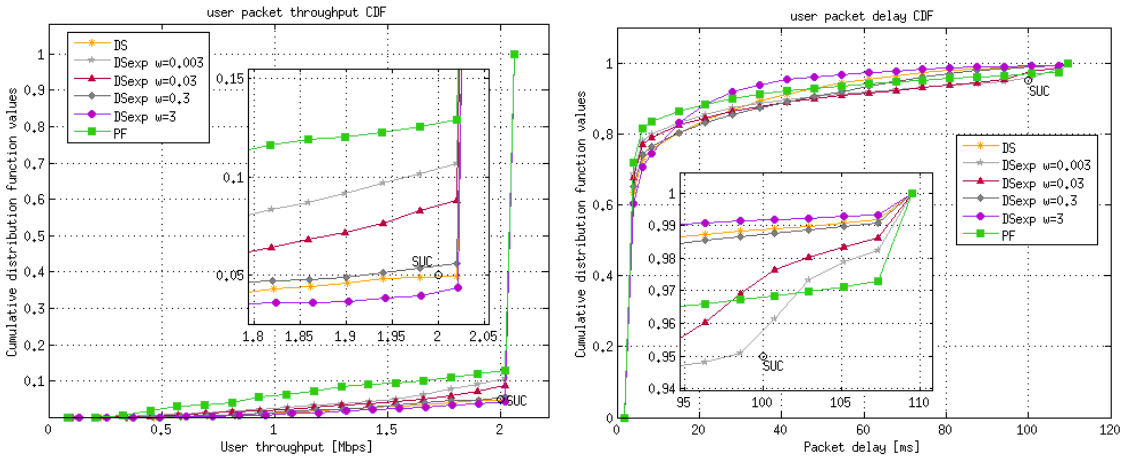

Figure 4-27: CDFs CDFs of user packet delay (left) and user packet throughput (right) for a 4x2 Grid-of-Beams + SDMA configuration and different scheduler variants (56 users per sector)

A comparison of the spectral efficiency obtained for full buffer simulations and CBR with different scheduler variants is given in Figure 4-28 for both GoB (left) and GoB+SDMA (right). For the full buffer model, simply the successfully transmitted bits are counted, whereas packets, segmentation and padding are modeled for the CBR service. In the full buffer simulations, all users have permanently an infinite amount of data to transmit and therefore can be allocated many resources. Results with the same simulator and simulation parameters (see Section 4.4.2) have shown that in this case the maximum load for GoB is 28 users per sector in order to fulfill the throughput SUC (95% of users having 2 Mbps user throughput or more). For CBR traffic only a few or just one packet might reside in the transmit buffer. Therefore, as stated above 40 users can be served using GoB due to the reduced offered traffic load of 2.06 Mbps per user. While the spectral efficiency vs. number of users curve is already in saturation for the full buffer assumption, multi-user scheduling gain is still considerable for the CBR traffic in Figure 4-28. It is therefore important to compare the loss in spectral efficiency not at equal number of users, but at the maximum load supported for this particular service. In this operational point the degradation in spectral efficiency is around 23% (from 2.2 bps/Hz/sector for full buffer and 28 users to 1.7 bps/Hz/sector for CBR and 40 users).

For GoB+SDMA similar trends are observed: spectral efficiency is decreased by 21 % for CBR traffic and delay-aware scheduler compared to full buffer (from 2.9 bps/Hz/sector for full buffer and 30 users to 2.3 bps/Hz/sector for CBR and 56 users).

It can be therefore concluded that full buffer simulations overestimate spectral efficiency but underestimate the maximum number of users that can be served in case all simulations are using the same throughput SUC. The SUC, i.e. QoS constraints, prevent full exploitation of the multi-user scheduling gain for the CBR traffic investigations.

Amongst the different variants of the delay-aware schedulers, virtually no difference is visible in the spectral efficiency in Figure 4-28. Figure 4-25, Figure 4-26, and Figure 4-27 show that related to delay and average throughput the DSexp, w = 3 performs best. However, the DS metric (Eq. (4.2)) performs almost as good and avoids the use of the tuning parameters w and can therefore be used as a good and simple implementations of a delay-aware scheduler.

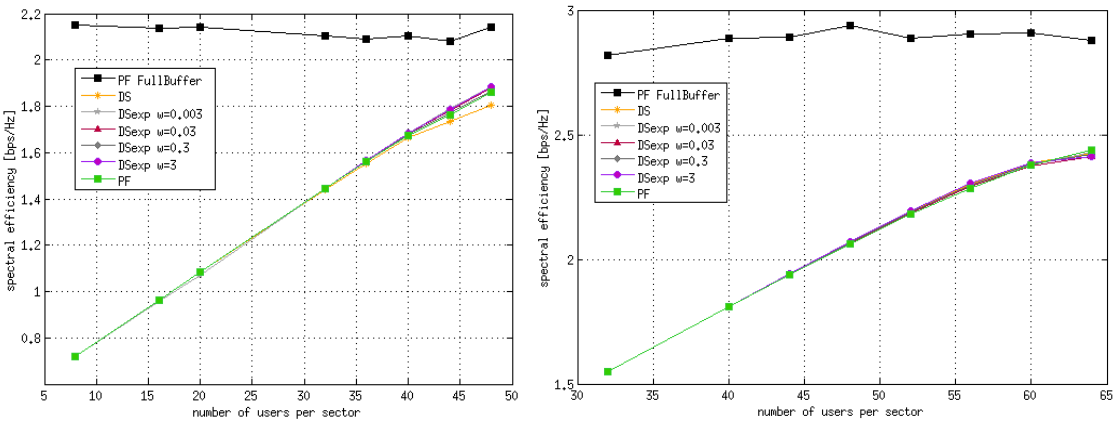

Figure 4-28: Comparison of spectral efficiency per sector for GoB (left) and GoB+SDMA (right)

If a standard PF scheduler is used instead of a delay-aware scheduler algorithm as outlined above, the maximum number of satisfied users decrease from 40 to 32 in case of GoB and from 56 to 48 for GoB+SDMA. The spectral efficiency obtained decreases accordingly from 1.7 bps/Hz/sector to 1.45 bps/Hz/sector for GoB and from from 2.3 bps/Hz/sector to 2.1 bps/Hz/sector for GoB+SDMA. The simple delay-aware scheduling algorithms used here can improve the maximum number of supported users and spectral efficiency notably. A comparison of the performance at the maximum number of satisfied users is provided in Table 4.7-1.

Table 4.7-1 Maximum number of satisfied users and spectral efficiency comparison

MIMO Scheme	Traffic Model - Scheduler	Max. number of satisfied users	Spectral Efficieny [bps/Hz/sector]
GoB	Full Buffer - PF	28	2.2
	CBR – PF	32 (+15%)	1.45 (-34%)
	CBR – DS	40 (+43%)	1.7 (-23%)
GoB+SDMA	Full Buffer - PF	30	2.9
	CBR – PF	48 (+60%)	2.1 (-28%)
	CBR – DS	56 (+87%)	2.3 (-21%)

4.8. Radio Resource Management

In this section we evaluate the performance of the WINNER handover algorithm, focusing on intramode (i.e., between LA cells) and intermode (i.e., between LA and WA cells) handovers.

The algorithm we propose combines all the available quality parameters (SINR, estimated instantaneous throughput and network load) and consists of two independent triggers, one for maintaining the wireless connection, and another for maximizing the network performance.

The wireless connection trigger aims at guaranteeing an available wireless connection for the mobile station and only takes place when the actual connection degrades and is likely to be lost. This algorithm is reported in Figure 4-29. A SINR target is defined, to obtain a PER < 0.01 with packets of 1500 bytes on the basic modulation scheme. By default the period of evaluation for the SINR is 0.2 s, but, when the SINR becomes lower than the target, it can be increased to 0.02 s for an intensive evaluation. From the collected values an average SINR is determined. If the average SINR is lower than the target, the handover is triggered.

The network performance trigger instead combines the measured SINR and the network load in order to maximize MAC layer performance. The metric used to activate the trigger is called "Residual throughput" and it is defined as: Data Rate * (1 – PER) * (1 – Channel Occupation). The word "residual" means that a part of network resource is already occupied by other users, then the handover decision is only based on the remaining bandwidth at the user disposal. The handover trigger is based on a comparison between the estimation of the residual throughput on the current cell (namely, Current_residual_throughput) with the one that could be achieved on another cell (namely, Target_residual_throughput). If the ratio between Target_residualt_throughput and Current_residual_throughput is bigger that a threshold,

Target_residualt_throughput / Current_residual_throughput > throughput_margin

then the handover is triggered.

After extensive simulations we decided to set the *throughput_margin* to 1.1, a value that avoids ping-pong effects and at the same time does not limit the gain that can be achieved with handovers.

Compared to the wireless connectivity trigger which periodically evaluates the link quality for maintaining the connection, evaluations of the network performance trigger are less frequent. A time average of more samples can better express the network performance in "long term".

To derive the Data Rate, the Channel Occupation and the PER, the UT performs measurements in the used cells and on broadcast messages sent by the BSs of neighbouring cells. For detailed description please refer to D4.8.2.

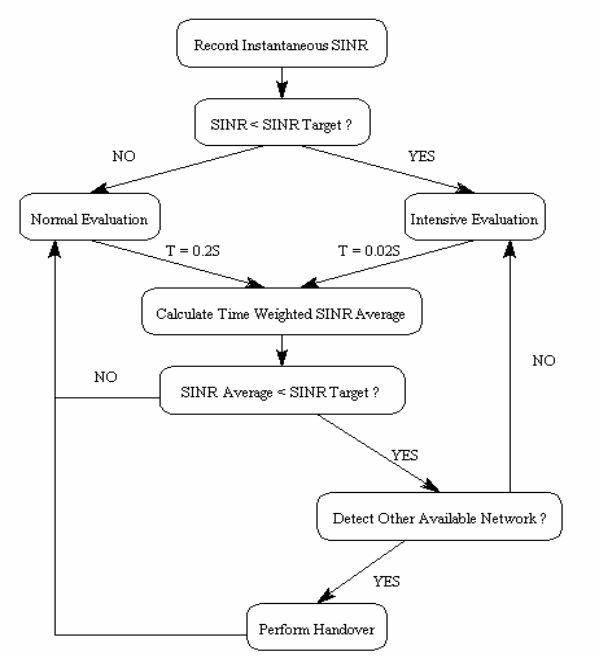

Figure 4-29 - Wireless Connection trigger

Moreover, in order to restrict the number of cells to measure, we assume that the user terminal is supplied with a list of the neighbouring cells, that are the most likely to fulfil the SINR or quality requirements at the user terminal location. In this way, measurements are performed only on the cells included in the neighbours list.

We evaluate the performance of the proposed algorithm providing simulation results derived with OPNET, by modifying the simulator distribution to implement the considered handover criteria.

In our simulations all user terminals have two radio interfaces with different PHY, MAC stacks and IP addresses corresponding to the wide area and the local area modes. These two interfaces constantly monitor the link quality of each mode and forward this information to a "mobility management" process implemented on the mobile device, which controls continuously the performance of each wireless connection and triggers the inter-mode handover if needed.

It must be highlighted that:

- In one instant only one interface is used for *data* transmission.
- Both stacks (MAC and PHY) are always on, and are able to receive and send *control* packets (e.g. to probe the channel quality).
- Each interface (WA and LA) has its own IP address, thus an IP handover is performed switching from WA to LA modes.

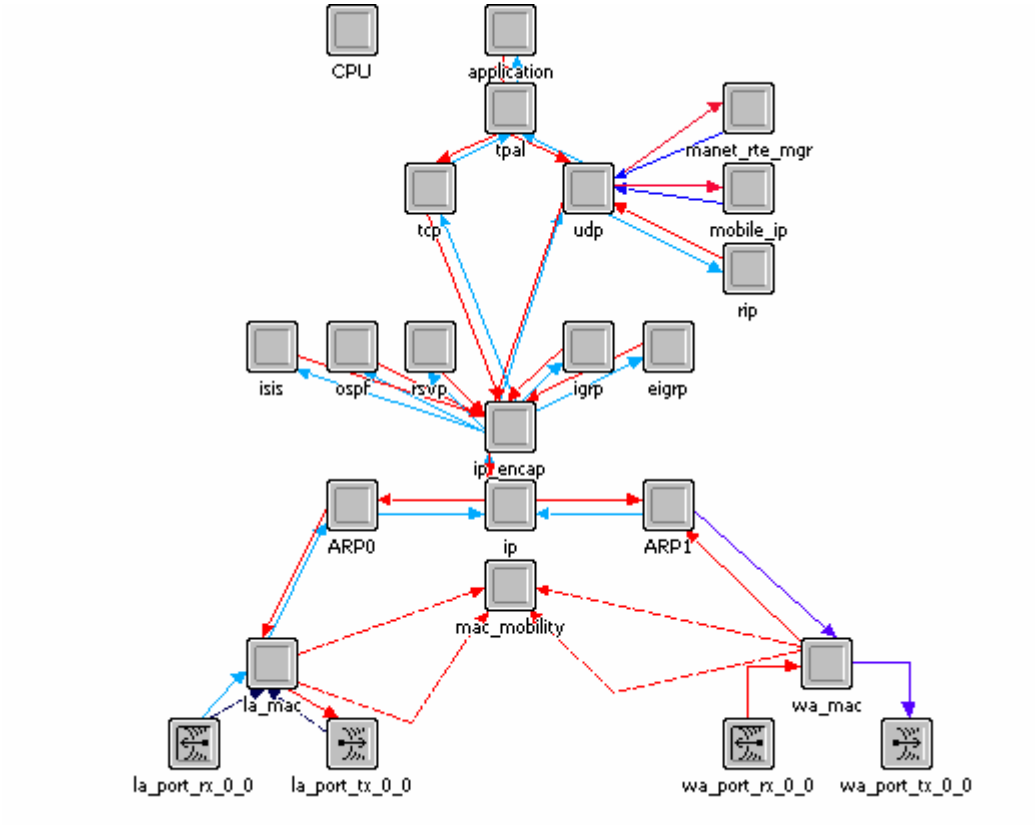

Figure 4-30– Hybrid station structure with two interfaces, WA and LA

Figure 4-30 reports a schematic representation of the user terminal, as implemented in the OPNET simulator. Each multi-mode terminal, able to transmit and receive on the WA and LA WINNER modes, is characterized by double PHY and MAC layers in the protocol stack. Since the PHY and MAC WINNER layers are not totally defined yet and an implementation in the OPNET simulator is not available, we represent the wide area mode with IEEE 802.16e and the local area mode with IEEE 802.11g. The 802.16e addresses LOS and NLOS operations within the 2 to 11GHz frequency range and provides some mobility support capabilities. It has almost 400 meters of radius with 20 Mbps of theoretical throughput. The 802.11g operates in the 2.4GHz licensed band and offers coverage of 70-80 meters with a theoretical throughput of 54Mbps.

The architecture of the upper layers is the reference one. On top of the IP layer, we find all the possible routing protocols and resources reservation protocols: *rsvp* (Resource ReSerVation Protocol), developed for supporting different QoS classes in IP applications; *ospf* (Open Shortest Path First), a routing protocol that determines the best path for routing IP traffic over a TCP/IP network; *eigrp* (Enhanced Interior Gateway Routing Protocol), *rip* (Routing Interchange Protocol), *isis* (Intermediate System - Intermediate System) and *igrp* (Internet Gateway Routing Protocol) that are distance vector routing protocols.

The transport layer is either TCP or UDP, and a process model called TPAL connects the transport layer to the application layer.

The UT implementation includes also the Mobile IP process and the *mac_mobility* entity, needed to perform inter-mode handover. The *mac_mobility* entity is the key element of the dual stack mobile

station: it continuously controls the performance of each mode and triggers the inter-mode handover if needed.

Now we present the performance assessment of inter-mode handover between Local Area and Wide Area WINNER modes: we show the impact of the two different combined WINNER triggers, that is the wireless trigger and the throughput based, focusing on intermode handover. We consider the scenario represented in Figure 4-31: a mobile station crosses the wide area cell passing through two different local area cells. The mobile station activates the wireless interfaces in the following order: LA – WA – LA - WA.

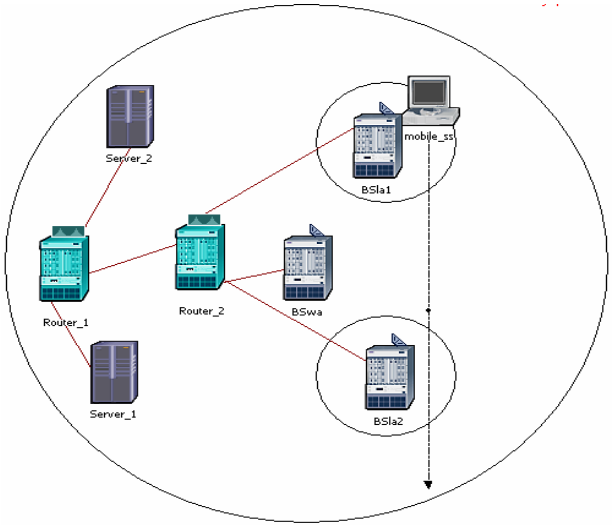

Figure 4-31 - Handover scenario with residual throughput criterion

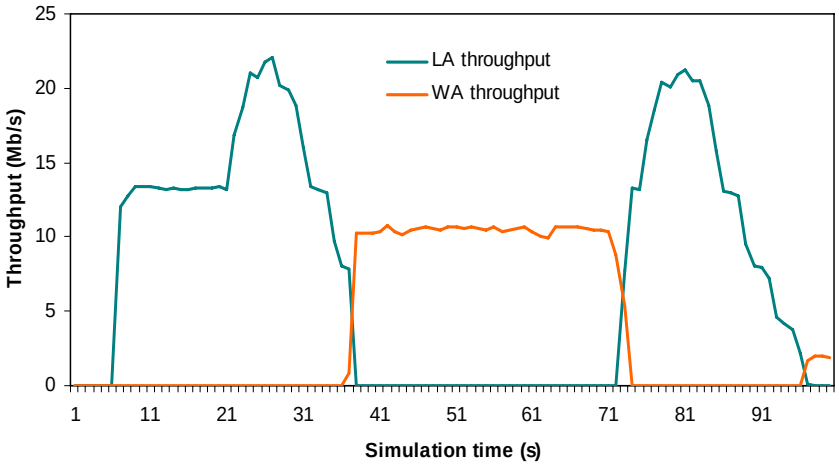

Figure 4-32 – Estimated throughput of mobile_ss

Figure 4-32 depicts the throughput achieved by the station mobile_ss when using LA or WA modes. The station, initially in the local area coverage, performs a handover to wide area when the throughput estimate on the wide area overcomes the one in the local area. Then, it enters the coverage of the second BSla and, when the LA throughput increases over the WA one, the second handover, from wide area to local area, is performed. Finally, the third handover from LA to WA is triggered by the wireless connectivity criterion. Indeed, the wide area throughput is lower than the local area throughput because the station is far away from the BSwa. For this reason the network performance trigger is not activated. In this case the wireless connectivity trigger lets maintain the connection and avoid packets loss.

4.9. Spectrum Technologies

In this section, we address the performance evaluation of Spectrum Resource Management (SRM) developed in WINNER, where we focus on the sharing capabilities of WINNER system in general and mainly with FSS (Fixed Satellite Service).

4.9.1. General overview of the Spectrum Resource Management (SRM)

It is envisioned that because of the scarce of spectrum, future mobile systems will have to coexist with other usage and share spectrum in an efficient manner. For that reason two mechanisms for spectrum management are being developed inside WINNER: Spectrum Sharing and Coexistence (SSC) and Flexible Spectrum Use (FSU). Both functions are not separated ones, but rather they have interrelations and common blocks to manage the spectrum usage inside WINNER: [WIN2D591][WIN2D592].

- SSC aims at facilitating the coexistence of WINNER with other systems in the same frequency band. The requirement of sharing the spectrum is without a doubt a constraining factor for the system concept, especially if it is assigned a secondary, non-prioritized position in accessing the spectrum. The expected gains from SSC will depend substantially on the properties of the involved systems and also on the regulatory environment. When considering the system requirements, especially Quality-of-Service (QoS) guarantees, operation in shared spectrum (from a secondary system position) can only be seen as a possibility for capacity enhancement.
- FSU considers the spectrum usage of different Radio Access networks (RAN) between the same RATs. The major advantages of FSU result from the enhanced spectral scalability of the system. Prior results from a simplified assessment model [HOOLI] showed that significant benefits can be expected from FSU between the RANs, even when the RANs carry partially correlated traffic patterns and knowing that FSU implementation involves considerable use of guard bands. The spectrum functionalities proposed will lead to a better utilization of the spectrum throughout multi-operator solutions, therefore increasing the availability of the spectrum.

The spectrum functionalities blocks are presented in **Figure 4-33**. .

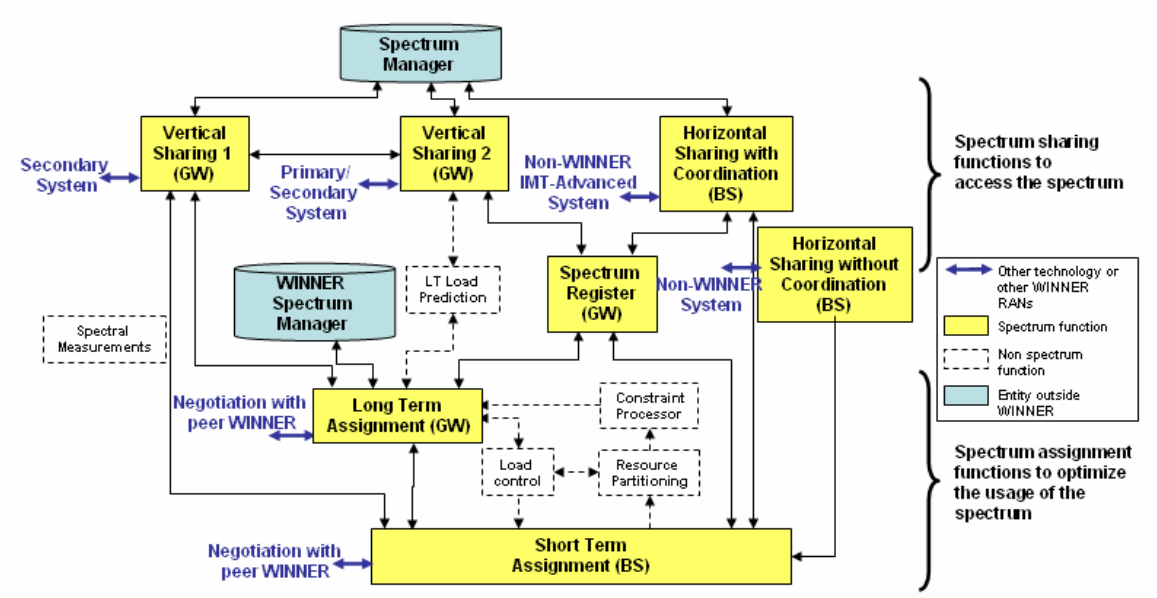

Figure 4-33 - Illustration of the interactivity between the spectrum sharing and spectrum assignment functions in the WINNER concept

In general, spectrum functions consist of concurrently triggered procedures. A normal spectrum control procedure (e.g. actualization of a given resource set measurement collection, etc.) is the result of several individual action calls.

The **general functionalities** common to both SSC and FSU (**Figure 4-33**) that are needed for the spectrum management are:

- Spectrum Manager. It is responsible for the overall usage of the spectrum in coexistence with non-WINNER RATs. It is a policy and rules maker so that peer to peer negotiation between WINNER and non-WINNER RANs follows the same rules. It resides outside the WINNER system.
- WINNER Spectrum Manager. It manages the usage of the spectrum within WINNER RANs only. It is a policy rules maker so that peer to peer negotiation between the proposed system RANs follows the same rules.
- Spectrum Register. It conveys information on exclusion zones, availability of spectrum from spectrum sharing functions to the spectrum assignment functions within WINNER's RAN. Each GW has its own spectrum register. The information in the register is dynamically updated. The introduction of the register is motivated by SSC with FSS, i.e. related exclusion zones may be large.

The main functions needed for **Spectrum Sharing and Coexistence** are:

- Vertical Sharing 1 (VS1). WINNER system has the access to the spectrum and it may assist a secondary system by sharing its spectrum resources (primary or not) when they are not needed.
- Vertical Sharing 2 (VS2). If WINNER system has a secondary access to the spectrum, it has to implement mechanisms not to interfere the primary system. For that purpose, considerable knowledge about the deployed primary system may be required. This knowledge can be obtained from two manners: In a blind mode, the proposed system would require information from a third party (i.e. central database maintained by regulator or another authorized entity) or in the second manner, the secondary system can negotiate with the primary system with regards to the operational characteristics and the amount of interference acceptable for the primary system. It is in general the task of VS2 to gather enough knowledge about the primary system.

  Note that VS2 does not preclude VS1, because though WINNER could be a secondary system and at the same time it could assist other system to use the spectrum.
- Horizontal Sharing with Coordination (HwC). WINNER and other system (i.e. other IMT-Advanced system RATs) have the same priority in access spectrum, and they coordinate their spectrum access based on a set of predefined rules (SSC rules) that all the involved systems are submitted to.
- Horizontal Sharing without Coordination (HwoC). Same as before but for the case that there are no possibilities of coordination (e.g. in licensed exempt RLAN band within 5GHz). Each system needs to come up with its own methods of sensing of spectrum holes or spectrum opportunity.

For **Flexible Spectrum Use** the main functionalities are:

- Long Term Spectrum Assignment: The function coordinates and negotiates the spectrum assignments between multiple WINNER RANs for large geographical areas (this function resides inside a GW). It takes into account the average traffic demand and predictions. The spectrum assignments are updated periodically at a slow rate, that is, in time frame of several tens of minutes and above.
- Short Term Spectrum Assignment: On the other hand, this function controls the short-term and local, i.e. cell-specific, variations of the large-scale spectrum assignments. Hence, it enables faster adaptation to the local traffic load variations and geographically more accurate spectrum assignments than the LT assignment. The assignments are performed in the time scale of several super-frames, i.e. 100 ms to several minutes. The ST assignment requests spectrum resources from other RANs after being triggered by the LT assignment or by preventive load control.

4.9.2. WINNER Sharing with FSS

Fixed Satellite Service has been identified due to its spectrum allocations and technical characteristics as one good candidate for sharing spectrum with [WIN2D592] [WIN2D5103], and this possibility is being studied inside the ITU-R during preparatory work for WRC-07, in accordance with (Resolution 228 (Rev.WRC-03). The frequency bands 3.4-4.2 and 4.4-4.9 GHz have been considered as two of the candidate bands for the future development of the terrestrial component of IMT 2000 and IMT-Advanced systems. The former is fully allocated to FSS, and the portion 4.5 to 4.8 GHz from the latter.

For a co-existence between FSS and WINNER, it is needed to guarantee that no harmful interference to the FSS systems will be caused. The techniques to mitigate the interference are:

- Exclusion zones around the FSS earth Station. The magnitude of the required protection distance is very dependent of each site, such as local conditions, terrain profile, parameters of the networks and the deployment of the two services.

  WINNER will have to know the location, frequency usage, working hours, direction and movement (in case of non geostationary satellites) of the antennas, etc. of the FSS ES. For this purpose, a central data base can be used (managed by the Spectrum Manager). In this case FSS ES operation has to be declared to the local administration. Another possibility is the use of beacon signals that will be transmitted by FSS (in a different frequency of operation) to assist WINNER in knowing the relevant parameters. In this way the working hours, path loss and direction can be easily measured.

  Without any mitigation technique and based on the worst assumptions of system parameters and terrain profile, these distances can range from less than a kilometre to more than a hundred kilometres. When employing other mitigation techniques (see bellow), these distances are significantly improved and are reduced to 0.05km in some cases.

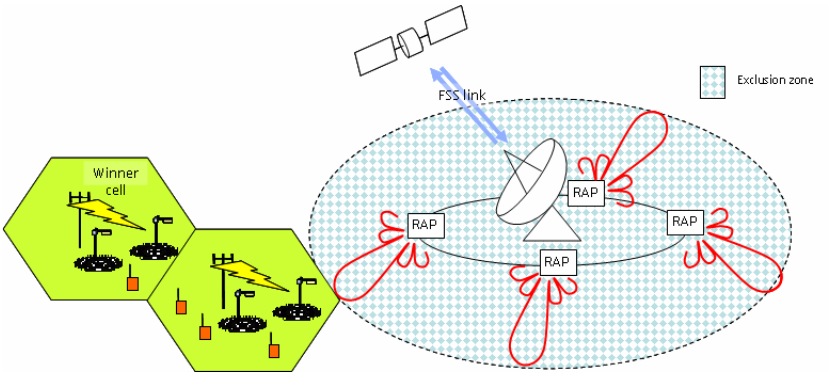

Figure 4-34 - Illustration of a WA deployment when sharing the spectrum with FSS

- Multiantenna technologies are helpful to prevent the BS from transmitting signals in the direction which would create a source of potential interference. In [WIN2D341] is described the Spatial-Temporal processing in WINNER. The envisaged multiantenna solutions rely either on sector-wise power adjustment (sectorized cells) or beamforming capabilities.

In countries where FSS usage is extensive and their locations or characteristics cannot be determined by a reasonable effort, band segmentation is a good solution. In many cases FSS Earth Stations use only part of the entire band. So the remaining frequency can be use for WINNER that due to the FSU capabilities can transmit only in the non-harmful band in the surroundings of the FSS ES.

In [WIN2D592] a numerical tool is developed for calculating the optimum power that can be assigned to every "chunk frequency" in all the BSs closed to a FSS ES,. This tool considers as an input, the long-term propagation (path-loss) between BS and FSS of a real environment in a scenario with multiple BS and multiple FSS ES. The output is the combination of maximum powers emitted by a set of BS's surrounding the FSS ES in order to maximize the throughput. The combination of powers is constrained not to exceed the aggregate maximum interference level at FSS earth stations. Though a solution can be obtained always by numerical methods, (e.g. the constrained non-linear optimization libraries built-in in Matlab such as "fmincon"), this tool uses a gradient-search–based algorithm.

4.9.2.1. Hard exclusion zones calculation

This section summarized the results of spectrum sharing studies performed in [WIN2D5103] and the improvements in [WIN2D5101], between WINNER and FSS systems in the candidate bands of 3.4 to 4.2 and 4.5 to 4.8 GHz. The studies cover both co-channel and adjacent band scenarios. The work is based on WINNER system characteristics and sharing related technical parameters, ITU agreed sharing parameters for a generic IMT-Advanced technology and FSS parameters contained in ITU-R Recommendations. The simulations have partly been conducted with an updated version of CEPT tool SEAMCAT 3.

Typical FSS parameters consider for the simulation

The following table summarizes the FSS earth station parameters considered.

Table 4.9-1: Typical downlink FSS parameters considered in the 4 GHz band

Parameter	Typical value						
Range of operating frequencies	3 400-4 200 MHz, 4 500-4 800 MHz						
Earth station off-axis gain towards the local horizon (dBi)[1]	Elev. angle[2]	5°	10°	20°	30°	48°	>85°
	Off-axis gain	14.5	7.0	–0.5	–4.9	–10	0
Reception bandwidth	50 MHz						
Receiving system noise temperature / Noise floor	100 K / –101.6 dBm						
Antenna height, / diameter	15 m / 5.5m						
Antenna peak gain	44.4 dBi						
Antenna reference pattern [10]	Recommendation ITU-R S.465 (up to 85°)						

[1] The values were derived by assuming a local horizon at 0° of elevation.

[2] 5° is considered as the minimum operational elevation angle.

Two interference criteria limits to FSS have been considered [ITU-R S.1432]: I/N=-12.2 dB and I/N=-20dB, considering N as the noise received by FSS earth station.

For propagation path loss the recommendation ITU-R P.452[5] ha been used in a flat terrain profile. This profile comes down to a free space model below 40 km (for ranges above 40 km, Earth radius impacts the path loss). A terrain model will reduce the protection distances due to the presence of obstacles.

WINNER parameters considered for the simulation

The following parameters were considered for simulations. They agree within the generic IMT-Advanced sharing parameters defined in the ITU-R, to represent IMT-Advanced technologies. (Doc. 8F/899, Attachment 5.20).

Table 4-1: Parameters for WINNER simulations

SUBURBAN MACRO CELL		
Bandwidth (MHz)	50 MHz	
	Base station (BS)	**User Terminal (UT)**
Antenna type (Tx/Rx) (the gain is assumed to be flat within one sector)	Tri-Sector	omnidirectional
Thermal noise floor including noise figure (dBm)	–92	–88
Tx output power(dBm)	43	24
Antenna gain (dBi)	20	0
Antenna down tilt (°)	2	0
Antenna height (m)	30	1.5
Intersite distance (separation	5	Uniform distributed in a

[5] This model has been implemented into SEAMCAT 3 tool by WINNER.

between BS) (km)		circle of 5km diameter

Results

The following tables show the different exclusion distances calculated for a WINNER system. These have been calculated to comply with the interference threshold of [ITU-R S.1432]. For the simulation, a single BS was first targeted, with different FSS ES elevation angles. The tables show the minimum and maximum distances obtained for these angles.

In the aggregate case, the effect of all the BSs is taken into account. A certain number of BSs have been uniformly (equi-spaced) located on a circle around the FSS earth station The radius is the result of the required protection distance meeting the interference criterion. The number of BSs is assessed according to the protection distance and the BS intersite distance range.

Finally the simulation was running considering that BS and FSS ES is working in adjacent channels. In this case the results logically are better.

Table 4.9-2: Exclusion distances between BS and FSS ES to avoid harmful interference

Macro (WA for WINNER, urban for FSS)		**Protection distance (km) –12.2 dB criterion**		**Protection distance (km) –20 dB criterion**	
		Min	**Max**	**Min**	**Max**
co-channel	**Single BS**	46	59	50	66
	Aggregate BS	52	61	56	74
adjacent channel	**Single BS**	3	31	6	41
	Aggregate BS	8	32	18	41

The interference caused by UTs is also simulated. The results are given considering the mean value of I/N achieved on earth station when WINNER UTs are randomly distributed around the BS coverage. The random distribution is run with a mobile density range from 10 to 50 per km².

Table 4.9-3: Interference caused for UT to FSS in co-channel interference

Density of MS per km²	**10**	**20**	**30**	**40**	**50**
I/N (dB) co-channel	–20,8	–19,7	–19,1	–18,8	–18,7
I/N (dB) adjacent channel	–23,8	–22,7	–22,3	–22,0	–21,8

In all the cases, I/N does not exceed –18.7 dB showing that no protection distance is required with regards to –12.2 dB criterion.

In [WIN2D5101] more mitigation techniques are considered, **Figure 4-35** shows the differences in the protection distance when considering disabling one of the three sectors in the tri-sectored configuration that points towards the FSS earth station, in the BS closer to the FSS ES, with the –12.2 dB criterion. The protection distance is reduced quite a lot in the worst cases of elevation angle.

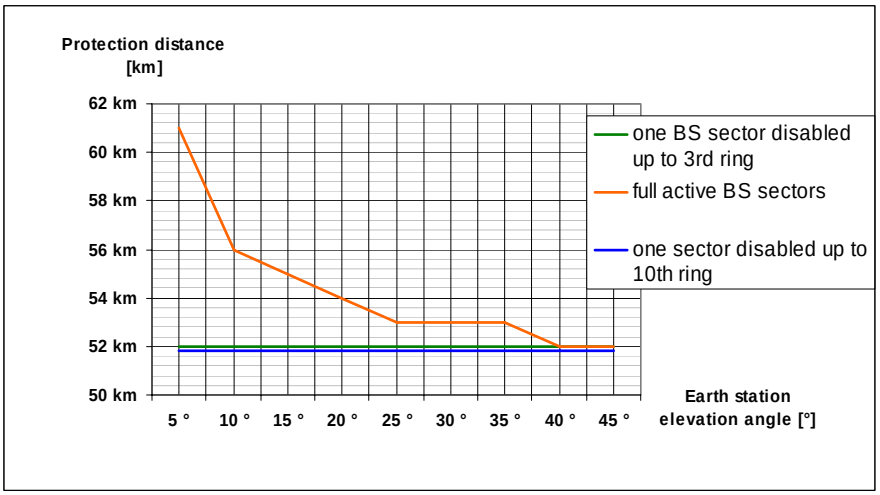

Figure 4-35 – Protection distance where one of the tri-sectored nodes are disabled

Other studies have been conducted in a real terrain profile (taken the example of the earth station in "Bercenay-en-Othe" that is located in a rural area in France). In this scenario the protection distance varies from 4 to 23 km (up to 83% compared with normal full active sector).

The final conclusion is that WINNER can share the FSS frequency band using adjacent channels or exclusion distances that have been calculated for flat terrain profiles. When taking into account the terrain profiles in a concrete deployment the exclusion distances are much shorter.

4.10. End-to-end performance degradation due to link and system level procedures

To simplify analysis and presentation of performance evaluation, models had to be used and simplifying assumptions had to be made,. In the following section, the impact of “real-world-effects” of link-level procedures and hardware effects on the performance is assessed. The results presented are an important guideline for the reference design [WIND21314], were the right trade-off points between performance, complexity, overhead and cost had to be found.

In particular, the following effects are studied:

- Channel estimation errors in SISO and MIMO links
- Timing and synchronization errors
- Hardware impairment effects
- Network synchronization accuracy
- Feedback errors such as SNR mismatch

4.10.1. Channel Estimation Errors

Receivers and adaptive transmitters need accurate estimates of channel state information (CSI) for their detection, equalization, decoding, interference mitigation and/or resource allocation operations. In this section we describe the effect on receiver performance of imperfect CSI derived from pilot-aided channel estimation algorithms, combined with equalization and interference rejection combining (IRC) using the minimum mean squared error (MMSE) criterion. The results are compared with those for perfect CSI. The effect on error rate performance of channel estimation errors, modelled as Gaussian random variables, was derived and discussed in [WIN2D233]. These models are most accurate at low signal to noise ratios, where the effects of additive noise dominates over interpolation errors. For higher SNR and for iterative channel estimation methods used in the presence of significant Doppler, we must resort to simulated error rate performance for the various channel estimation schemes and modulation, multiple access and coding methods. The channel estimation schemes discussed and evaluated here are applicable to MA and LA scenarios as well as to the WA scenario. Differences among scenarios, duplexing schemes and frequency-adaptive or –non-adaptive schemes are mainly due to corresponding differences in pilot arrangements. Most of the performance results shown here are for FDD WA non-frequency-adaptive and full-band schemes. Pilot arrangements for other modes are described in [WIN2D233].

This section displays simulation results, extracted from ,[WIN2D233], for equalization and channel estimation schemes, and their penalties relative to the case of perfect channel state information, for the wide area FDD scenario. Full-band (40 MHz, 40 Mbaud))[6] and 1.25 Mbaud IFDMA, B-EFDMA and B-IFDMA are shown. Two channel estimation approaches are used: (1) a non-iterative purely pilot-aided approach using Wiener interpolation in the full band cases case and the single pilot per block without interpolation in the case of B-EFDMA, B-IFDMA and IFDMA; (2) a soft-decision iterative approach (DFICE) to supplement the pilot-aided estimation, using soft decoder outputs. In addition, the improvement available from estimating channel parameters over several successive frames is also shown for full-band DFT-precoded OFDM, B-IFDMA and IFDMA. OFDM and B-EFDMA systems used linear equalization and interference rejection (similar to the IRC schemes assessed in [WIN2D473]) and CSI-aware decoding. DFT-precoded OFDM, IFDMA and B-IFDMA systems used iterative block decision feedback equalization (IBDFE), described in Chapter 4 of [WIN2D233]. Table 4.10-1 displays the approximate complexity of the pilot interpolation, IBDFE, DFICE and least squares (LS) algorithms. Fehler! Verweisquelle konnte nicht gefunden werden. displays the simulation parameters, and **Table 4.10-3** displays the required SNR to achieve a 10^{-2} frame error rate, and also the SNR degradation between ideal CSI and non-ideal CSI with the various channel estimation schemes for SISO (single input single output) links with no interference. While SISO links are somewhat peripheral to the WINNER reference design, they are included here for comparison with the channel estimation performance of of SDMA and MIMO links, and also because SISO may play a role for relay-enhanced cells. **Table 4.10-3** also shows the pilot overhead percentage for each scheme.

As indicated in the table, B-IFDMA, B-EFDMA and IFDMA require significantly higher pilot overhead, and exhibit higher SNR degradation due to channel estimation errors than do full-band OFDM and DFT-precoded OFDM. This is mainly due to the reduced opportunity to interpolate pilot estimates and exploit correlation in the frequency domain. There is in fact no frequency domain interpolation in the B-EFDMA, B-IFDMA and IFDMA cases, since for B-(E&I)FDMA there is only one pilot per 4X3 block, and blocks are separated in frequency by more than the correlation bandwidth. The use of larger block sizes (e.g. 8X6), with more pilots, has recently been proposed for B-EFDMA and B-IFDMA, and should give more scope for interpolation between pilot locations in frequency and time, while keeping pilot overhead reasonable. Results for both 4X3 and 8X6 blocks are shown as well.

Table 4.10-3 also shows that iterative channel estimation can yield significant improvement relative to non-iterative estimation, and furthermore that estimation over multiple frames yields 0.5 to 1 dB improvement, at least for the moderate vehicle speed of 50 kmh.

Table 4.10-1 Complexity, per ICE iteration and per in-cell transmitted signal, of soft decision iterative block decision feedback equalization (SD-IBDFE) equalization, pilot-based channel estimation interpolation, iterative channel estimation (DFICE) and least squares (LS) processing

Frequency Domain Channel Transfer Function	$M\lfloor\log_2(M)\rfloor$
Initial CE/Interpolation	$(.)^{-1}{}_{Df}+(.)^{-1}{}_{Dt}+M+M\lfloor(.)^{-1}_{M_R}+1\rfloor$
SD-IBDFE	$I_E M\lfloor(.)^{-1}_{M_R}+2\log_2(M)+3\rfloor+M$
LS Forward Processing	$M\lfloor(.)^{-1}_{M_R}+2+\log_2(M)\rfloor$
DFICE processing	$M\lfloor 1+\log_2(M)\rfloor$

Notation: M=OFDM symbol length

M_R=number of receive antennas

$(.)^{-1}_{M_R}$ matrix inversion (matrix size M_R)

I_F=number of SD-IBDFE iterations (typically 2)

Df=pilot spacing

[6] The WINNER reference FDD bandwidth is 45 MHz. Differences in channel estimation performance from this bandwidth are minor.

Table 4.10-2 Parameters for single input – single output channel estimation simulations for wide area FDD scenario

Modulation Scheme	QPSK
Code, decoder	Conv. rate ½ const. length 7, Viterbi decoder
Interleaving	Random
Carrier frequency	3.7GHz
Signal BW	40 MHz
Sub-Carrier spacing	39.0625KHz
Used sub-carriers	1024
Sampling rate	80 MHz
Number of OFDM symbols per chunk	12
Block configuration for B-EFDMA and B-IFDMA	(4 subcarriers) X (3 OFDM symbols) per block. Blocks spaced at 32-subcarrier intervals in frequency
Number of pilots per chunk per OFDM symbol	4 for full-band 2 for IFDMA, 1 for B-EFDMA and B-IFDMA
OFDM symbols containing pilots	1st and 12th OFDM symbols for full-band and IFDMA, 2nd for 4X3 B-EFDMA and B-IFDMA
Prior information available to interpolator	Channel response<CP length Vehicle speed<100 kph
Number of receiving elements	M_R=1
Equalization scheme	IBDFE for DFT-precoded OFDM, linear for OFDM
DFICE Iterations	2 or more
Channel, user terminal speed	C2, 50 kph

Table 4.10-3 SNR and SNR degradation (with respect to perfect CSI) for frame error rate = 10^{-2} for noniterative and iterative channel estimation schemes (wide area scenario)

Pilot Schemes	**SNR for ideal CSI (dB) for 10^{-2} frame error rate**	**SNR degradation due to channel estimation (dB)**		
		Non-iterative channel estimation **Wiener pilot** **Interpolation** **(W2X1D)**		**Iterative channel estimation with decoding in iteration loop**
OFDM –full band **(4.1% pilot overhead)**	10.5	1.5		0.2
DFT-precoded OFDM-full band **(4.1% pilot overhead)**	9.4	**1-frame channel est.**	2.1	0.4
		4-frame channel est.	1.5	0.0
B-EFDMA **(4X3 blocks; 32-**	8.2	4.0		2.8

subcarrier spacing ; 8.3% pilot overhead)				
B-IFDMA (4X3 blocks; 32-subcarrier spacing; 8.3% pilot overhead)	8.4	**1-frame channel est.**	4.3	3.0
		4-frame channel est.	3.6	2.4
IFDMA (32-subcarrier spacing; 16.7% pilot overhead)	8.5	**1-frame channel est.**	2.8	1.5
		4-frame channel est.	1.9	1.0

In SDMA and MIMO scenarios, there is interference from in-cell co-channel users (ICUs) due to the sharing of spectrum among different data streams. In this scenario orthogonal pilot patterns are used in order to avoid interference between the pilot signals from different SDMA streams. Pilot overhead increases as the number of individual streams increases. When slow power control is employed in the uplink, ICUs can be expected to be received with equal average powers.

In SDMA and MIMO scenarios there may also be interference from out-of-cell interferers (OCIs). OCIs' average received powers at a given base station will depend on their propagation paths to their own base stations. In-cell users are assigned orthogonal pilots; thus there is no in-cell interference to pilots. However to avoid excessive pilot overhead, the same pilots may be assigned to users in other cells; thus there may be pilot interference from adjacent cells.

Inter-cell pilot interference can be minimized by adopting a frequency reuse partitioning strategy, in which user terminals with low path loss to their base stations, but which are in different cells, have frequency reuse of one, while user terminals experiencing higher path loss have a higher frequency reuse factor, and thus experience out of cell interference only from more distant cells [WIN2D471].. A representative frequency reuse partitioning scenario is presented and analyzed in [[WIN2D233], in which the frequency reuse factors for terminals within and beyond 70% of the cell radius are 1 and 3, respectively. It is shown that based on a WINNER wide area propagation model, average received power from each OCI in this deployment scenario is at least 15 dB below that of in-cell users. Other techniques may be employed to reduce out of cell interference, such as dynamic channel allocation and scheduling among base stations [WIN2D471],[WIN2D742], [WIN2D473]. For evaluation of channel estimation performance for SDMA with out of cell interference, we assume that one or more of these techniques have been applied, so that uplink out of cell interferer signals arrive at a victim base station with an average received power of -15 dB relative to the average power of each in-cell received signal.

Table 4.10-4 is based on simulations of an uplink DFT-precoded SDMA system with 2 in-cell user terminals sharing a common channel, and (in all but the first row of the table) 4 out-of-cell interferers (OCIs), each with an average received power 15 dB below that of each in-cell user's average received power. The base station has 4 receiving antennas (M_R=4). Independently fading C2 channel models with 50 kph Doppler are assumed between each transmitting/receiving antenna pair. The base station's MMSE-based receiver uses the IBDFE equalization algorithm, for the multi-antenna, multi-user case, described in Section 4.4 of [WIN2D233]. An exception is in the third row of the table, where a rate ½ regular (3,6) LDPC code with 4608 block length, and turbo equalization, instead of IBDFE, is used [SF06], [NLF07]. As in the SISO cases, non-iterative channel estimation based on interpolation of frequency-multiplexed pilots, is evaluated, as is iterative channel estimation. Both the pilot-based and iterative channel estimation schemes estimate only the in-cell users' channels, while OCIs are ignored. The last column in the table shows results for a least squares (LS) decision directed algorithm (described in Section 4.4 of [WIN2D233]), which is used in addition to pilot interpolation and iterative ICU estimation. This LS algorithm is aimed at suppressing OCI interference without having to explicitly estimate OCI channels (essentially, the algorithm estimates the out-of-cell interference autocorrelation matrix, instead of out-of-cell interferers' channels). Full-band DFT-precoded OFDM uses 4 orthogonal pilots per chunk per in-cell user. **Table 4.10-4** also shows required SNR and SNR degradation for B-

IFDMA with 4X3 blocks and for 8X6 blocks. For the 4X3 case, there are two pilots per block per in-cell user; thus the pilot overhead in this case is 33.3%.. For the 8X6 case, there are 4 pilots per block per user; the corresponding total pilot overhead is 16.6%.

Table 4.10-4 One-Frame Estimation for uplink DFT-precoded OFDM with 2X4 SDMA

MA schemes ↓	SNR for ideal CSI (dB) for 10^{-2} frame error rate	SNR degradation due to channel estimation (dB)		
		Non-iterative channel estimation	Iterative channel estimation	Iterative channel estimation plus least squares
Full-band DFT-precoded OFDM No OCIs 8.3% pilot overhead	0.3	3.9	3.3	2.0
Full-band DFT-precoded OFDM 4 OCIs, each at -15 dB 8.3% pilot overhead	1.3	5.0	3.7	2.2
Full-band DFT-precoded OFDM with turbo equalization and rate ½ LDPC codes 4 OCIs, each at -15 dB 8.3% pilot overhead	-0.4	4.1	3.4	2.7
B-IFDMA with 4X3 blocks, 32-subcarrier spacing between blocks. 4 OCIs, each at -15 dB 33.3% pilot overhead	-1.0	8.5	6.0	6.0
B-IFDMA with 8X6 blocks, 32-subcarrier spacing between blocks. 4 OCIs, each at -15 dB 16.6% pilot overhead	0.3	6.5	5.1	4.4

Note that "SNR" is signal to noise ratio per receive antenna.

As seen in the table, non-ideal channel estimation causes significant SNR degradation relative to the ideal CSI case, largely due to the OCI interference to the ICU pilots. This is apparent by noting that the SNR degradations in **Table 4.10-4** are significantly worse than those for SISO. This degradation is reduced by iterative channel estimation, and is further reduced for the full-band case by the application of least-squares processing using receiver hard decisions, to suppress OCI interference.

While the FER performance of B-IFDMA and B-EFDMA with ideal CSI is much better than that of the full band system (due to the enhanced frequency diversity and smaller number of data symbols per frame of the B-IFDMA and B-EFDMA systems), the SNR degradation for non-ideal CSI is significantly larger than that for full-band transmission, even when pilot overhead is about 33%. The use of larger B-IFDMA blocks, with more pilots per block, significantly improves channel estimation accuracy and enables reduced pilot overhead. For relatively low bit rate data streams, B-IFDMA and B-EFDMA, in spite of

their less efficient channel estimation properties, exhibit lower frame error rates than L-FDMA with the same overall bit rate. L-FDMA corresponds to B-IFDMA or B-EFDMA where the blocks are contiguous, instead of being separated in frequency, so the band of frequencies spanned by a L-FDMA signal is much smaller. Separate comparisons of L-FDMA and B-IFDMA (not shown here) indicated the superiority of B-IFDMA for coded QPSK symbol rates up to 5 Mbaud.

Least squares processing produces no benefit in the 4X3 B-IFDMA case, since the number of OFDM symbols per block (3) is inadequate for the least squares averaging. While the 8X6 B-IFDMA case has 1.3 dB higher required SNR for perfect CSI (due to its slightly diminished frequency diversity), its SNR degradation for non-perfect CSI with ICE and least squares processing is 1.6 dB less than that for the 4X3 case. The main reason for this is the use of 4, instead of 2 pilots in the 8X6 block, allowing better interpolation from pilot estimates, while also reducing overhead. The resulting gain in channel estimation accuracy more than compensates for the reduced diversity of the 8X6 case. The required SNR in this case is 4.7 dB, while for 4X3 it is 5.0 dB. Note that the LDPC/turbo equalization combination reduces required SNR by roughly 1.5 dB, but that the SNR degradation due to non-ideal CSI remains roughly the same.

ICE can be further aided by application of genetic algorithms (GA) as described in [WIN2D233]. Channel estimation results for a 2X2 SDMA OFDM system with GA-assisted ICE are shown in [WIN2D233] for the metropolitan area scenario.

4.10.2. Timing and Synchronization Errors

Link level synchronisation consists of two stages: first when coarse timing synchronisation and fractional frequency offset estimation are performed, and second when fine timing synchronisation and integer frequency offset estimation are performed. Algorithms are described in[WIN2D233].

Inter-carrier interference (ICI) occurs when the frequency synchronisation algorithms are not able to estimate the exact value of the frequency offset caused by the Doppler shift and the mismatch between frequencies of the transmit and receive oscillators. The SNR degradation due to ICI versus normalised frequency synchronisation error is presented in Figure 4-36[7].

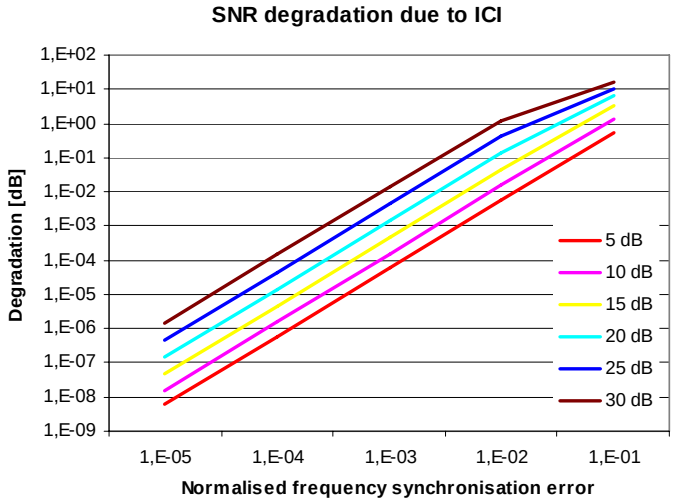

Figure 4-36 SNR degradation due to frequency synchronisation error

The ICI depends on both SNR and frequency synchronisation error. The maximum values of frequency offset estimation error normalised by subcarrier spacing are shown in Table 4.10-5. Comparison of Figure 4-36 and Table 4.10-5 reveals that in all scenarios considered in Table 4.10-5 SNR degradation due to ICI is lower than 0.1 dB.

[7] Note that the vertical axis showing the SNR degradation in dB has a logarithmic scale for better visualisation of the results.

Table 4.10-5 Frequency offset estimation errors - maximum values

Transmission mode	Channel mode	SNR [db]							
		5	7.5	10	12.5	15	17.5	20	22.5
TDD	A1 LOS	9.34e-3	7,04e-3	5.23e-3	3.84e-3	3.09e-3	2.3e-3	1.73e-3	1.32e-3
TDD	A1 NLOS	9.13e-3	6.83e-3	4.96e-3	3.54e-3	2.95e-3	2.23e-3	1.65e-3	1.25e-3
TDD	B1 LOS	8.79e-3	6.89e-3	5.46e-3	4.55e-3	3.99e-3	3.59e-3	3.31e-3	3.13e-3
TDD	B1 NLOS	7.72e-3	6.08e-3	4.59e-3	3.59e-3	2.91e-3	2.3e-3	1.88e-3	1.63e-3
FDD	C2 NLOS	9.39e-3	6.93e-3	5.26e-3	4.0e-3	3.11e-3	2.55e-3	2.03e-3	1.67e-3

- Inter-block interference (IBI) occurs only if timing synchronization error is excessively large, or the channel impulse response is longer then the cyclic prefix. For the WINNER case only the first scenario takes place. The IBI-free ranges for different transmission modes and channel models are presented in Table 4.10-6. The channel length counted in samples is computed for the transmitted signal sampling time.

Table 4.10-6 Timing synchronisation errors not causing IBI

•Transmission mode	•Prefix length (samples)	•Channel model	•Channel length (ns)	•Channel length (samples)	•IBI-free range
TDD	128	A1 LOS	75 ns	8	<-120, 0>
TDD	128	A1 NLOS	135 ns	14	<-114, 0>
TDD	128	B1 LOS	105 ns	11	<-117, 0>
TDD	128	B1 NLOS	485 ns	49	<-79, 0>
FDD	256	C2 NLOS	1420 ns	117	<-139, 0>

For the given system and channel parameters if the timing synchronisation error is within the above range then the SNR degradation is equal to 0 dB. Otherwise, the SNR degradation is greater then 0 dB and its value depends on the timing synchronisation error and on the SNR of the desired signal. The relationship between the SNR degradation and the timing synchronisation error is shown for different WINNER channel types in Appendix E of.[WIN2D233].

In general, both phenomena, i.e., ICI and IBI can take place jointly as a result of timing and frequency synchronisation errors occurring simultaneously. The results of the estimated SNR degradation are presented for different WINNER channel types in Appendix E of.[WIN2D233].

Complexity:

Coarse timing and fractional frequency offset synchronisation requires 17 real multiplications, 5 real additions and one complex division per received signal sample. Furthermore IFFT-512 and FFT-512 are computed after coarse timing synchronisation. Other computations are performed once, after successful coarse timing synchronisation and require 13000 real multiplications, 256 complex divisions and 4096 real additions.

Conclusions:

- Simulation results of the link level synchronisation, presented in Appendix F of [WIN2D233] showed that the error range of timing synchronisation is much less than IBI-free range (Table 4.10-6). Thus it can be assumed that the received signal will not be distracted by inter-block interference.
- Since the synchronisation of the fractional part of the frequency offset is not perfect, the inter-carrier interference will occur in all scenarios. Thus, assumed SNR of the received signal should be decreased by values read from Figure 4-36 or computed using formula (3.67) from Appendix F of [WIN2D233] However, as shown in Table 4.10-5, SNR degradation due to ICI is marginal

in all considered scenarios. For the purposes of link level synchronization an overhead of three OFDM symbols which are situated in preamble of the super-frame is induced.

4.10.3. Hardware Impairment Effects

Phase Noise

Phase noise causes inter-symbol interference in multi carrier systems, as well as common phase rotation. In single carrier systems it causes a slowly varying phase rotation to the data symbols. However, in both systems the impact of the phase noise can be estimated, tracked and compensated as given in [WIN2D233]. Table 4.10-7 shows performance results for iterative phase noise correction. The phase noise compensation algorithm for multi carrier systems is applicable for any pilot patterns and does not need any additional overhead. For the performance results given in the table the pilot pattern defined in [WIN1D210] was used. For the single carrier case the time-varying phase process can be tracked with a second order soft decision directed phase locked loop (PLL), which uses log likelihood ratio (LLR) information from a turbo equalizer. For both schemes (multi and single carrier) the complexity of the correction algorithm can be neglected compared to the decoding complexity.

The general performance of the proposed phase noise mitigation techniques do not differ very much among different channel models. For the sake of simplicity an urban channel model was used for single carrier system and a typical indoor channel model was used for multi carrier system. A high quality oscillator might have a phase noise determined by the VCO of -115dBc/Hz at 1MHz offset from the carrier, resulting in a two-side 3dB linewidth of 20Hz. If such a high quality oscillator and low modulation schemes are going to be used the impact of phase noise can easily be corrected without any significant SNR loss. This can be done using standard compensation algorithms, e.g. common phase error correction in multi carrier systems with the help of known pilots. However, in order to reduce the costs of hardware components or to allow higher order modulation schemes more complex phase noise mitigation algorithms have to be used as presented in [WIN2D233].. Applying the proposed algorithms, Table 4.10-7 delivers an insight in the maximum oscillator linewidths values where the compensation algorithms are still able to achieve a target block error rate of 1%.

Table 4.10-7 Iterative Phase Noise correction

	Channel Model	Modulation Scheme	Coding Scheme	Phase Noise two-side 3dB linewidth	SNR los @ 0.01 BLER after iterative compensation
Single Carrier	C 2	QPSK	LDPC Code	6.4kHz	~1.5dB
Multi Carrier	A1 NLOS (TDD)	QPSK	Memory 6 Convolution Code	195.3Hz	~1.5dB
		16-QAM		97.6Hz	~1.5dB

HPA Nonlinearities

Neighbouring desired and undesired user spectra may be received with large power variability due to differing path losses. Avoidance of adjacent channel interference then requires low transmitted power spectral sidelobes and rather stringent spectral masks. For example, allowable interference to adjacent-frequency receivers is usually specified in terms of maximum interference power at a certain distance and at a certain frequency offset from the interferer's carrier. Under typical transmitted power and path loss conditions, this may imply spectral masks with as much as 40 to 60 dB of out of band attenuation. A WINNER spectral mask scaled to fit current assumed wide area system bandwidth, is illustrated in the following figures. Control of power spectrum sidelobe levels to obey a spectral mask is normally achieved by an appropriate power backoff at the HPA input.backoff. Signal processing techniques to reduce the dynamic range of the transmitted waveform can also be used to reduce spectrum sidelobe levels, and have been discussed and evaluated in other WINNER reports and references therein.

Minimising the power backoff required for high power amplifiers is very important in terms of cost and battery recharging intervals, especially for mobile terminals. Large required backoff lowers amplifier

efficiency and increases the maximum output power required from the HPA, thus increasing its cost, and battery drain.

The minimum required power backoff depends on several factors:

- The distribution of the transmitted signals' amplitude; i.e. its dynamic range. A large dynamic range implies larger minimum to maximum amplitude swings and hence larger backoff to minimise distortion. A commonly used, but not necessarily very useful, criterion is "peak to average power ratio" (PAPR).
- The nonlinear input-output characteristic of the HPA. In our studies, we have used the Rapp model for amplitude to amplitude conversion, which is considered reasonably typical for solid state power amplifiers. The model has one parameter, p. A low value of p; e.g. p= 2, results in an input-output characteristic which has a visible nonlinearity below the saturated output. It may be typical of a moderate-cost HPA. A higher quality HPA, or one whose input-output characteristic below saturation is linearized by adaptive pre-distortion, has a higher value of p, such as p=10.
- The power spectrum mask to which the HPA output power spectrum must be confined. It is determined by consideration of allowed power leakage into adjacent users' spectral allocations. In this study we use the spectral mask that was derived for WINNER narrowband mobile terminal outputs , scaled to the used wide area signal bandwidths of 40 MHz and 10 MHz.

In general, different nonlinearity characteristics and spectral masks will change the absolute values of backoffs for different types of signals, but would not be expected to change the relative values.

Various OFDMA and DFT-precoded OFDMA signals transmitted through a Rapp model nonlinearity with p=2 and 10 were simulated, and their resulting average output power spectra were measured. Typical results are shown in the figures below. Each signal block is time-windowed with a raised cosine window after the IFFT operation. For each signal, the average power was adjusted by trial and error so that the power spectrum barely grazed the spectral mask. Then the difference between that average power and the saturated output power from the nonlinearity was the signal's required power backoff.

Figure 4-37 shows p=2 HPA output power spectra for full-band 16-QAM OFDM and DFT-precoded OFDM (serial modulation) for 40 MHz nominal bandwidth (50 MHz system bandwidth), Serial modulation requires nearly 2 dB less backoff to comply with the scaled WINNER spectral mask that is shown in the figure.

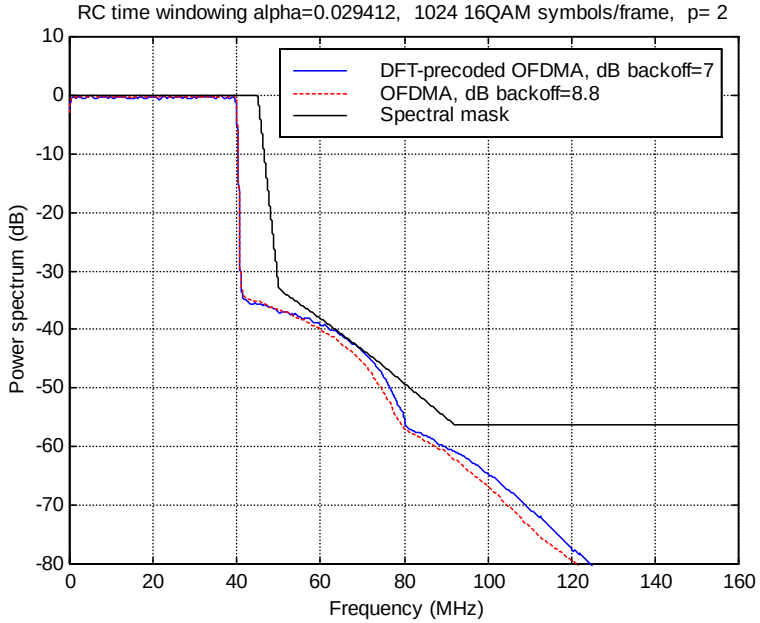

Figure 4-37 HPA output power spectra for full-band (40 MHz) 16-QAM OFDMA and DFT-precoded OFDMA signals. HPA has Rapp model nonlinearity with parameter p=2.

Required backoff is further reduced if the HPA has a nearly linear characteristic below saturation, as exemplified by the power spectra for p=10, shown in Figure 4-38. The backoffs for both signal formats are reduced by 1 dB. The p=10 characteristic produces flatter out of band radiation, but at very low levels.

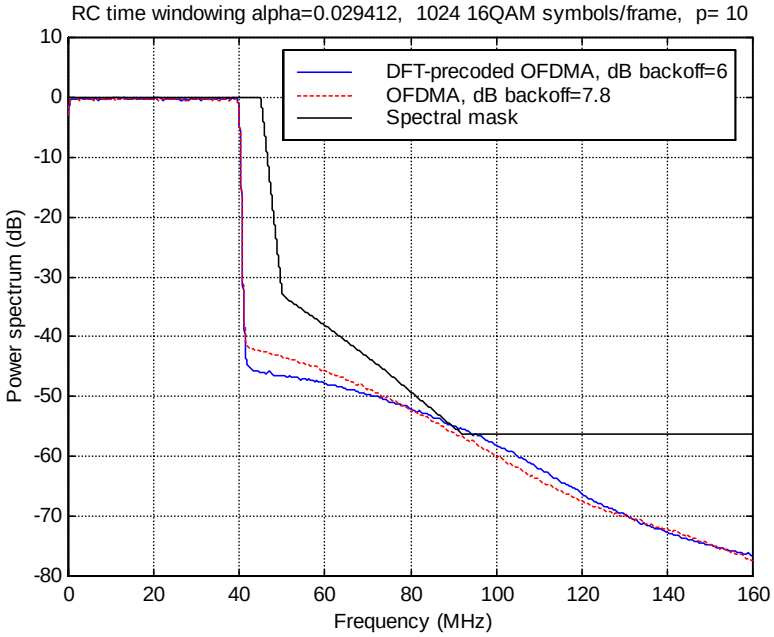

Figure 4-38 HPA output power spectra for full-band (40 MHz) 16-QAM OFDMA and DFT-precoded OFDMA signals. HPA has Rapp model nonlinearity with parameter p=10.

It is worth noting that for a typical spectral mask such as the scaled WINNER mask shown in these figures, it is mainly the out of band radiation, rather than nonlinear distortion of the transmitted signal, that determines the required power backoff. For example, for Figure 4-37 and subsequent figures, the in-band distortion of the transmitted signals is at least 30 to 35 dB below the signal power, and total out of band distortion is at least 35 to 40 dB below the signal power. This statement should be modified somewhat for high level modulation, such as 64- and 256-QAM. Figure 4-39 shows HPA output signal constellations for 256-QAM signals emerging from a p=10 HPA,. The signal to nonlinear distortion ratios are 37.3 and 38.4 dB, for backoffs of 7.9 dB and 6.1 dB, for OFDM and DFT-precoded OFDM, respectively.

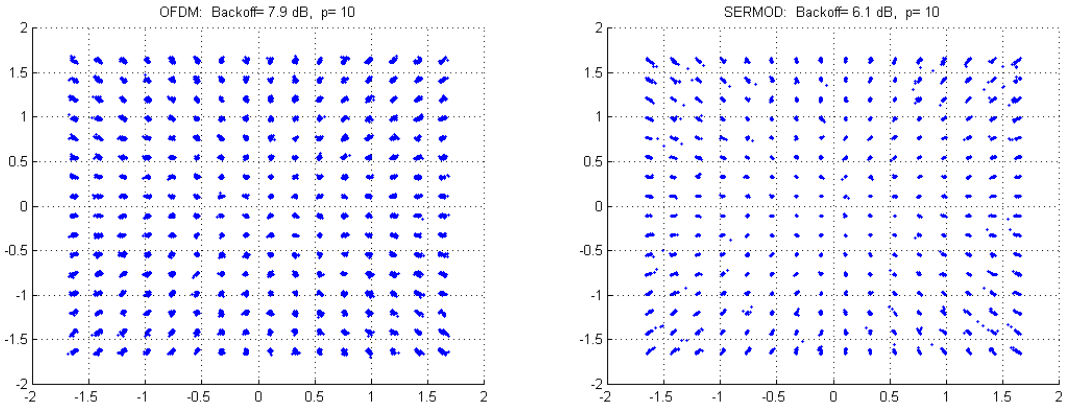

Figure 4-39 Signal constellations for 256-QAM full-band (40 MHz) OFDM and DFT-precoded OFDM (labelled "SERMOD") at the output of a p=10 Rapp model HPA. The signal to nonlinear distortion ratios are 37.3 and 38.4 dB for OFDM and DFT-precoded OFDM, respectively.

The backoff requirements for QPSK B-EFDMA and B-IFDMA signals with a 4-subcarrier block width, with 32 blocks spaced at 32 subcarrier intervals, are shown in.Figure 4-40. Although the B-IFDMA signal

waveform is not exactly equivalent to a single carrier waveform, its required backoff is close to that of the full-bandwidth case. IFDMA has similar backoff properties to B-IFDMA and full-band DFT-precoded OFDM.

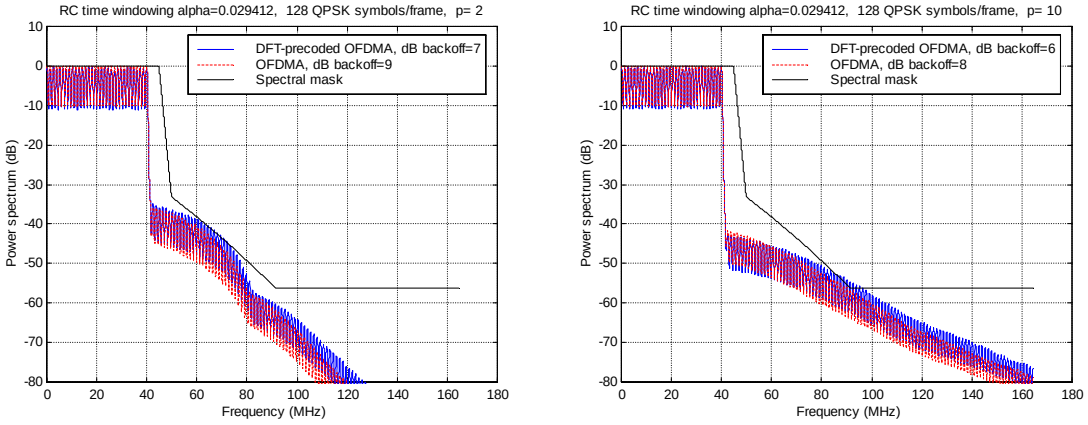

(a) (b)

Figure 4-40 HPA output power spectra for QPSK OFDMA and DFT-precoded OFDMA signals, corresponding to B-EFDMA and B-IFDMA respectively, with block width=4 and with 40 MHz nominal bandwidth. (a) HPA has Rapp model nonlinearity with parameter p=2; (b) HPA has Rapp model nonlinearity with parameter p=10;

The power spectra shown above are for signal waveforms which do not include frequency-multiplexed pilots for channel estimation and synchronisation. Full-band and B-IFDMA signals' peak to average ratio and HPA output spectra will be affected, since frequency multiplexed pilots essentially add another waveform to the data waveform. It is to be expected that the power spectrum for B-EFDMA will be little affected by frequency multiplexed pilots, since the signal is the sum of many waveforms in parallel anyway. As shown in [CoFrRe+07] E. Costa, A. Frediani, S. Redana, Y. Zhang, "Dynamic Spatial Resource Sharing in Relay Enhanced Cells", in 13th European Wireless Conference, EW 2007, April 2007.

[DFL+07], the presence of pilots in the B-IFDMA signal increases the backoff required from 7.0 dB to 7.8 dB, and the difference from B-EFDMA decreases from 1.9 dB to 1 dB. Note that only a fraction of OFDM symbols contain pilots and need this extra backoff. Thus the effect of frequency multiplexed pilots on the required power backoff is minimal

The effect on output power spectra of adaptive frequency domain resource partitioning was also evaluated. It was found that it has no adverse effect on the emitted power spectrum, relative to the spectral mask. This is because in order for a spectrum to fall within a spectrum mask, power control can only **reduce** power from its spectrum mask limit at a given frequency. Figure 4-41 illustrates this. Note that the backoff difference between OFDMA and DFT-precoded OFDMA is reduced, but is still positive.

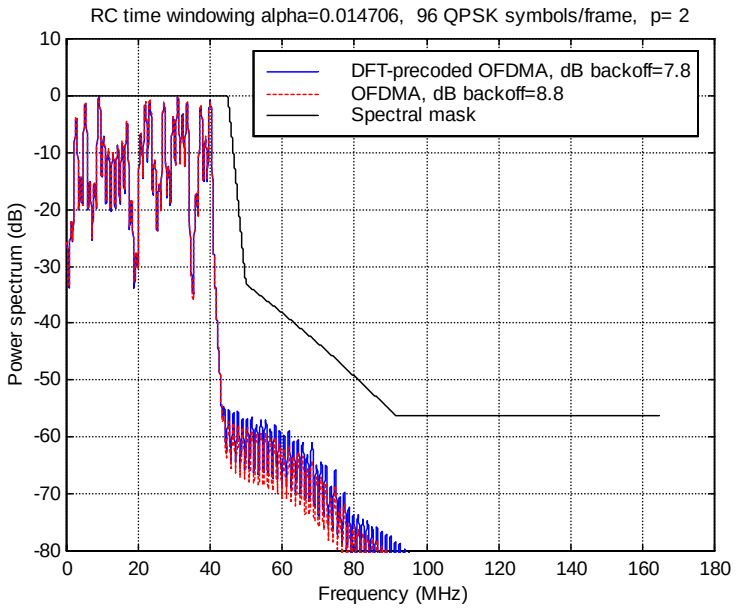

Figure 4-41 Illustration of output HPA power spectrum for nonuniformly-spaced spectrum chunks – typical of frequency-adaptive resource partitioning for OFDMA and DFT-precoded OFDMA, Rapp parameter *p*=2.

Table 4.10-8 summarizes the results for required power backoff, for in-band signal to nonlinear distortion, and for signal to adjacent user distortion. For the full-band (40 MHz) cases, adjacent user refers to the adjacent 40 MHz frequency band. For B-EFDMA and B-IFDMA, adjacent user means the frequencies occupied by a user whose blocks are immediately adjacent and interleaved in frequency with those of the transmitting user; e.g. the transmitting user occupies subcarriers [1, 2, 3, 4, 33, 34, 35, 36,..] and the adjacent user occupies subcarriers [5, 6, 7, 8, 37, 38, 39, 40,…].

Table 4.10-8 Required power backoffs and signal to distortion ratios to comply with WINNER spectral mask, for Rapp HPA parameter values *p*=2 and 10

	Rapp parameter *p*=2			**Rapp parameter *p*=10**		
	Required power backoff (dB)	**Signal to in-band distortion Ratio (dB)**	**Signal to adjacent user distortion ratio (dB)**	**Required power backoff (dB)**	**Signal to in-band distortion ratio (dB)**	**Signal to adjacent user distortion ratio (dB)**
QPSK (4-QAM)						
OFDM (full-band)	8.8	32.7	38.6	7.9	40.2	44.7
DFT-precoded OFDM (full-band)	6.8	37.0	39.5	5.7	49.3	51.3
B-EFDMA	9.0	35.7	41.7	8.0	42.9	47.6
B-IFDMA	7.0	36.3	40.2	6.0	44.3	47.9
16-QAM						
OFDM (full-band)	8.8	31,8	38.5	7.8	37.8	44.4
DFT-precoded OFDM (full-band)	7.0	33.3	38.2	6.0	39.6	46.9
B-EFDMA	8.8	29.8	40.8	8.0	32.1	49.1
B-IFDMA	7.3	29.8	39.6	6.5	32.1	49.3

64-QAM						
OFDM (full-band)	8.7	31.5	38.1	7.9	37.5	44.7
DFT-precoded OFDM (full-band)	7.0	32.6	37.8	6.1	38.6	45.8
256-QAM						
OFDM (full-band)	8.7	31.6	38.2	7.9	37.3	44.5
DFT-precoded OFDM (full-band)	7.0	32.6	37.6	6.1	38.4	45.6

To summarise the results:

- The backoff required to satisfy the spectral mask does not increase significantly in going from QPSK to 256QAM.
- The same holds true for backoffs required to maintain a given signal to nonlinear distortion ratio (SNDR). e.g. for p=2 Rapp model nonlinearity, backoffs required to satisfy spectral mask also yield approx. 32 dB SNDR for QPSK through 256QAM. (although it would probably be desirable to have a higher SDNR, and therefore somewhat more backoff, for 256QAM).
- DFT-precoded OFDM and B-IFDMA have 1.5 to 2 dB less required power backoff than do OFDM and B-EFDMA, respectively (~2 dB for QPSK, ~1.5 dB for 256QAM).
- For all modulations, and for Rapp parameter p=10 (HPA approximating an ideal linear clipper), required backoff is roughly 1 dB less than that for p=2 (corresponding to more nonlinearity in the unsaturated region of the HPA). p=10 also reduces SNDR by about 5 dB.
- Thus DFT-precoded OFDM and higher quality (or adaptively-predistorted) HPAs are desirable, especially for uplink transmission high level modulations.
- Required backoff of course depends on the choice of the spectral mask.
- Adaptive resource partitioning for frequency adaptive transmission can only reduce the required backoff to comply with the spectral mask.

4.10.4. SNR Mismatch Impact on LDPC Codes

Whilst evaluating performance of advanced coding techniques, namely iterative coding such as Turbo-Codes, and LDPC Codes, it is necessary to take into account multiple impairments resulting from the system itself in which such coding techniques are used.

As a result, optimal decoding algorithms such as Log-MAP for Turbo-Codes, or LLR-BP for LDPC Codes even though they allow reaching close to Shannon Capacity performances, might experience severe degradations due to external impairments.

One of the key parameter common to both decoders, is the SNR estimation. Therefore it is mandatory to evaluate the accuracy requested by SNR estimation algorithms (impacted by Channel Estimation), in order to avoid prohibitive performance degradations.

In this part, we'll restrict ourselves to LDPC Codes only, since these have been selected for WINNER Reference system.

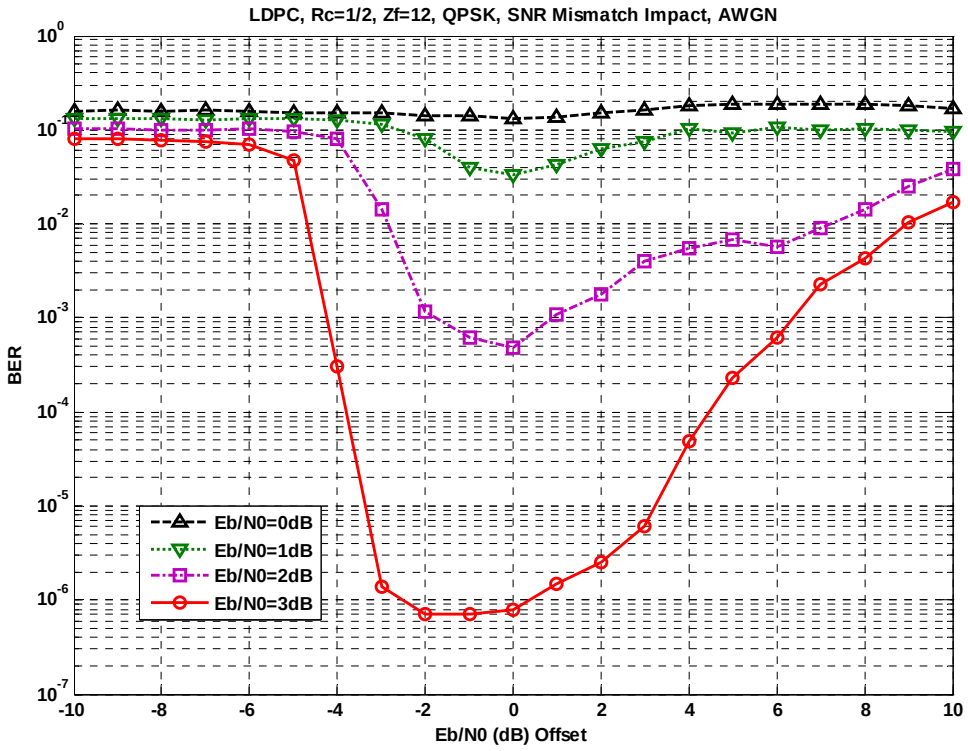

Figure 4-42 SNR Mismatch Impact on LDPC Codes, Rc=1/2, QPSK

In order to obtain sufficient valuable and relevant results, different modulations have been taken into account namely QPSK (Figure 4-42), 16-QAM (Figure 4-43) and finally 64-QAM (Figure 4-44), with a half-rate Rc=1/2 LDPC Codes, as defined in [WIN1D210].

Depending on the acceptable degradation in term of performance (BER or CWER), this curves can then be used for checking suitability of Channel Estimation algorithms through their impact on the SNR estimation.

For instance, with QPSK for an operating point of Eb/N0=3dB, the SNR Offset can be in the range [-3;+3] dB, if we want to avoid a BER above 10^{-5}.

Besides, it's worth noticing that an offset of -5dB (Underestimation) will force such QPSK transmission (True Eb/N0=3dB) to be degraded up to a BER close to 0.1! On the contrary, even after +10dB offset (overestimation) we are still around BER=10^{-2}

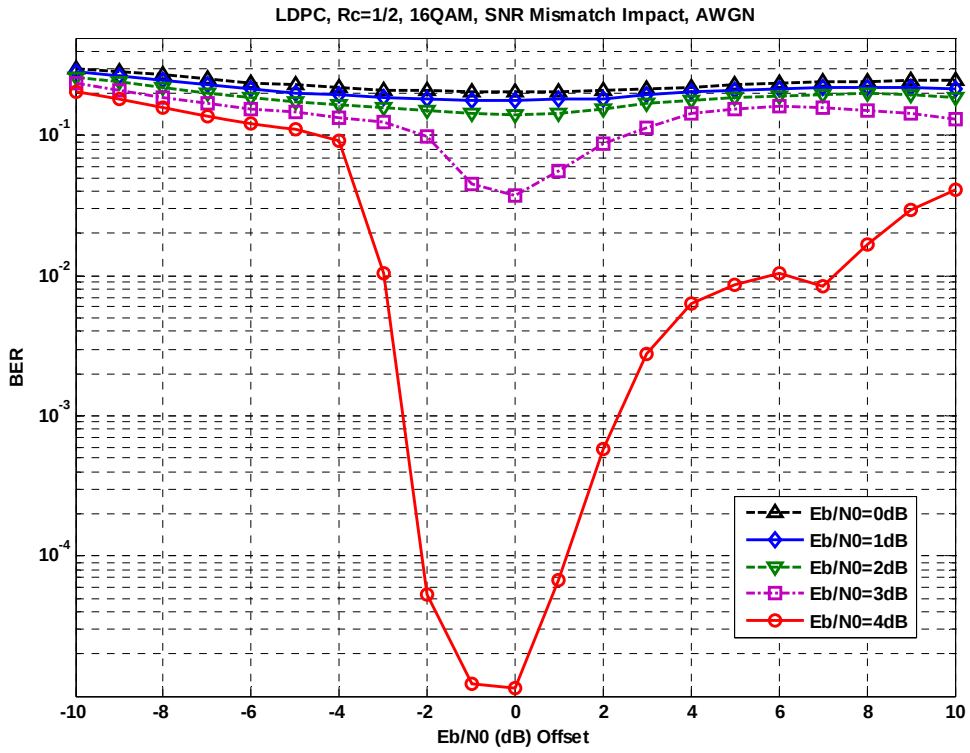

Figure 4-43 SNR Mismatch Impact on LDPC Codes, Rc=1/2, 16-QAM

On the figure above (Figure 4-43), we can notice the same key behaviour w.r.t. overestimation and underestimation: we only need -3dB Offset with a True Eb/N0=4dB to be above BER=10^{-2}, when an overestimation of +6dB is necessary!

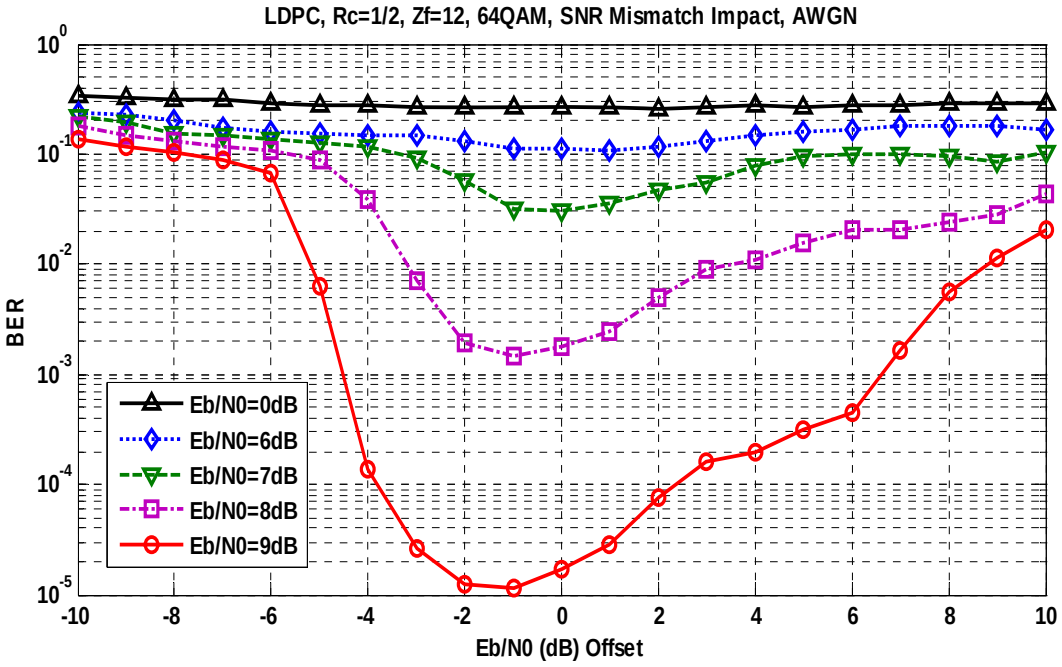

Figure 4-44 SNR Mismatch Impact on LDPC Codes, Rc=1/2, 64-QAM

As a conclusion, even though the Log-BP decoding of LDPC Codes is optimal in terms of performance, it might lose this advantage due to mismatched SNR estimation.

Besides, it has been pointed out that the sensitivity of such decoding algorithm is more robust to overestimation than underestimation.

4.10.5. Network Synchronisation

Network synchronisation is defined as aligning all internal time references within the network, so that all nodes agree on the start and end of a super-frame. To do so in a self-organised manner, similar rules to the ones used in nature by fireflies are applied: each node maintains a time reference, referred to as the phase function, which is updated upon reception of a pulse from other nodes. The update rule is extremely important, and it was shown by Mirollo and Strogatz in their seminal paper [MS90] that the phase increment, which is a function of the internal phase, needs to be always strictly positive.

In this section, we first review the super-frame preamble structure that is currently defined and used for synchronisation. In [WIN2D233] a self-organised network synchronisation scheme derived from the firefly synchronisation principle is extended to fit into the super-frame preamble. Thanks to the coarse misalignment mode, cells that are initially completely misaligned are always able to synchronise.

In the wide area scenario, given the large propagation delays, the main concern for the network synchronisation scheme is the achieved accuracy. Thus the following simulations investigate the misalignment in time between base stations and user terminals, and the misalignment between base stations, rather than the time needed for a network to synchronise.

The accuracy is defined as follows. Let $\tau_{\mathrm{UT},i}$ and $\tau_{\mathrm{BS},j}$ respectively denote the timing reference instants of, respectively, user terminal *i* and base station *j*. Given the constant misalignment between BSs and UTs, which is known and equal to the durations of the UL, Sync word and the RAC, the accuracy between the *i*th UT and the *j*th BS is defined as:

$$\text{accuracy} = \left| \tau_{\mathrm{UT},i} - \left(\tau_{\mathrm{BS},j} - \left(T_{\mathrm{UL,Sync}} + T_{\mathrm{RAC}} \right) \right) \right| \quad .$$

Given this definition, if the nodes are perfectly aligned in time, the accuracy is equal to zero. However, given the propagation delay between two nodes, it is rarely equal to zero.

In the following, the accuracy of the self-organized network synchronisation scheme is verified considering seven loaded cells with 150 user terminals distributed in the network and participating to the network synchronisation procedure by transmitting the UL Sync word. Participating UTs are chosen if their distance from their own base station is superior to $d_{\mathrm{selection}}$. Such a topology is represented in Figure 4-45 for a cell radius of 1000 metres and a selection range of $d_{\mathrm{selection}} = 950\mathrm{m}$.

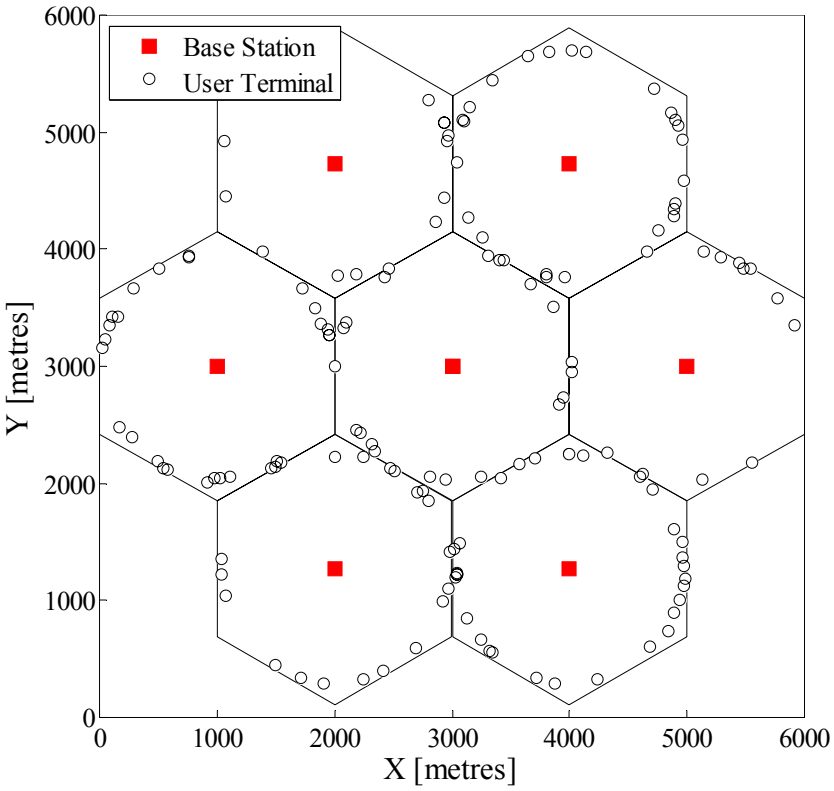

Figure 4-45: Example of a network topology for 7 BSs and 150 participating UTs.

Simulations are conducted as follows. Initially nodes start from a random misalignment that is restricted to $T_{\mathrm{UL},sync}$ for user terminals and $T_{\mathrm{DL},sync}$ for base stations with an average spacing of $T_{\mathrm{UL,Sync}} + T_{\mathrm{RAC}}$ between the two groups. This way, nodes synchronise more quickly than if the misalignment is as large as the super-frame duration. Base stations parameters are set to: $\alpha_{\mathrm{BS}} = 1.20$, $\beta_{\mathrm{BS}} = 0.01$ for the coupling, and $T_{\mathrm{refr,DL}} = 25 \cdot T_{\mathrm{s}}$ where T_{s} is the duration of an OFDM symbol. User terminal parameters are set to $\alpha_{\mathrm{BS}} = 1.40$, $\beta_{\mathrm{UT}} = 0.01$ and $T_{\mathrm{refr,UL}} = 15 \cdot T_{\mathrm{s}}$. Figure 4-46 plots the synchronisation accuracy between user terminals and base stations versus the propagation delay between them.

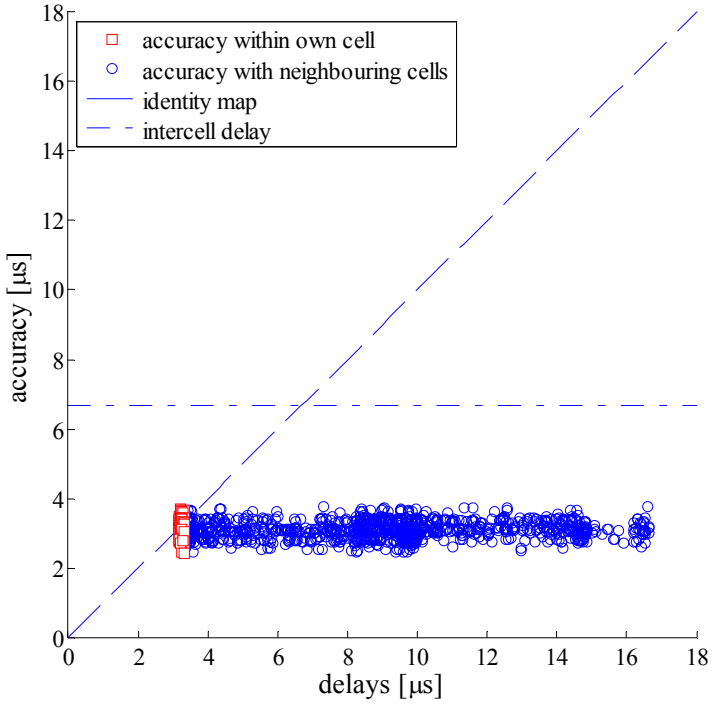

Figure 4-46: Network synchronisation accuracy without compensation of propagation delays.

In Figure 4-46 two accuracy groups are considered: the accuracy between the UTs and their closest base station (accuracy within own cell), and the accuracy between these users and the six surrounding base stations (accuracy within neighbouring cells) for a selection range of $d_{\text{selection}} = 950\text{m}$.

In both cases, the accuracy is much lower than the inter-BS delay, denoted intercell delay, which is constant between the central base stations and the six surrounding ones, and is equal to $2000/3\cdot10^8 \approx 6.67\mu s$. The achieved accuracy of nodes with their own base station is centred around their respective propagation delay, as shown with the identity map. Surprisingly, the accuracy with surrounding base stations is also centred around this value. Therefore when compensating by the propagation delay, the accuracy should centre around zero.

To verify the accuracy in the case of timing advance, the timing reference instant of user terminals $\tau_{\text{UT},i}$ is advanced by the propagation delay with their own base station $\theta_{\text{UT},i,\text{BS(i)}}$, so that the new definition for the accuracy is equal to:

$$\text{accuracy}_{\text{TA}} = \left|\tau_{\text{UT},i} - \theta_{\text{UT},i,\text{BS(i)}} - \left(\tau_{\text{BS},j} - \left(T_{\text{UL,Sync}} + T_{\text{RAC}}\right)\right)\right|$$

Figure 4-47 plots the synchronisation accuracy when advancing the timing references of user terminals.

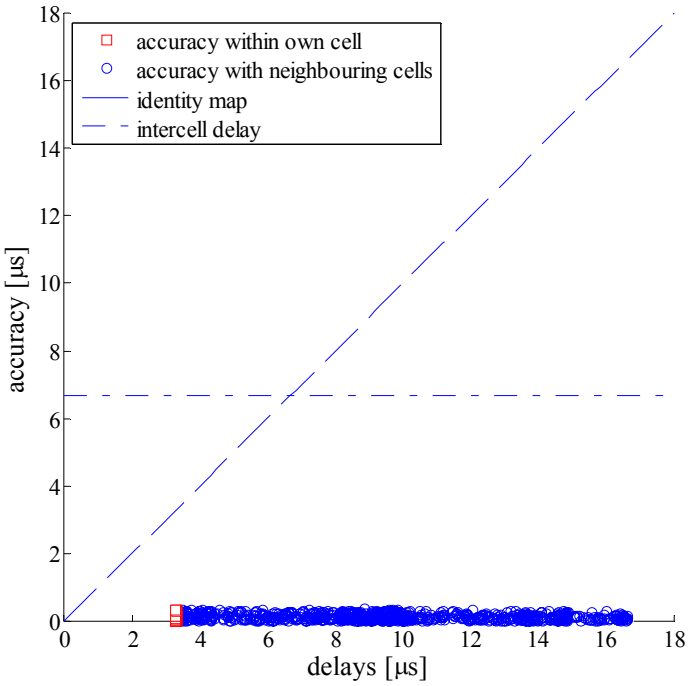

Figure 4-47: Network synchronisation accuracy with compensation of propagation delays.

Compensation of the propagation delay within the own cell effectively greatly improves the accuracy between user terminals and base stations. From Figure 4-47 the accuracy is always below $1\mu s$.

Another important result for the network synchronisation is the misalignment among base stations, which is measured by looking at the time difference between the firing instants of base stations:

$$\text{accuracy}_{\text{BS}} = \left| \tau_{\text{BS},i} - \tau_{\text{BS},j} \right|$$

In Figure 4-48 the inter-base station accuracy is plotted as a function of the propagation delay between them for a selection range of $d_{\text{selection}} = 950\text{m}$ based on 100 generated networks. As the position of base stations is fixed and BSs are disposed in an hexagonal fashion as shown in Figure 4-45, only three propagation delays are possible, namely $6.67\mu s$, $11.4\mu s$ and $13.3\mu s$, and respectively correspond to inter-BS distances 2000 m, 3409 m and 4000 m.

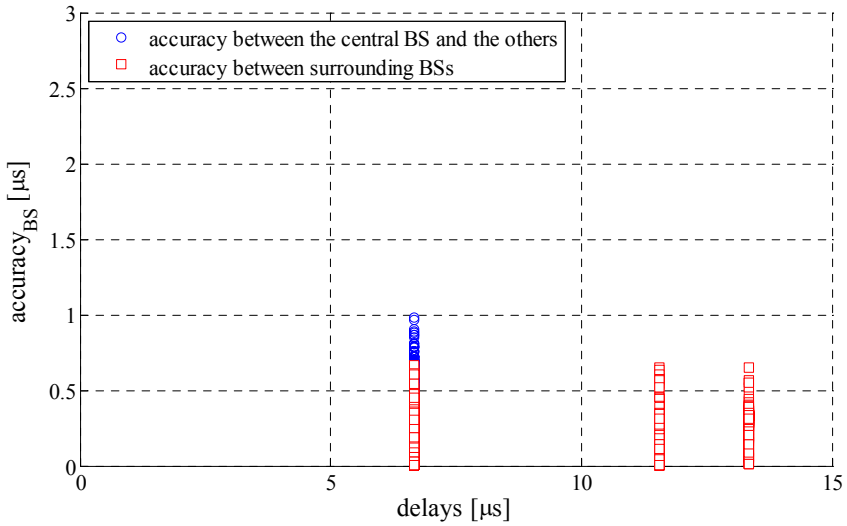

Figure 4-48: Inter-Base Station Accuracy when $d_{\text{selection}}$=950 m.

From Figure 4-48 the maximum misalignment between two base stations is $1\mu s$ and concerns for the central cell. Surprisingly base stations that are further apart are better aligned than the central one.

So far the achieved accuracy was examined for a selection distance of 950 metres. Figure 4-49 plots the maximum misalignment between a UT and a BS with and without timing advance.

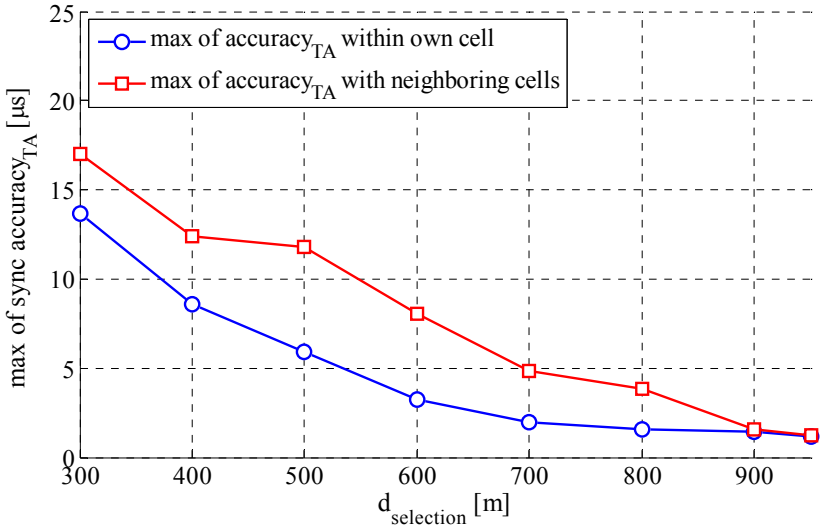

Figure 4-49: Maximum misalignment as a function of the selection distance $d_{selection}$ for N_{UT}=150.

From Figure 4-49 the selection range $d_{selection}$ is an important parameter for the accuracy of the network synchronisation algorithm. For a low range, the worse achieved accuracy is around $15\mu s$, and performing timing advance does not improve this, because timing references are spread too far apart. Increasing the selection range enables to reduce the spread in timing references, and forces nodes to form one group, as observed in Figure 4-46. Thus relying on the cell edge users, i.e. $d_{selection} < 900\text{m}$, to perform network synchronisation presents the advantage that the synchronisation accuracy is far lower than if the selection range is low, and an accuracy in the range of $1\mu s$ can be achieved. Furthermore transmissions from UTs that are close to their BS is less likely to be heard by surrounding BSs than transmissions from cell edge UTs.

In conclusion the proposed self-organised network synchronisation procedure is able to achieve the required accuracy. In general a maximum accuracy equal to the guard interval of an OFDM symbol is needed. In the wide area case, this duration is equal to $3.2\mu s$, and the network synchronisation algorithm is able to synchronise with a maximum misalignment of $1\mu s$. Thus it is an appropriate candidate for the WINNER system.

5. Summary – Performance of WINNER in Wide Area Scenario

It was shown that WINNER building blocks outperform methods used in legacy systems both using very specific metrics such as BER performance or SNR degradation as well as end-2-end metrics such as spectral efficiency measured in bit/s/Hz/sector. It was also shown, that some methods used today are already close to achievable limits – very valuable input to target further research in the right direction, and to have confidence to base standards in development on the right methods.

The WINNER system offers flexibility in deployments to adapt to the needs of an operator or of a user. For instance, the number of antenna elements can be changed at the base station, or systems could operate with and without relays. Comparing these modifications of the outer environment to the WINNER baseline configuration provide very useful insight – especially also in conjunction with cost-modelling.

The key performance results in terms of spectral efficiency for the Wide Area deployments are the following:

- Spectral efficiency results are obtained at an operating point, where 95% of users in a particular area are provided with a data rate of 2 Mbit/s in the downlink, and 1.3 Mbit/s in the uplink ("satisfied user criterion"). Results are obtained using the WINNER channel models developed for wide area situations, which also include links to fixed and mobile relay stations.
- The spectral efficiency targets set by WINNER in [WIN2D6114] (R38) are reached and outperformed significantly in the downlink for a 4x2 configuration, and almost for a 2x2 full buffer configuration but with a smaller number of supported users per sector. The spectral efficiency requirement for the uplink is also reached. More particularly:
    - In a 4x2 MIMO configuration, a downlink spectral efficiency of 2.9 bits/s/Hz/sector can be achieved using Grid of Beams (GoB), SDMA and interference rejection combining (IRC) at the receiver.
    - For uplink, a spectral efficiency of more than 3 bits/s/Hz/sector has been demonstrated by implementing SDMA based on a BS receiver with IRC and successive interference cancellation (SIC).
- Relaying can in certain scenarios increase the spectral efficiency by 60 %. Relaying is even more important in the uplink than in the downlink. This improvement can however only be realized by the usage of intelligent and dynamic resource partitioning and reuse schemes to adapt the available capacity on the relay and the access links to the actual distribution of the offered traffic within the relay-enhanced cell.

The following key insights can be obtained regarding the performance of the WINNER building blocks in the context of end-2-end system design and performance:

- B-IFDMA is one WINNER multiple access scheme, where its parameterization is a major issue. Evaluations resulted in a proposal for dimensioning of blocks for non-frequency adaptive transmission in the SISO case. A basic block size of 4 subcarriers x 3 symbols is recommended for low data rates and sufficient frequency diversity is achieved with 16 blocks each separated by 4 chunks in SISO case; if spatial diversity is used 8 or 4 blocks are sufficient. For larger data rates several basic blocks can be combined into larger blocks, as described in [WIN2D61314].
- For spatial processing it has been demonstrated that SDMA implemented with a GoB as basis is a simple but very efficient downlink scheme. The gains of spatial multiplexing for wide area scenarios are limited, even if beamforming is applied and additionally adaptive switching to single stream schemes is allowed. These schemes hardly outperform the GoB based schemes.
- Relaying can improve spectral efficiency for MBMS transmission significantly, especially if outdoor-to-indoor coverage is required.
- Intercell interference is a major challenge in wide area deployments. A range of techniques were developed and investigated with different complexity-performance trade-offs. The most suitable techniques are:
    - Downlink: The use of spatial processing schemes such as transmit beamforming (GoB) in conjunction with receivers with interference suppression capabilities (e.g. IRC).
    - Common Control Channels: Resource partitioning such as FFR is recommended for user throughput improvements at the cell edge if the associated possible sector throughput degradation can be afforded, since beamforming can typically not be applied.
    - Uplink: Receivers with interference suppression capabilities, e.g. IRC.
- In contrast to most beyond 3G standardization activities (such as LTE and mobile WiMAX), WINNER has not only evaluated full-buffer traffic scenarios, but also the impact of realistic traffic models such as constant bit rate (CBR) on key performance metrics, e.g. the spectral efficiency, supported number of users per cell and SINR distribution. Full buffer simulations overestimate the spectral efficiency by ~20-30%. The application of the satisfied user criterion (2 Mbits/s) for full buffer simulations (where each user offers infinite load) and proportional fair scheduling leads to a significant underestimation of the number of supported users, since for realistic services only a finite offered load per user is present. Packet-delay-aware scheduling further improves performance under QoS constraints.

-
- WINNER includes a concept of handovers within modes (intramode) and between modes (intermode). At the example of local area to wide area handover it is shown, that both wireless connectivity and throughput triggers are essential to maintain undisrupted high throughput.
- The WINNER Spectrum Resource Management concept governs, how sharing is accomplished to access spectrum resources and how to optimize the usage of spectrum.
- WINNER can share the FSS frequency band using adjacent channels or exclusion distances. Exclusion distances depend on the pathloss criterion, the consideration of co-channel or adjacent channel interference, and of the antenna configuration of the BSs. They range from 3 km to 74 km. This has been calculated for flat terrain profiles. When taking into account the terrain profiles in a concrete deployment the exclusion distances are much shorter.
- The performance degradation of non-iterative channel estimation compared to perfect channel knowledge is between 1.5 and 4.3 dB considering SISO links, but can be reduced to 0.2-3.0 dB, if iterative channel estimation is applied.
- SDMA and MIMO impose interference from in-cell co-channel users, which is especially significant for channel estimation with a low-overhead pilot design. Iterative channel estimators can reduce the SNR degradation significantly – being an enabler for low-overhead pilot designs.
- It is shown that inter-block interference due to timing and synchronization errors is negligible.
- Phase noise is no major issue for high-quality hardware components. However, it was shown that low-cost oscillators can be used for WINNER as well, where phase noise compensation algorithms can limit the SNR degradation to tolerable amounts.
- B-IFDMA and DFT-precoded OFDMA have 1.5-2dB lower required power backoff than OFDM or B-EFDMA.
- A self-organized network synchronization procedure developed within WINNER is able to achieve the required accuracy. The maximum misalignment of 1 μs is below the cyclic prefix of 3.2 μs.

6. References

Public WINNER project deliverables can be downloaded from the project website http://www.ist-winner.org, and a list of all publications is available there as well.

WINNER I Deliverables

[WIN1D14] IST-2003-507581 WINNER, "D1.4 Final requirements"

[WIN1D21] IST-2003-507581 WINNER, "D2.1 Identification of Key Radio Link Technologies", June, 2004.

[WIN1D23] IST-2003-507581 WINNER, „D2.3 Assessment of Radio Link Technologies", February, 2005.

[WIN1D71] IST-2003-507581 WINNER, "D7.1 System Requirements", July 2004

WINNER II Deliverables

[WIN2D111] IST-4-027756 WINNER II, "D1.1.1 WINNER II Interim Channel Models", November 2006.

[WIN2D112] IST-4-027756 WINNER II, "D1.1.2 WINNER II Channel Models", September 2007.

[WIN2D223] IST-4-027756 WINNER II "D2.2.3 Modulation and Coding Schemes for the WINNER II system", November 2007.

[WIN2D233] IST-4-027756 WINNER II, "D2.3.3 Link level procedures for the WINNER II System", November 2007.

[WIN2D341] IST-4-027756 WINNER II "D3.4.1 The WINNER II Air Interface: Refined Spatial-Temporal Processing Solutions", November 2006.

[WIN2D352] IST-4-027756 WINNER II, "D3.5.2 Assessment of relay based deployment concepts and detailed description of multi-hop capable RAN protocols as input for the concept group work", June 2007.

[WIN2D353] IST-4-027756 WINNER II, "D3.5.3 Final assessment of relaying concepts for all CGs scenarios under consideration of related WINNER L1 and L2 protocol functions", September 2007.

[WIN2D461] IST-4-027756 WINNER II, "D4.6.1 The WINNER II Air Interface: Refined multiple access concepts," November 2006.

[WIN2D471] IST-4-027756 WINNER II, "D4.7.1 Interference Averaging Concepts", June, 2007.

[WIN2D472] IST-4-027756 WINNER II, "D4.7.2 Interference Avoidance Concepts", June, 2007.

[WIN2D473] IST-4-027756 WINNER II, "D4.7.3 Smart Antenna Based Interference Mitigation" June 2007.

[WIN2D5101] IST-4-027756 WINNER II "D5.10.1 The WINNER Role in the ITU Process Towards IMT-Advanced and Newly Identified Spectrum", November 2007.

[WIN2D5103] IST-4-027756 WINNER II "D5.10.3 WINNER II Spectrum Sharing Studies", November 2006.

[WIN2D591] IST-4-027756 WINNER II "D5.9.1 Flexible Spectrum Use Functionalities for WINNER II", November 2007.

[WIN2D592] IST-4-027756 WINNER II "D5.9.2 Implementation of efficient Spectrum Sharing and Coexistence Capabilities for WINNER II", November 2007.

[WIN2D6137] IST-4-027756 WINNER II, "D6.13.7 Test scenarios and calibration case issue 2," December 2006.

[WIN2D6139] IST-4-027756 WINNER II, „D 6.13.9 State-of-the-art evaluation (issue 2) ", June 2007

[WIN2D61311] IST-4-027756 WINNER II, "D6.13.11 Final concept group metropolitan area description for integration into overall System Concept and assessment of key technologies", October 2007

[WIN2D61312] IST-4-027756 WINNER II, “D6.13.12 Final concept group local area description for integration into overall System Concept and assessment of key technologies”, October 2007

[WIN2D61314] IST-4-027756 WINNER II, “D6.13.14 WINNER II system concept description“, November 2007.

Other References

[3GPP06a] 3GPP: “Requirements for Evolved UTRA (E-UTRA) and Evolved UTRAN (E-UTRAN) (Release 7)”, 3GPP TR 25.913 V7.3.0, March 2006

[3GPP06b] 3GPP: “Physical layer aspects for evolved Universal Terrestrial Radio Access (UTRA) (Release 7)”, 3GPP TR 25.814 V7.0.0, June 2006

[3GPP07] 3GPP: “Feasibility study for evolved Universal Terrestrial Radio Access (UTRA) and Universal Terrestrial Radio Access Network (UTRAN)”, 3GPP TR 25.912, V.7.2.0, June 2007

[3GPP204] 3GPP2 C.R1002-0; “cdma2000 Evaluation Methodology”. Rev. 0, 10.12.2004

[8F0568] ITU-R WP8F, Document 8F/TEMP/568-E, " WORKING DOCUMENT TOWARDS PROPOSED DRAFT NEW [REPORT / RECOMMENDATION] [GUIDELINES FOR EVALUATION OF RADIO INTERFACE TECHNOLOGIES FOR IMT-ADVANCED], May 2007.

[BAS+05] Karsten Brueninghaus et al., “Link Performance Models for System Level Simulations of Broadband Radio Access Systems”, PIMRC 2005

[Bon04] T. Bonard, “A Score-Based Opportunistic Scheduler for Fading Radio Channels,” in Proceedings of the European Wireless Conference, Barcelona, February 2004

[CoFrRe+07] E. Costa, A. Frediani, S. Redana, Y. Zhang, “Dynamic Spatial Resource Sharing in Relay Enhanced Cells”, in 13th European Wireless Conference, EW 2007, April 2007.

[DFL+07] F. Danilo-Lemoine, D. Falconer, C-T Lam, M. Sabbaghian and K. Wesołowski, “Power Backoff Reduction Techniques for Generalized Multicarrier Waveforms”, in *EURASIP J. on Wireless Communications and Networking special issue on multicarrier systems*, Nov., 2007.

[ETSI1] ETSI TR 101 112 v3.2.0, Universal Mobile Telecommunications System (UMTS); Selection procedures for the choice of radio transmission technologies of the UMTS (UMTS 30.03 version 3.2.0), ETSI, 1998.

[FAO07] Website of Food and Agriculture Organization of the United Nations (FAO): “Bridging the Rural Digital Divide”, http://www.fao.org/rdd/

[FrReCo+07] A. Frediani, S. Redana, E. Costa, A. Capone, Y. Zhang, “Dynamic Resource Allocation In Relay Enhanced Cells based on WINNER System”, in 16th IST Mobile & Wireless Communication Summit, IST Summit 2007, July 2007.

[FKC+05] T. Frank, A Klein, E. Costa and E. Schultz, "IFDMA-a promissing multiple access scheme for future mobile radio systems", in *Proc*. of PIMRC05, pp1214-1218.

[HOOLI] K.Hooli, S. Thilakawardana, J. Lara, J-P. Kermoal, and S. Pfletschinger, “Flexible Spectrum Use between WINNER Radio Access Networks”, IST mobile and wireless summit, Mykonos, Greece, June 2006

[HoElPaSc07] C. Hoymann, J. Ellenbeck, R. Pabst, M. Schinnenburg, “Evaluation of Grouping Strategies for an Hierarchical SDMA/TDMA Scheduling Process”, Proceedings of ICC2007, Glasgow, Scotland

[IEEE05] IEEE P 802.20: “802.20 Evaluation Criteria”, V. 1.0, IEEE P 802.20 PD-09, 23. September 2005

[ITU-R S.1432] Recommendation ITU-R S.1432. " Apportionment of the allowable error performance degradations to fixed-satellite service (FSS) hypothetical reference digital paths arising from time invariant interference for systems operating below 30 GHz". January 2006

[KW02] M.Kuhn and A. Wittneben, "A new scalable decoder for linear space-time block codes with intersymbol interference," *Proc. Of IEEE VTC'02 spring*, 6-9 May. 2002.

[MS90] R.E. Mirollo and S.H. Strogatz, “Synchronization of pulse-coupled biological oscillators”, *SIAM J. APPL. MATH*, 50(6):1645–1662, Dec. 1990.

[NeP2000] R. van Nee, R. Prasad, “OFDM for Wireless Multimedia Communications,” Artech House Publishers, Boston, London, 2000.

[NGMN07a] China Mobile, KPN, NTT DoCoMo, Orange, Sprint, T-Mobile, Vodafone: “LTE physical layer framework for evaluation”, 3GPP TSG-RAN1#48, St. Louis, February 2007

[NGMN07b] R. Irmer et.al.: “Next Generation Mobile Networks Radio Access Performance Evaluation Methodology`”, NGMN White Paper, July 2007

[NeP2000] R. van Nee, R. Prasad, “OFDM for Wireless Multimedia Communications,” Artech House Publishers, Boston, London, 2000.

[NLF07] B. Ng, C-T Lam and D. Falconer, “Turbo Frequency Domain Equalization for Single Carrier Broadband Wireless Systems”, *IEEE Transactions on Wireless Communications*, Vol. 6, No. 2, February 2007.

[ReCoCa+07] S. Redana, L. Coletti, A. Capone, L. Moretti, “A Novel Resource Request and Allocation Strategy for Relay based Beyond 3G Networks”, in 8th World Wireless Congress, WWC 2007, May 2007.

[SBO06] R. Stridh, M. Bengtsson, and B. Ottersten. System evaluation of optimal downlink beamforming with congestion control in wireless communication. IEEE Trans. Wireless Commun., 5(4), April 2006.

[SF06] M. Sabbaghian, D. D. Falconer, ”Comparison between Convolutional and LDPC Code based Turbo Frequency Domain Equalization”, *IEEE International conference on communications*, vol. 1, pp. 5432-5437, June 2006.

[SSO+07] M. Sternad, T. Svensson, T. Ottosson, A. Ahlén, A. Svensson and A. Brunstrom,"Towards systems beyond 3G based on adaptive OFDMA transmission", Invited Paper, Proceedings of the IEEE, Special Issue on Adaptive Transmission, vol. 95, no. 10, 2007.

[ST06] G. Senarath, W. Tong et.al.: “Multihop System Evaluation Methodology – Performance Metrics”, IEEE C802.16j-06/025, May 2006

[SZ07] S. Srinivasan and J, Zhuang et.al.:” Draft IEEE 802.16m Evaluation Methodology Document”, IEEE C802.16m-07/080r1, 17. April 2007

[TA07] A. Tyrrell, and G. Auer, “Imposing a Reference Timing onto Firefly Synchronization in Wireless Networks”, in *Proc. VTC Spring 2007,* Apr. 2007.

[TFF07] M. Trivellato, F. Boccardi and F. Tosato, “User Selection Schemes for MIMO Broadcast Channels with Limited Feedback”, *Proc. IEEE Vehic. Technol. Conf.*, 2007, pp. 2089-2093.

[Yua06] Y. Yuan-Wu, "An enhanced MAP-DFE multiuser detection technique for uplink MC-CDMA systems" *Proc. of IEEE PIMRC'06*, Helsinki, Finland, 11-14 Sept. 2006.

[YG06] Taesang Yoo and Andrea Goldsmith. On the optimality of multi-antenna broadcast scheduling using zero-forcing beamforming. IEEE J. Select.Areas Commun., 24(3), March 2006.

[Zet95] P. Zetterberg. A comparison of two systems for down link communication with base station antenna arrays. IEEE Trans. Veh. Technol., 48(5), November 1995.

A. Appendix

A.1 Further Aspects of Spatio-Temporal Processing

This section of the appendix contains additional details and results of the spatio-temporal processing.

A.1.1 MU-MIMO with long- and short-term CSI in the Downlink

Simulations have been performed using a 19-cell simulator based on the assumptions in [WIN2D6137] for the base-coverage urban scenario. 1000 users are dropped over 57 sectors resulting in an average of 17.5 users per sector. The detailed simulation parameters can be found in Appendix D.1.3.4 of [WIN2D341]; i.e., four transmit antennas at the base station and two receive antennas at the mobiles.

For comparison, the SIMO reference case with two receive antennas under 5%-SUC shows a sector rate of 1.3 bit/s/Hz/sector and about 450 users are served in 19 cells under ideal channel estimation and ideal link adaptation.

Num BS antennas (beams)	TDMA/ SDMA	Scheduler	Actual/Ideal channel estimation	5% outage user spectral efficiency [bit/s/Hz]	Average site spectral efficiency [bit/s/Hz/sector]
4	SDMA	MT	Ideal	0.0	6.06
4	SDMA	PF	Ideal	0.0203	5.31

Table A.1.1 Individual and sector spectral efficiency for combined short- and long-term CSI with SDMA in WA downlink.

In comparison with the results reported in [WIN2D341], it can be observed that they are in the same order of magnitude. The main drawback of the MU-MIMO with long- and short-term CSI scheme is that the intersector interference changes from the timepoint when the SINR is reported to the actual downlink transmission. This is clearly an advantage of GoB based schemes because the intersector interference can be computed if all BS will use all beams. A remedy can be to include interference avoidance methods like those reported in [WIN2D472].

A.1.2 MU-MIMO with SDMA-GoB in the Downlink

Simulations have been performed using a 19-cell simulator based on the assumptions in [WIN2D6137] for the base-coverage urban scenario. 1000 users are dropped over 57 sectors resulting in an average of 17.5 users per sector. The detailed simulation parameters can be found in Appendix D.1.3.4 of [WIN2D341], i.e. four transmit antennas at the base and two receive antennas at each UT. For comparison, the SIMO reference case with two receive antennas under 5%-SUC shows a sector rate of 1.3 bit/s/Hz/sector and about 450 users are served in 19 cells under ideal channel estimation and ideal link adaptation.

The impact of the GoB design on the sum performance can be observed in Table A.1.2. Always, the score-based scheduler was used. Ideal channel estimation and ideal link adaptation are assumed.

Num BS beams	**TDMA / SDMA**	**GoB design**	**Average sector spectral efficiency**

			[bit/s/Hz/sector]
8	TDMA	Ref	2.99
8	TDMA	Grass	2.667
64	TDMA	Ref	3.048
64	TDMA	Grass	2.839
128	TDMA	Ref	3.021
128	TDMA	Grass	2.879
8	SDMA (2 beams)	Ref	4.158
8	SDMA (2 beams)	Grass	2.772
16	SDMA (2 beams)	Ref	4.023
16	SDMA (2 beams)	Grass	3.387
64	SDMA (2 beams)	Ref	3.9225
64	SDMA (2 beams)	Grass	3.413
24	TDMA	Ref	3.035
24	SDMA (2 beams)	Ref	3.417
24	SDMA (2 beams)	Ref	4.211
24	SDMA (4 beams)	Ref	4.8

Table A.1.2: Sector spectral efficiency for TDMA-GoB and SDMA-GoB in WA downlink with different GoB designs (reference vs. Grassmannian)

The conclusions from Table A.1.2 are the following: The reference GoB design performs better than the ideal Grassmannian design because the channels are spatially correlated in the WA scenario. Furthermore, the reference scheme (one beamset with 4 beams) performs better than multiple beamsets because the number of users per sector is too low. SDMA-GoB outperforms TDMA-GoB even if a much larger number of beams is used in TDMA-GoB mode.

A.1.3 Baseline TDMA/SDMA Grid of Beams

The baseline Grid of Beams scheme has been simulated for both TDMA (one scheduled user per chunk) and SDMA (one user scheduled per beam in each chunk). Particular aspects of the simulation setup include the following.

- All piloting and channel estimation was simulated. The pilots are orthogonal between the sectors of a site but scrambled to obtain random correlation between sites. The pilot length is six symbols per chunk and transmit antenna (per antenna pilots are used).
- The results include 24/96 (for 4 Tx antennas) overhead for the pilots, but no other control signaling overhead.
- Score based scheduling.
- Ideal link adaptation.
- MMSE combining at the receivers (also known as IRC).
- Full data buffers.
- For the SUC results, the load was varied from 3.5 to 17.5 average number of users per sector.
- No HARQ.

Results for single antenna receivers are presented in Figure A.1.1 and are summarized in Table A.1.3 below.

Antenna config.	Technique	Spectral efficiency in bits/s/Hz/sector (interpolated)	Max supported satisfied users (interpolated)
SISO	TDMA	SUC not achieved	SUC not achieved
1x4	TDMA	1.5	6.7
1x4	SDMA	SUC not achieved	SUC not achieved

Table A.1.3: Spectral efficiency for satisfied user criterion. Baseline GoB.

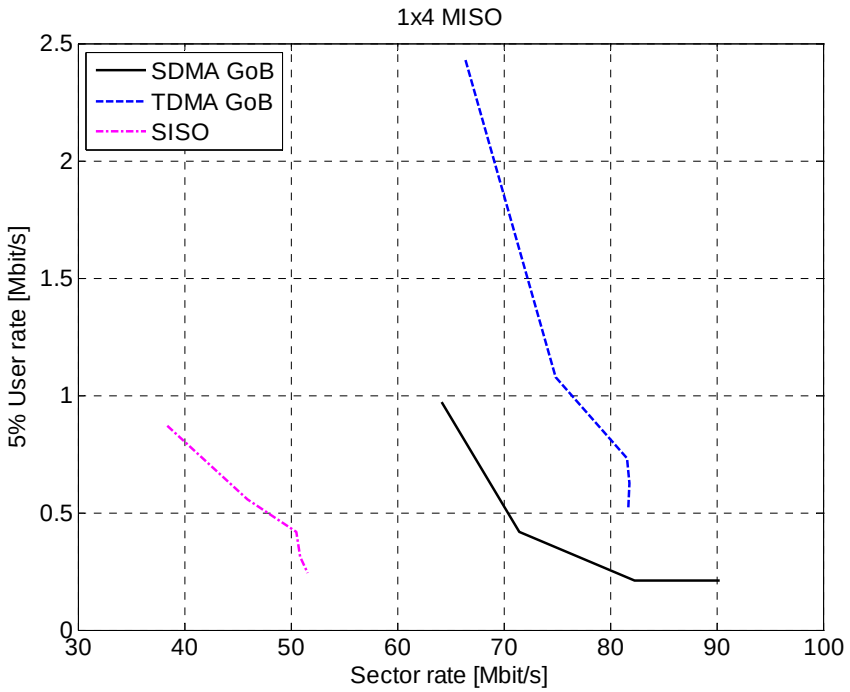

Figure A.1.1: 5% User rate versus sector rate for single antenna user terminals.

For the case of multiple receive antennas, beamformers both with and without tapering were considered. In contrast to [WIN2D341], Sect. 3.2.3.2, we used the same number of beams and scheduled users as the number of transmit antennas here. In this deployment, at least with SDMA, the negative influence of the wider main lobe seems to be larger than the gain in decreased sidelobes.

Results for 2x1, 2x4 and 4x4 are presented in Figure A.1.2 through Figure A.1.4, respectively. The results for the SUC at 5% user throughput of 2MB/s are summarized in Table A.1.4.

Antenna config.	Technique	Spectral efficiency in bits/s/Hz/sector (interpolated)	Max supported satisfied users (interpolated)
2x1	TDMA	0.9	4.7
2x1	SDMA	1.1	6.5
2x4	TDMA	1.6	11
2x4	SDMA	2.3	7.5
4x4	TDMA	1.5	12

4x4	SDMA	3.5	18

Table A.1.4: Spectral efficiency for satisfied user criterion. Baseline GoB.

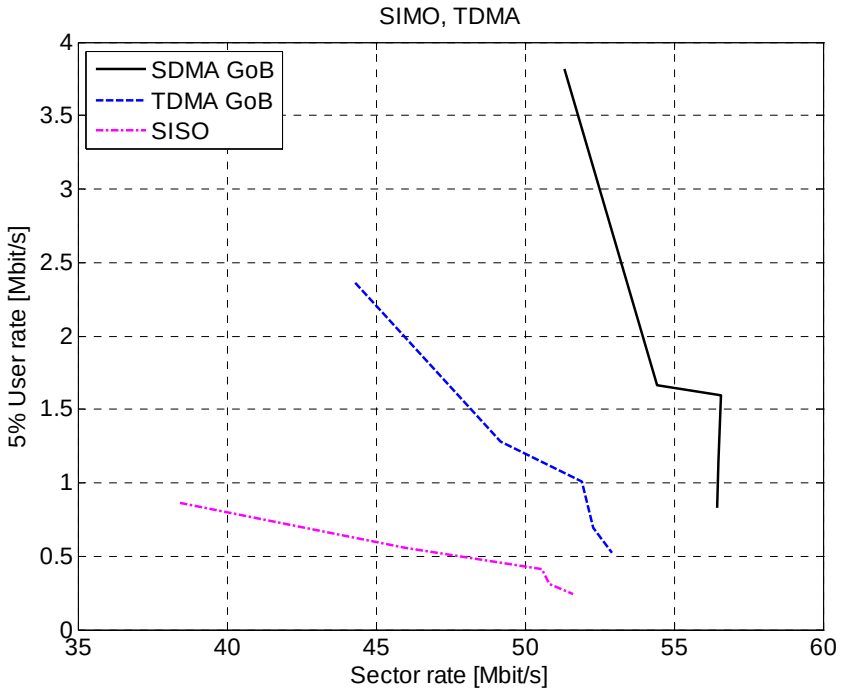

Figure A.1.2: 5% User rate versus sector rate for single antenna base station, 2 Rx antennas.

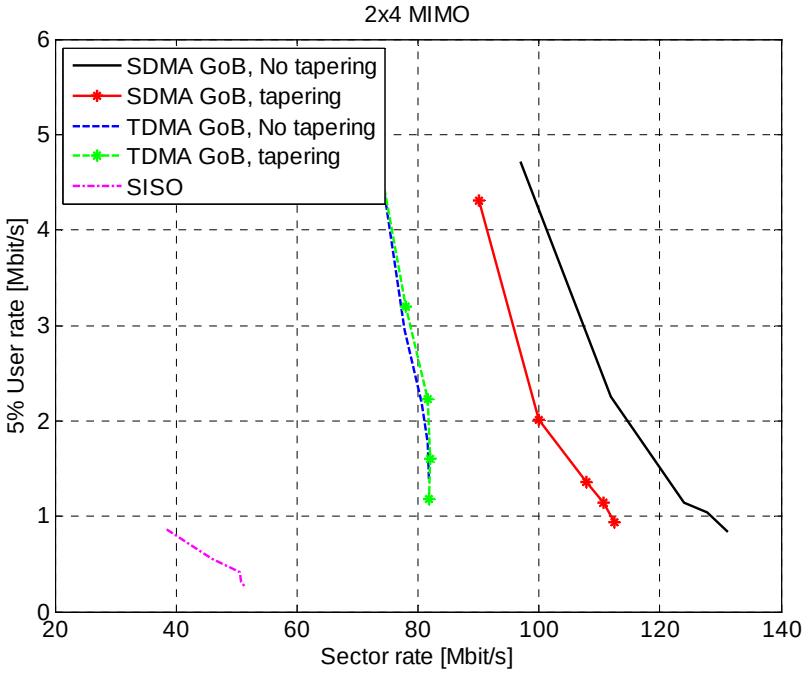

Figure A.1.3: 5% User rate versus sector rate for 4 Tx, 2 Rx antennas.

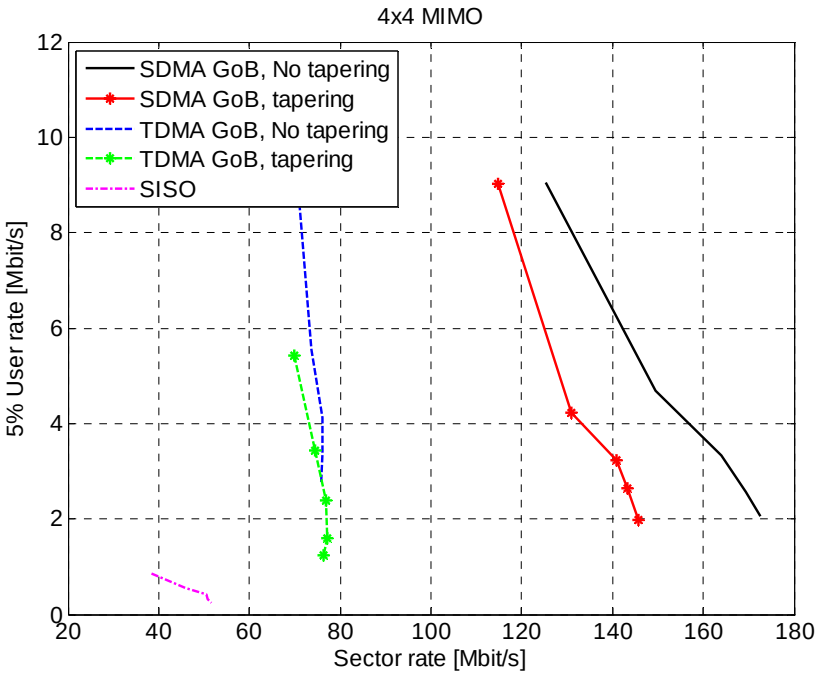

Figure A.1.4: 5% User rate versus sector rate for 4 Tx, 4 Rx antennas.

A.2 Further Aspects of Multiple Access

This section of the appendix contains additional details and results of the Multiple Access schemes.

A.2.1 Parameterization for B-IFDMA in Wide Area

In the following, the dependency of essential properties of B-IFDMA on different parameters is discussed. The basic parameters of B-IFDMA are:

- the number of consecutive OFDM symbols assigned to a user,
- the number of subcarriers per block and
- the number of blocks.

The effect of a variation of these parameters on performance, pilot symbol overhead required for channel estimation, envelope fluctuations, power efficiency and on the computational complexity is addressed. In the following, parameters for a Wide Area scenario and FDD are assumed.

A.2.1.1 Pilot Symbol Overhead required for Channel Estimation

The pilot symbol overhead for channel estimation results in an additional amount of energy per payload data symbol required for transmission compared to a transmission without pilots. Let Q denote the number of symbols per user including payload and pilot symbols and let P denote the number of pilot symbols per user. The additional amount of energy is given by

$$\Lambda = 10\log_{10}\left(\frac{Q}{Q-P}\right) \tag{A.2.1}$$

According to [WIN2D231], for the WINNER FDD mode the distance D_f of the pilots in frequency domain is given by $D_f = 4$, whereas the distance D_t of the pilots in time domain is given by $D_f = 11$. The values for the required additional amount of energy per payload symbol for different numbers of consecutive OFDM symbols assigned to a user and different numbers of subcarriers per block are given in Table A.2.1. From Table A.1.1 follows that for an increasing number of consecutive OFDM symbols and for an increasing number of subcarriers per block the pilot symbol overhead and, hence, the additional required energy per payload symbol decreases. Moreover, it can be concluded that for IFDMA using only one OFDM symbol the overhead is infinite, i.e., no payload data is transmitted as long as the distance of adjacent subcarriers is greater than $D_f = 4$.

Additional energy per payload symbol in dB		**Number of subcarriers per block**			
		1	**2**	**3**	**4**
Number of consecutive OFDM symbols assigned to a user	**1**	∞	3	1.8	1.2
	2	3	1.2	0.8	0.6
	3	1.8	0.8	0.5	0.4
	4	1.2	0.6	0.4	0.3
	6	0.8	0.4	0.2	0.2

Table A.2.1: Additional energy per payload symbol in dB for different numbers of consecutive OFDM symbols and subcarriers per block assigned to a user.

A.2.1.2 Envelope fluctuations

In the following, the envelope fluctuations for the B-IFDMA signal dependent on the parameters are discussed. Basically, increased envelope fluctuations have the following consequences: On the one hand, dependent on the envelope fluctuations, the required power amplifier class has to be determined. The higher the envelope fluctuations, the more linear and the more expensive is the required power amplifier. On the other hand, for transmit signals with high envelope fluctuations a high power back-off for the power amplifier is required. The higher the power back-off, the less power efficient the use of the power amplifier. Thus, high envelope fluctuations results in higher costs and increased power consumption.

In the following Figures the cumulative PAPR distributions for B-IFDMA signals with different numbers M of subcarriers per block are shown. Additionally, OFDMA signals with corresponding subcarriers allocation are given in order to show the effect of DFT precoding. The results consider an oversampled and windowed transmit signal of a single user.

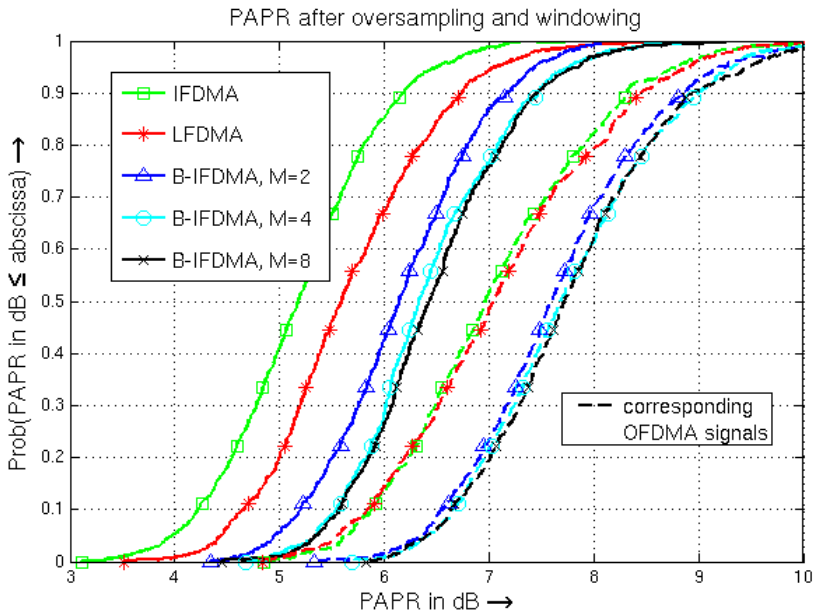

Figure A.2.1: PAPR of B-IFDMA signals with different numbers M of subcarriers per block with Q=32 subcarriers per user and QPSK modulation. Assuming rate ½ coding this corresponds to an instantaneous data rate of 1.11 Mbps (pilot overhead not considered).

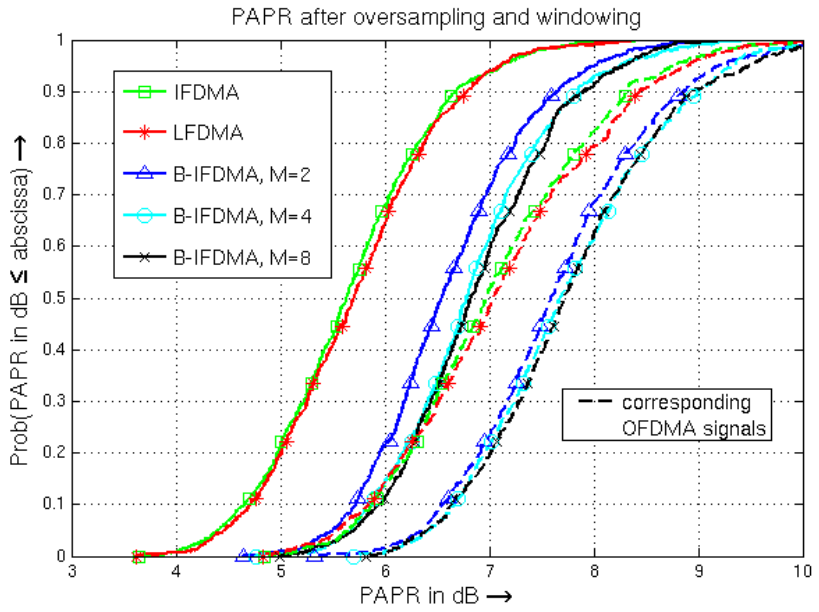

Figure A.2.2: PAPR of B-IFDMA signals with different numbers M of subcarriers per block with Q=32 subcarriers per user and 16 QAM modulation

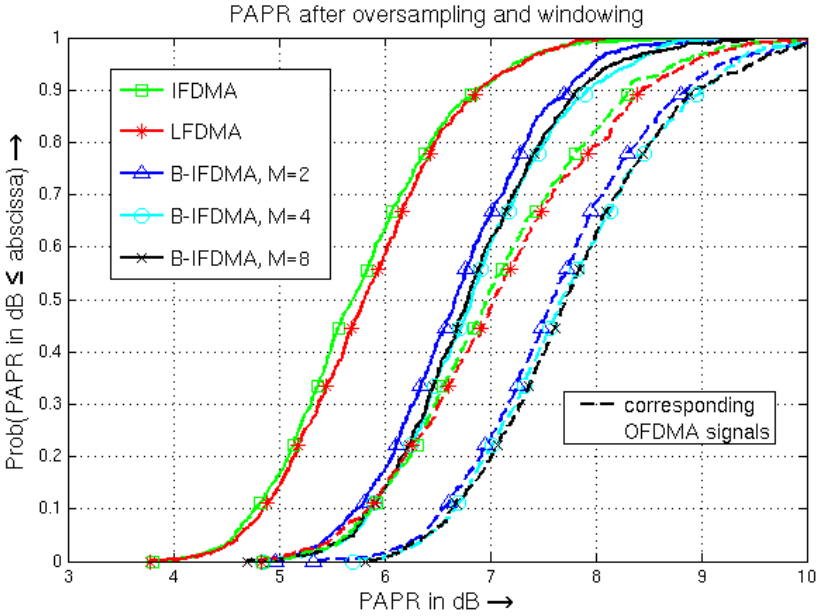

Figure A.2.3: PAPR of B-IFDMA signals with different numbers M of subcarriers per block with Q=32 subcarriers per user and 64 QAM modulation

In Table A.2.2 the average PAPR from Figures A.2.1 to A.2.3 and the corresponding Raw Cubic Metrics are given. Let $x_n^{(k)}$ denote the transmit signal of user *k* with *N* samples. The Raw Cubic Metric is defined as

$$RCM = 20\log_{10}\left(\mathrm{RMS}\left(\left(\frac{|x_n^{(k)}|}{\mathrm{RMS}(x_n^{(k)})}\right)^3\right)\right)$$

with

$$\mathrm{RMS}(x_n^{(k)}) = \sqrt{\frac{1}{N}\sum_{n=0}^{N-1}|\,x_n^{(k)}\,|^2}\ .$$

From Figures A.2.1-A.2.3 and Table A.2.2 follows that, in general, the envelope fluctuations increase with increasing number M of subcarriers per block. IFDMA which can be regarded as B-IFDMA with M=1 provides the lowest envelope fluctuations. As a special case, LFDMA which can be regarded as B-IFDMA with L=1 block provides a similar PAPR compared to IFDMA. In all cases, DFT precoding provides a significantly lower PAPR compared to OFDMA without DFT precoding. For QPSK, the PAPR is slightly better compared to 16 QAM and 64 QAM and the difference to the corresponding OFDMA signals is more pronounced. For 64 QAM the difference in the average PAPR between IFDMA and B-IFDMA with M=4 subcarriers per block is similar to the difference in the average PAPR between B-IFDMA with M=4 subcarriers per block and the corresponding OFDMA scheme. The differences in the PAPR between B-IFDMA signals with M= 2, 4, and 8 subcarriers per block are rather small. The RCM values point in the same direction as the average PAPR.

	Mod. Scheme	RCM	Average PAPR
B-IFDMA (OFDMA) M=8	QPSK	5.34 (7.82)	6.49 (7.80)
	16 QAM	6.20 (7.83)	6.87 (7.80)
	64 QAM	6.24 (7.83)	6.84 (7.81)
B-IFDMA (OFDMA) M=4	QPSK	5.31 (7.83)	6.43 (7.79)
	16 QAM	6.18 (7.83)	6.84 (7.80)
	64 QAM	6.31 (7.83)	6.87 (7.80)
B-IFDMA (OFDMA) M=2	QPSK	4.96 (7.77)	6.17 (7.68)
	16 QAM	5.97 (7.75)	6.62 (7.64)
	64 QAM	6.13 (7.77)	6.71 (7.70)
B-IFDMA (OFDMA) M=1	QPSK	3.87 (7.72)	5.19 (7.04)
	16 QAM	5.19 (7.72)	5.67 (7.04)
	64 QAM	5.47 (7.71)	5.80 (7.04)

Table A2.2: Average PAPR and RCM for B-IFDMA and corresponding OFDMA schemes (values in brackets) for different parameters and modulation schemes.

In Figure A.2.4 the dependency of the PAPR of a B-IFDMA signal with M=4 subcarriers per block on the number L of blocks is depicted.

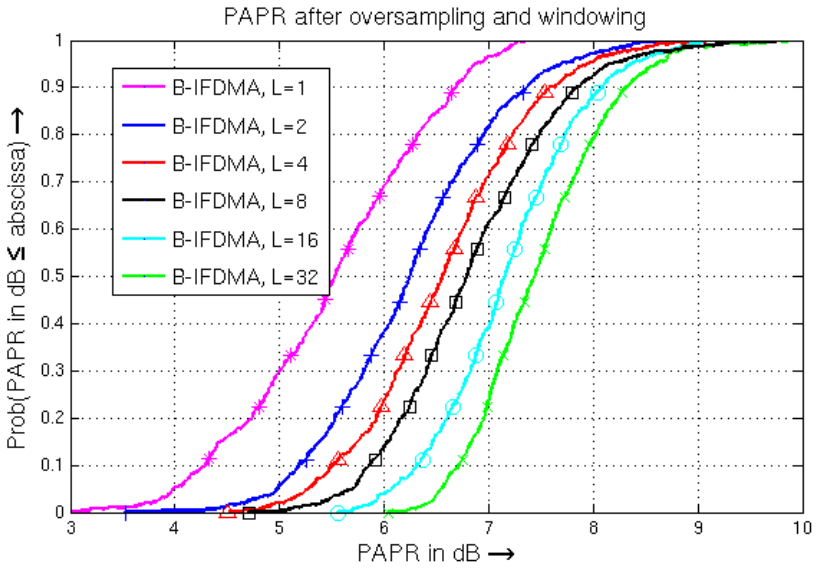

Figure A.2.4: PAPR of B-IFDMA signal for different numbers L of blocks for M=4 subcarriers per block using 16 QAM modulation

From Figure A.2.4 follows that the PAPR increases with increasing number L of blocks and, consequently, with increasing instantaneous [8]data rates.

Finally, in Figures A.2.5-A.2.8 the power spectral density of the B-IFDMA and OFDMA signals with a power back-off that is required to keep the WINNER spectral mask is shown. As an amplifier model, the Rapp model [NeP2000] with a Rapp-Parameter p=2 is used.

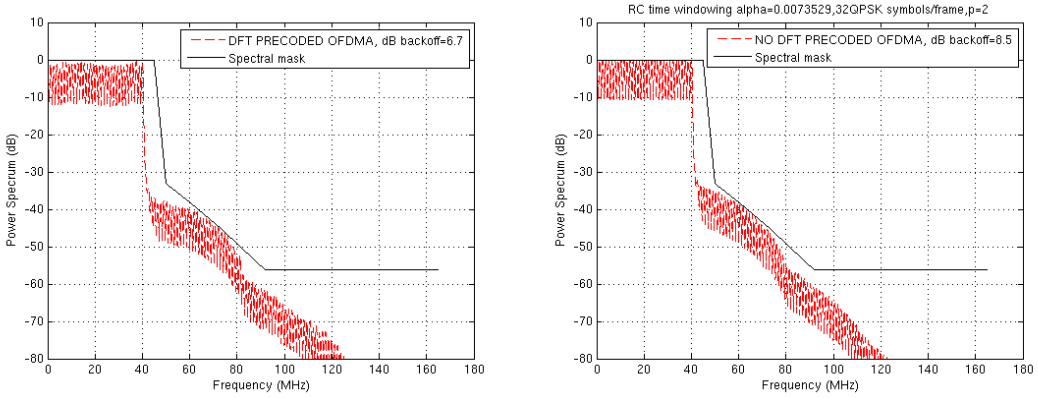

Figure A.2.5: Power spectral density keeping the WINNER spectral mask for IFDMA with 32 subcarriers per user and for OFDMA with corresponding subcarrier allocation using QPSK modulation.

[8] Although the data rate averaged over a frame can be made smaller if necessary compared to a given instantaneous data rate by introducing a TDMA component within the frame, as in the baseline assumption in [WIN2D6137], where a B-IFDMA block size of 4 subcarriers and 3 OFDM symbols is assumed out of 8 subcarriers and 12 OFDM symbols in an FDD chunk (half frame duration).

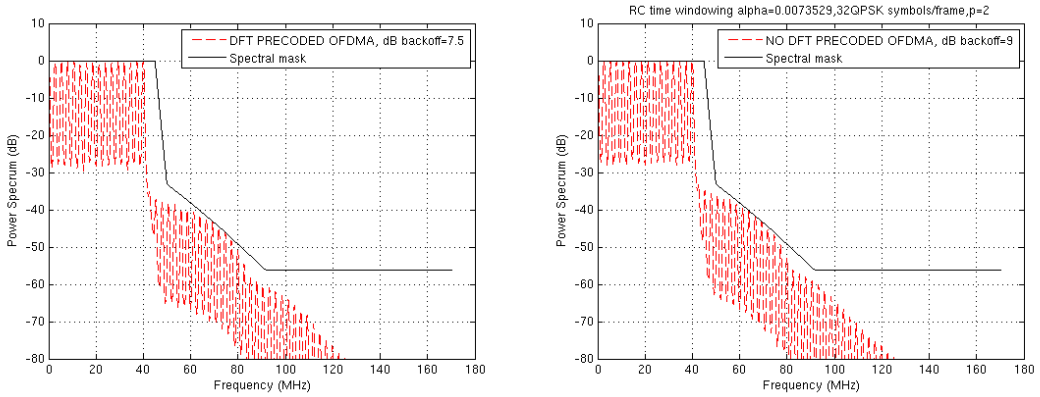

Figure A.2.6: Power spectral density keeping the WINNER spectral mask for B-IFDMA with M=2 subcarriers per block and with 32 subcarriers per user and for OFDMA with corresponding subcarrier allocation using QPSK modulation.

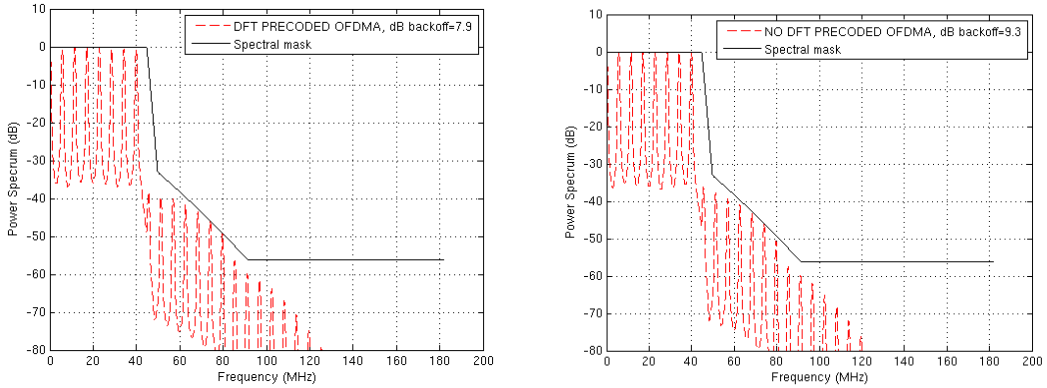

Figure A.2.7: Power spectral density keeping the WINNER spectral mask for B-IFDMA with M=4 subcarriers per block and with 32 subcarriers per user and for OFDMA with corresponding subcarrier allocation using QPSK modulation.

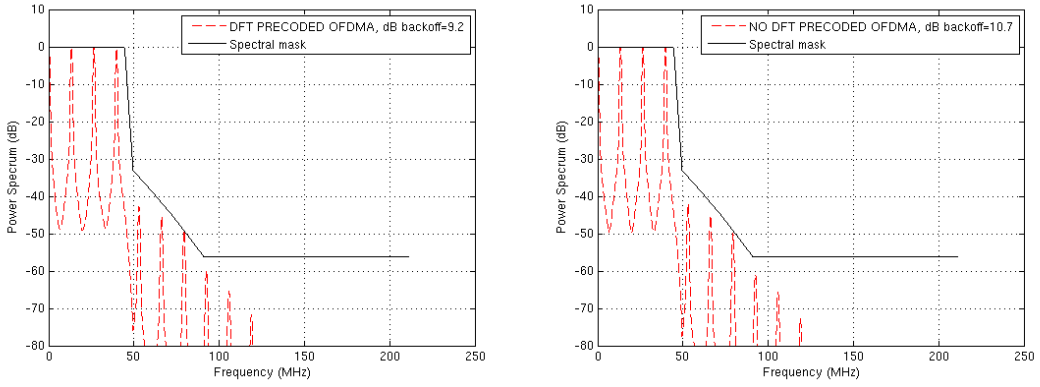

Figure A.2.8: Power spectral density keeping the WINNER spectral mask for B-IFDMA with M=8 subcarriers per block and with 32 subcarriers per user and for OFDMA with corresponding subcarrier allocation using QPSK modulation.

The required power back-offs from Figures A.2.5-A.2.8 and in a similar way obtained power back-offs for 16 QAM and 64 QAM modulation are summarized in Table A.2.3.

	QPSK		16 QAM		64 QAM	
Scheme	with DFT precoding	w/oDFT precoding	with DFT precoding	w/oDFT precoding	with DFT precoding	w/oDFT precoding
IFDMA	6,7 dB	8,5 dB	7.2 dB	8,5 dB	7.2 dB	8,5 dB
B-IFDMA, M=2	7,5 dB	9,0 dB	7.8 dB	9,0 dB	7.8 dB	9,0 dB
B-IFDMA, M=4	7,9 dB	9,3 dB	8.4 dB	9,3 dB	8.4 dB	9,3 dB
B-IFDMA, M=8	9,2 dB	10,7 dB	9.4 dB	10,7 dB	9.4 dB	10,7 dB

Table A.2.3: Required power back-off for a power spectral density keeping the WINNER spectral mask for B-IFDMA with M=8 subcarriers per block and with 32 subcarriers per user and for OFDMA with corresponding subcarrier allocation..

From Table A.2.3 it can be concluded that in case of B-IFDMA for QPSK the required power back-off is slightly lower than for 16 QAM and 64 QPSK whereas for OFDMA the required power back-off is independent from the modulation scheme. For QPSK the difference in the required power back-off of the different B-IFDMA signals is more pronounced than in 64 QAM. However, for the given parameters for 64 QAM the required power back-off for B-IFDMA with M=4 subcarriers per block is 1.2 dB higher than for IFDMA.

A.2.1.3 Performance

a) Diversity and Array Gain

In the following, the amount of frequency diversity exploited by B-IFDMA is analyzed for different parameters. In Figures A.2.9-A.2.11 performance results for B-IFDMA with an instantaneous data rate of 278 kbps, 1.11 Mbps and 2.22 Mbps (pilot overhead not considered), respectively, are given. The simulation parameters are summarized in Table A.2.3.

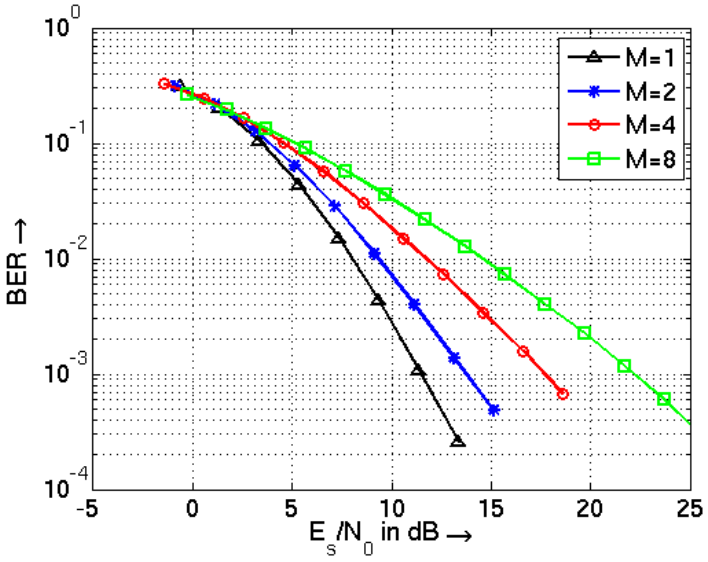

Figure A.2.9: Performance of B-IFDMA with 278 kbps, i.e., Q=8 subcarriers per user for single antenna transmission.

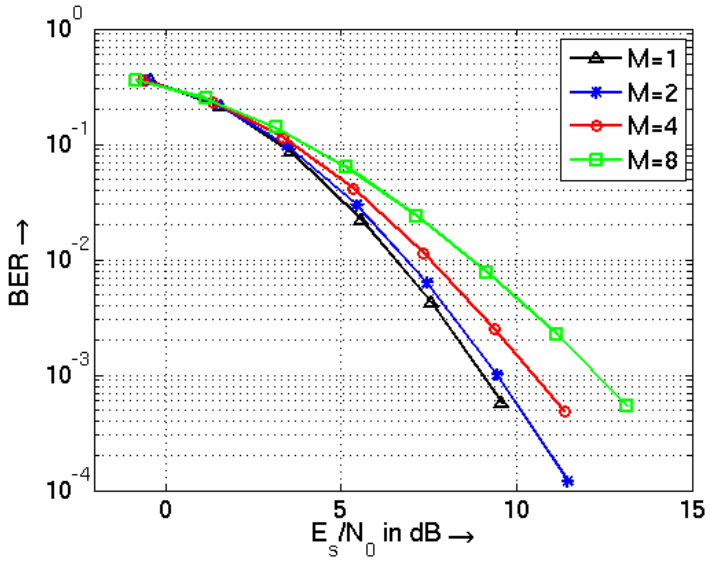

Figure A.2.10: Performance of B-IFDMA with 1.11 Mbps, i.e., Q=32 subcarriers per user for single antenna transmission.

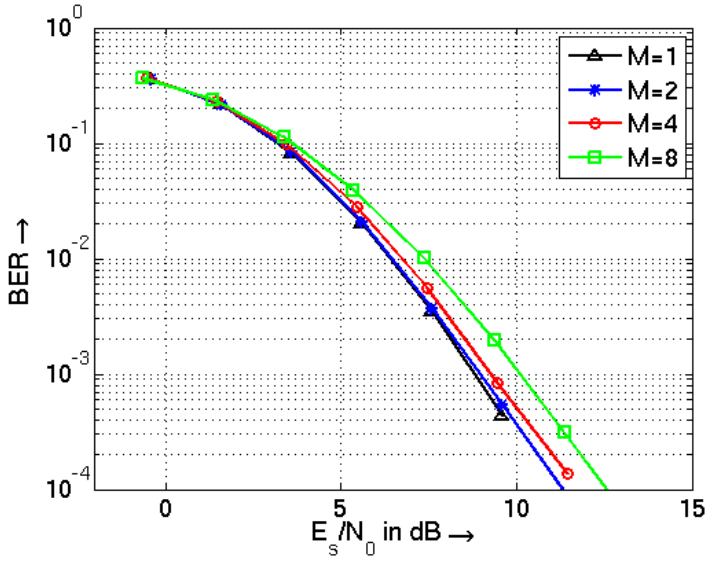

Figure A.2.11: Performance of B-IFDMA with 2.22 Mbps, i.e., Q=64 subcarriers per user for single antenna transmission.

Bandwidth	40 MHz
Total number of subcarriers	1024
Carrier frequency	3.7 GHz
Sampling rate	1/(25 ns) = 40 MHz
Modulation	QPSK
Code	Convolutional Code

Code polynomials	133, 171
Code rate	½
Constraint length	6
Code word length	1000 information bits
Decoder	BCJR [BCJR74]
Final state of the decoder	Terminated
Type of interleaving	Random
Interleaving depth	0.3 ms
Channel model	WINNER, Base Coverage Wide Area
User velocity	50 km/h
Multiple antenna scheme at Tx	Alamouti Space-Time Coding
Multiple antenna scheme at Rx	Maximum Ratio Combining (MRC)

Table A.2.3: Simulation Assumptions

The required E_s / N_0 at a BER of 10^{-3} are summarized in Table A.2.4. From the simulation results follows that, for a given data rate, i.e., for a fixed number of subcarriers assigned to a user, for a lower number M of subcarriers per block a higher frequency diversity is provided. A lower number of subcarriers per block results in a higher number of blocks. For the given parameters, within each block the channel can be assumed to change only slowly. Thus, the frequency diversity provided is higher the higher the number of blocks. This effect is reinforced for lower instantaneous data rates, i.e., for a low number of subcarriers per user since at lower instantaneous data rates the level of frequency diversity is lower and, thus, the benefit from additional diversity due to a higher number of blocks for decreasing number M is higher.

	M=1	**M=2**	**M=4**	**M=8**
278 kbps	11.5 dB	13.75 dB	17.65 dB	22.2 dB
1.11 Mbps	9 dB	9.5 dB	10.5 dB	12.25 dB
2.22 Mbps	8,75 dB	8,9 dB	9,25 dB	10.1 dB

Table A.2.4: Required E_s / N_0 at a BER of 10^{-3}

In Figures A.2.12 and A.2.13 the performance of B-IFDMA using Alamouti STC at the transmitter as well as the performance using Alamouti STC at the transmitter and in addition Maximum Ratio Combining (MRC) at the receiver is given. Compared to the single antenna case a significant spatial diversity gain and, in case of MRC, array gain is provided. Moreover, the difference in the required signal to noise ratio for different numbers of subcarriers per block is reduced. The required E_s / N_0 at a BER of 10^{-3} are summarized in Table A.2.5 assuming Alamouti STC at the transmitter and in Table A.2.6 assuming Alamouti STC at the transmitter and MRC at the receiver.

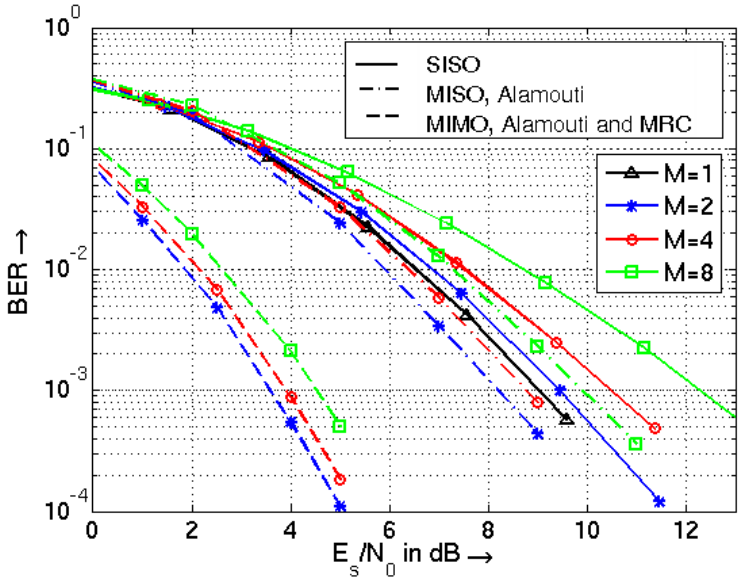

Figure A.2.12: Performance of B-IFDMA with 1.11 Mbps, i.e., Q=32 subcarriers per user for 2 transmit antennas and 2 receive antennas .

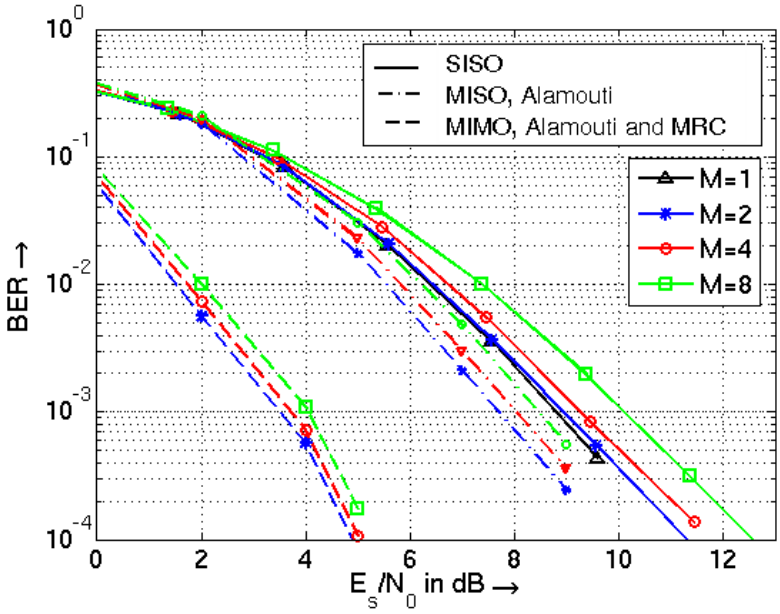

Figure A.2.13: Performance of B-IFDMA with 2.22 Mbps, i.e., Q=64 subcarriers per user for 2 transmit antennas and 2 receive antennas.

	M=2	M=4	M=8
1.11 Mbps	8.2 dB	8.8 dB	9.9 dB
2.22 Mbps	7.7 dB	8 dB	8.5 dB

Table A.2.5: Required E_s / N_0 at a BER of 10^{-3} for Alamouti STC at the trasnmitter

	M=2	M=4	M=8

1.11 Mbps	3.6 dB	3.9 dB	4.5 dB
2.22 Mbps	3.5 dB	3.7 dB	4.1 dB

Table A.2.6: Required E_s / N_0 at a BER of 10^{-3} Alamouti STC at the transmitter and MRC at the receiver.

b) Channel Estimation error

For different numbers of subcarriers per block not only different pilot symbol overhead for channel estimation is provided, but also different channel estimation errors since different interpolations depths in frequency domain are exploited and, thus, the signal experiences different interpolation errors. In Figure A.2.9 simulation results for B-IFDMA with different numbers of subcarriers per block are given assuming single antenna transmission. *IP* denotes the interpolation depth. E.g., *IP=4* denotes that within a block of 4 subcarriers one pilot symbol is transmitted. The additional required energy per symbol due to pilot symbol overhead as given in Table A.2.1 is considered as an according shift of the BER curve to the right.

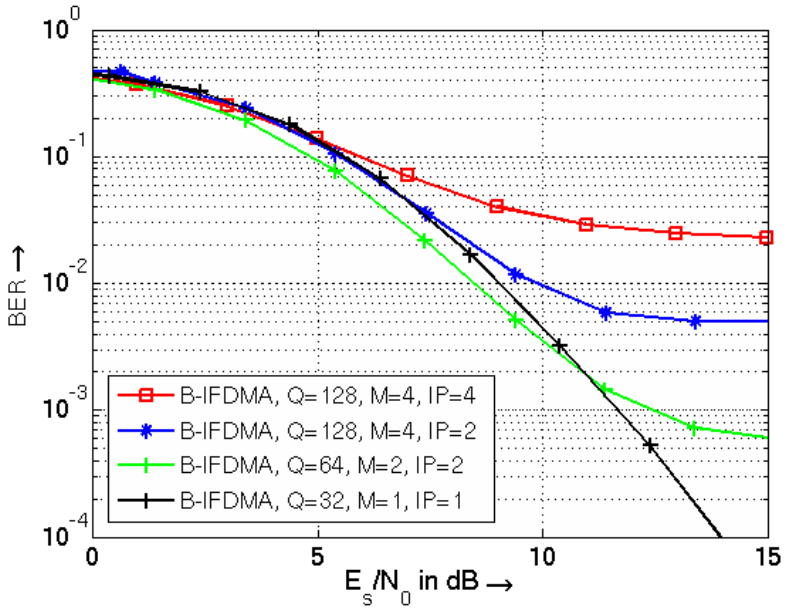

Figure A.2.14: Performance of B-IFDMA with pilot assisted channel estimation..

From Figure A.2.14 follows that although the overhead increases for lower numbers of subcarriers per block the channel estimation error decreases. Thus, for the given channel estimation algorithm and the given scenario at low BERs B-IFDMA with a low number of subcarriers per block provides better performance compared to B-IFDMA with a higher number of subcarriers per block, even if the higher pilot symbol overhead is taken into account.

A.2.1.4 Computational Complexity

Similar to IFDMA, also for B-IFDMA a low complexity implementation in time domain is possible. The computational complexity is dependent on the number of subcarriers per block *M* and can be shown to be given by

$$C_{Tx,eff.} = N \cdot M \quad , \tag{A.2.2}$$

where $C_{Tx,eff.}$ denotes the required number of complex multiplications, M denotes the number of subcarrier per block and N denotes the number of subcarriers in the system. Using the conventional implementation, the computational effort depends on the number Q of subcarriers assigned to a user and is given by

$$C_{Tx,conv.} = \frac{Q}{2}\mathrm{ld}(Q) + \frac{N}{2}\mathrm{ld}(N) \quad . \tag{A.2.3}$$

From Eq. (A.2.2) follows that the computational complexity decreases with decreasing number of subcarriers per block. Moreover, compared to the conventional implementation, for numbers of subcarriers per block smaller than 4 the efficient implementation requires up to factor 8 less complex multiplications compared to the conventional implementation.

A.2.1.5 Conclusions

Summarizing the investigation of the different properties of B-IFDMA it can be concluded that for a given number of 3 consecutive OFDM symbols assigned to a user, B-IFDMA combines good performance due to good exploitation of frequency diversity and promising signal characteristics such as low envelope fluctuations with potential power efficiency due to micro sleep modes. Regarding the effect on different numbers of subcarriers per block, the investigations provided here show that for the given number of 3 consecutive OFDM symbols assigned to a user, a further reduction of the number of subcarriers per block is possible and beneficial in terms of performance, complexity and envelope fluctuations, whereas a further increase of the number of subcarriers per block is not recommended. For a given number of subcarrier assigned to a user a reduction of the number of subcarriers per block enables a better exploitation of frequency diversity. Together with the decrease of the interpolation error for channel estimation the effect of increased pilot symbol overhead is nearly compensated. At the same time, a lower number of subcarriers per block for B-IFDMA leads to a reduced complexity of the user terminal for signal generation and lower envelope fluctuations.

A.2.2 Performance of B-IFDMA in the WINNER system concept

In this chapter, we have evaluated partially the link level performance of the B-IFDMA defined in the baseline of WINNER II system concept [WIN2D6137]. We have investigated two possibilities to improve the performance. One is a multi frames structure, and another corresponds to a multi receive antenna technique.

A.2.2.1 Baseline Evaluation

System Parameters

We have evaluated the performance of B-IFDMA uplink defined in [WIN2D6137] for the base coverage urban FDD mode. The system parameters are given in Table A.2.7. Each user spreads his coded and modulated symbols into 16 chunks and occupies a block of 4 subcarriers x 3 OFDM symbols in each chunk. The number of blocks is 16 with a distance of 4 chunks between two adjacent B-IFDMA blocks. Thus, a user can transmit 192 modulation symbols in a code block spanning one chunk duration, disregarding unusable pilot symbol positions. The numbers of information bits for all the code rates are given in Table A.2.8. The UMTS interleaver is considered.

Table A.2.7: Simulated system parameters

Sampling frequency	80 Mhz
Number of FFT points	2048
Guard interval	256
Number of available subcarriers	512
Mobile Channel, speed	C2, 50 km/h
Chunk size	8 subcarrieres x 12 OFDMA symbols
Block size	4 subcarrieriers x 3 OFDM symbols

IFDMA size	N=16
Chunk distance	4
Modulation	QPSK and 16-QAM
Mother code of convolution code	G1=561, G2=753
Mother code of turbo code	Code of UMTS with coding rate 1/3
Code Rate (R)	1/2, 2/3 and 3/4
Channel estimation	Perfect

Table A.2.8: parameters for modulation and coding scheme

MCS	3	4	5	6	8
Mod.	QPSK			16-QAM	
R	1/2	2/3	3/4	1/2	3/4
Info size	192	256	288	384	576

System Model

A B-IFDMA signal can be generated either as a sum of a few adjacent IFDMA signals, or with one common DFT precoding matrix [WIN2D461][9]. Here we assume the first method. Each IFDMA signal can be seen as a full load MC-CDMA [FKC+05] with particular spreading codes as following:

$$\mathbf{c}_k = \left(c_k^1, \cdots, c_k^l, \cdots c_k^N\right)^T = \left(1, \cdots e^{j\frac{2\pi}{N}(l-1)(k-1)}, \cdots, e^{j\frac{2\pi}{N}(N-1)(k-1)}\right)^T,\ k = 1,2,\cdots N \quad \text{(A.2.4)}$$

Each symbol k is spread into N subcarriers (chips) by $\mathbf{c}_k$. All the symbols are spread into the same group of N chips. As compared to the basic MC-CDMA, the number of users for MC-CDMA becomes the number of symbols for an IFDMA block. As one IFDMA block transmits always N modulated symbols, the corresponding MC-CDMA is always full load and all the symbols in an IFDMA block belong be the same user. The multiple access of IFDMA corresponds to assigning different groups of subcarriers to different users. For N_R receive antennas, the received signal as a vector of $N\,N_R$ elements can be defined as:

$$\mathbf{r} = \mathbf{A}\mathbf{d} + \mathbf{z} \quad \text{(A.2.5)}$$

where $\mathbf{d}$ consists of transmit N symbols in an IFDMA block and is called the N dimension data vector defined as

$$\mathbf{d} = \left(d_1, \cdots, d_k, \cdots, d_N\right)^T \quad \text{(A.2.6)}$$

the transition matrix, $\mathbf{A}$, containing the overall spreading and channel influence, is an $N\,N_R \times N$ matrix determined by spreading codes, c_k^l, and channel gain, $H_l^{(n_r)}$ with l = 1,2,…, N, and n_r = 1, …, N_R and is defined as

[9] In [WIN2D461] it is shown that generating the B-IFDMA signal as a sum of frequency-adjacent IFDMA signals results in larger envelope fluctuations, implying a larger requirement on power amplifier backoff to meet the spectral requirement mask. However, the overall conclusions on performance in this chapter should be similar also for receivers adapted to B-IFDMA signals generated with a common DFT precoding matrix.

$$\mathbf{A} = \begin{bmatrix} H_1^{(1)}c_1^1 & \cdots & H_1^{(1)}c_N^1 \\ \vdots & & \vdots \\ H_N^{(1)}c_1^N & & H_N^{(1)}c_N^N \\ \vdots & & \vdots \\ H_1^{(N_R)}c_1^1 & \cdots & H_1^{(N_R)}c_N^1 \\ \vdots & & \vdots \\ H_N^{(N_R)}c_1^N & & H_N^{(N_R)}c_N^N \end{bmatrix} = \begin{pmatrix} \mathbf{H}^{(1)}\mathbf{C} \\ \vdots \\ \mathbf{H}^{(N_R)}\mathbf{C} \end{pmatrix} \quad \text{(A.2.7)}$$

with $\mathbf{C} = \left(\mathbf{c}_1, \cdots, \mathbf{c}_k, \cdots \mathbf{c}_N\right)$and $\mathbf{H}^{(n_r)} = diag\left(H_l^{(n_r)}\right)$ and $\mathbf{z}$ is the noise vector with all elements being independent complex Gaussian variables with zero mean and variance $\sigma_0^2 = \sigma^2/(N\ N_R)$. The detectors estimate the $N \times 1$ data vector from the $N\ N_R \times 1$ received signal vector. Note that in our B-IFDMA, one user has 4 IFDMA blocks side by side and the channel gain, $H_l^{(n_r)}$, are constant for the other IFDMA blocks in the same frame as the channel gains are considered constant within a chunk. The receive signal can also be expressed as

$$\mathbf{r} = \begin{bmatrix} \mathbf{r}^{(1)} \\ \vdots \\ \mathbf{r}^{(N_R)} \end{bmatrix} = \begin{bmatrix} \mathbf{H}^{(1)}\mathbf{C} \\ \vdots \\ \mathbf{H}^{(N_R)}\mathbf{C} \end{bmatrix} \mathbf{d} + \mathbf{z} \quad \text{(A.2.8)}$$

Note that for the baseline conception, WINNER II considerer $N_R = 1$.

Symbol detection Techniques

MMSE

The symbol detector is also called as signal equaliser. The equaliser based on MMSE criterion is defined as a basic equalisation technique used for WINNER II [WIN2D6137]. The MMSE can be applied carrier by carrier, called here MMSE-PC (per carrier). For MMSE-PC, the data vector is detected by

$$\hat{\mathbf{d}}_{mmse\_pc} = \mathbf{C}^H \mathbf{W} \sum_{n_r=1}^{N_R} \left(\mathbf{H}^{(n_r)}\right)^* \mathbf{r}^{(n_r)} \quad \text{(A.2.9)}$$

$$\text{with} \qquad \mathbf{W} = diag\left(\frac{1}{\sum_{n_r=1}^{N_r} \left| H_l^{(n_r)} \right|^2 + \frac{\sigma^2}{N}} \right) \quad \text{(A.2.10)}$$

Another option is a symbol by symbol MMSE detector, called here MMSE-PS (per symbol). For MMSE-PS, the data vector is detected by

$$\hat{\mathbf{d}}_{mmse\_ps} = (\mathbf{A}^H\mathbf{A} + \sigma^2\mathbf{I})^{-1}\mathbf{A}^H\mathbf{r} = \mathbf{B}^{-1}\mathbf{A}^H\mathbf{r} \quad \text{(A.2.11)}$$

$$\text{with} \quad \mathbf{B} = \mathbf{A}^H\mathbf{A} + \sigma^2\mathbf{I} \quad \text{(A.2.12)}$$

For a no full load MC-CDMA system, the MMSE-PS outperforms the MMSE_PC. But for the one user and full load cases, they provide the same performance. As IFDMA corresponds to a full load MC-CDMA. These two detectors (A.2.9) and (A.2.11) are the same.

E-MAP-DFE

We have described the E-MAP-DFE in [Yua06], which is an enhanced version of MAP-DFE [KW02]. The Maximum A posterior Probability Decision Feedback Equaliser (MAP-DFE) is a local iterative

interference cancellation (IC) technique. At each iteration *i*, we perform four operations: MMSE-PS, MAP, threshold selection and IC. The key idea is to use the estimated a posteriori error probabilities of the MMSE-PS output symbols (Pes) to determine a segment of symbols to be output from MAP-DEF detector. The condition to determine the symbols in this segment is that the symbols' Pes be lower than a given threshold. If no candidate satisfies the above condition, the symbol with the lowest Pes will be assigned in the segment. At iteration *i*, The influences of the selected symbols on the matrices $\mathbf{A}^{(i)}$ and $\mathbf{B}^{(i)}$ and on the signal vector $\mathbf{r}^{(i)}$ will be cancelled by IC operation by supposing that the hard decisions on the selected symbols are correct.

In the enhanced MAP-DFE (E-MAP-DFE) [Yua06], two enhancement techniques are introduced: 1) an in phase and quadrature (IQ) separation for the received signal and for the channels coefficients in order to apply the MAP-DFE in the real domain, and 2) apply a Pes estimation more precisely by taking into account the influences of the nulling matrix, the end to end matrix and the MAI contribution. If only the IQ processing is considered, we call the corresmonding MAP-DFE as IQ-MAP-DFE. If only the more precise Pes is taken into account, we call it $\text{MAP}_{\text{optimum}}$-DFE. The E-MAP-DFE can also be noted as IQ-$\text{MAP}_{\text{optimum}}$-DFE.

Note that for a MAP-DFE based detector, MMSE-PS should be used except the initial iteration where all the *N* symbols are dealt with. For the iterations followed the initial one, as some symbols have been output, the MC-CDMA non full load case is encountered.

Iterative PIC

To construct the feedback symbols, the iterative Parallel Interference Cancellation (PIC) detector uses the output of the channel decoder. By considering the Viterbi decoder, the output of the channel decoding will be re-encoded, re-interleaved and re-mapped to form the feedback signal for the feedback input of the iterative PIC detector. At the initial iteration, in general, the MMSE-PC detector can be used. At the following iteration, after the interference cancellation, a maximum ratio combiner is used. Indeed, the PIC detector uses the iterative feedback input

$$\widetilde{\mathbf{d}}^{(fb)} = \left(\widetilde{d}_1^{(fb)},\ \widetilde{d}_2^{(fb)},\ \cdots,\ \widetilde{d}_N^{(fb)} \right)^T \tag{A.2.13}$$

to get the iterative output vector

$$\hat{\mathbf{d}}_{\textbf{iterative-PIC}} = (\hat{d}_{it\text{-}PIC,\,1}, \hat{d}_{it\text{-}PIC,\,2}, \cdots, \hat{d}_{it\text{-}PIC,\,N})^T, \tag{A.2.14}$$

where

$$\begin{aligned} \hat{d}_{it\text{-}PIC,k} &= \mathbf{A}^H(k)\left(\mathbf{r} - \mathbf{A}\widetilde{\mathbf{d}}^{(fb)} + \mathbf{A}(k)\widetilde{d}_k^{(fb)} \right) \\ &= \mathbf{A}^H(k)\left(\mathbf{r} - \sum_{k'=1, k'\neq k}^{N} \mathbf{A}(k')\widetilde{d}_{k'}^{(fb)} \right) \end{aligned} \tag{A.2.15}$$

and $\mathbf{A}(k)$ denotes the *k*-th column of $\mathbf{A}$. The vectors **A** and **r** are recorded in the detector for all iterations.

Genie PIC

To show the performance limit of a coded B-IFDMA system, we use also the Genie PIC detector, which corresponds to the PIC detector of (A.2.15) with the feedback input being the exact transmit symbols.

Simulation Results

In WINNER II concept, the non frequency adaptive B-IFDMA is used to substitute the frequency adaptive transmission when the later can not work well. The performance target is BLER= 10%. In Figure A.2.15, we show the performance of B-IFDMA with QPSK modulation and with MMSE detector. From the figure we can see that for the performance target, the required SNR= Eb/N0 are 6.4 , 7.6 and 8.6 dB for R= 1/ 2, 2/3 and 3/4 respectively. These performances can not be considered good when we have the minimum SNR of 7 dB for frequency adaptive transmission good working (see table III in [SSO+07]). In addition, with real channel estimation, we will have some performance loss, which we expect to be less than 2 dB.

To improve the performance, we can use some more complex symbol detectors as described above. Figure A.2.16 shows the obtained BLER performance for IQ-MAP-DFE and iterative PIC detectors. For comparison purpose, the performance curves of MMSE detector are also reported. At the performance target of BLER equal to 10^{-1}, The iterative PIC detector requires SNR of 5.5 , 6.8 and 7.6 dB for R= 1/ 2, 2/3 and 3/4 respectively, which corresponds to the gains of 0.9, 0.8 and 1.0 dB as compared to MMSE detector. For IQ-MAP-DFE, the gains with respect to (w.r.t.) MMSE are 0.4, 0.6 and 1.2 dB for R= 1/ 2, 2/3 and 3/4 respectively. We remark that the IQ-MAP-DFE is more robust at high data rate. However iterative PIC is stable for different data rate. To show the performance limit of the B-IFDMA system, we also provide the BLER curve of the genie PIC detector for R = 1 / 2. The required SNR is 4 dB. If a loss of 2 dB for a real channel estimation is considered, we can say that whatever we do on the optimisation of symbol detector, we can not decrease the required SNR less than 6 dB for the baseline configuration of B-IFDMA.

In Figure A.2.17, we illustrate the BER performance of B-IFDMA for all considered detectors. From the figure, we note that the iterative PIC has not any gain as compared to MMSE and that the IQ-MAP-DFE obtained a gain of 1.5 dB for R=3/4 and a gain of 0.9 dB for R=2/3, at BER=10^{-3}. No gain is observed for R=1/2.

For 16-QAM modulation, we show the BLER and BER performances in Figures A.2.18 and A.2.19. In addition to the MMSE, iterative PIC and IQ-MAP-DFE detectors as for QPSK, here we have considered other two detectors: IQ-MAP-DFE with α=0.4 and soft IC and E-MAP-DFE with α=0.4 and soft IC. The parameter α has been introduced in [Yua06]. The soft IC means that for the interference cancellation operation in IQ-MAP-DFE or E-MAP-DFE, the soft values of output symbols (not the hard decision) according to the Pes obtained at MAP operation are used to provide the interference cancelled signal vector $\mathbf{r}^{(i+1)}$. When we compared the three detectors: MMSE, iterative PIC and IQ-MAP-DFE, we observe that at the performance target of BLER=10^{-1} the iterative PIC detector performs a gain of 1.8 or 1.5 dB w.r.t. the MMSE detector for R=1/2 or ¾ respectively; but no gain for BER. However the IQ-MAP-DFE detector performs a gain of 0.5 or 2.0 dB w.r.t the MMSE detector at BLER=10^{-1} and for R=1/2 or ¾ respectively; the gain is 0.6 for R=1/2 or 2.8 dB for R=3/4 at BER=10^{-3}. Although the gain of IQ-MAP-DFE at low code rate is small, the gain at high code rate is important. The new detector, IQ-MAP-DFE (or E-MAP-DFE) with α=0.4 and soft IC, can compensate the shortage of IQ-MAP-DFE. The new detectors perform 1.3 and 2.5 dB of gain w.r.t the MMSE detector at BLER=10^{-1} and for R=1/2 and ¾ respectively; the gain becomes 1.3 or 3.6 dB for R=1/2 or ¾ respectively and at BER=10^{-3}.

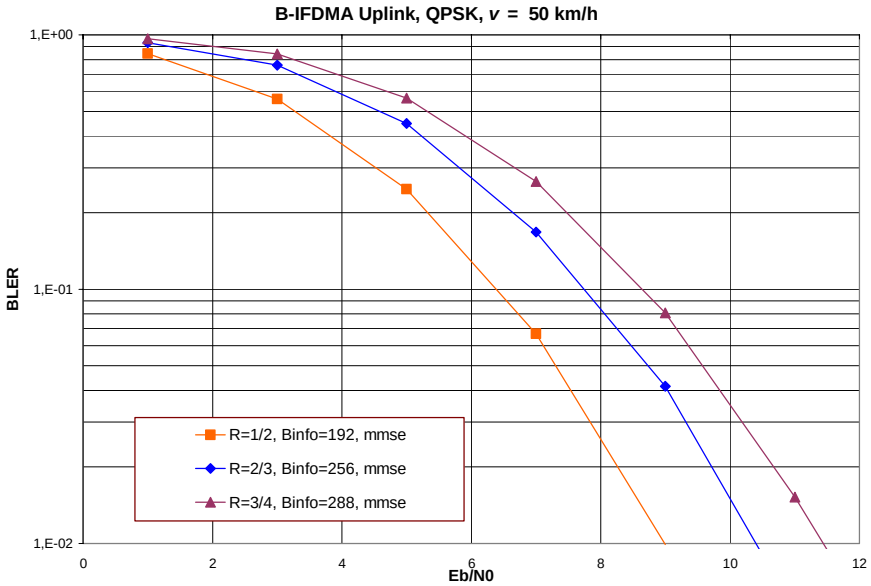

Figure A2.15: BLER performance of B-IFDMA for the basic configuration.

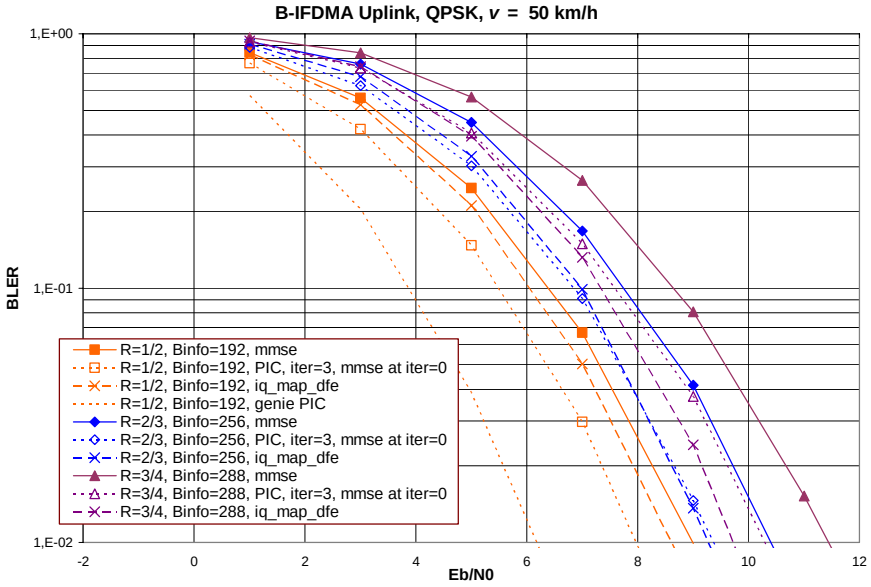

Figure A.2:16: BLER performance of B-IFMA for the improved detection techniques

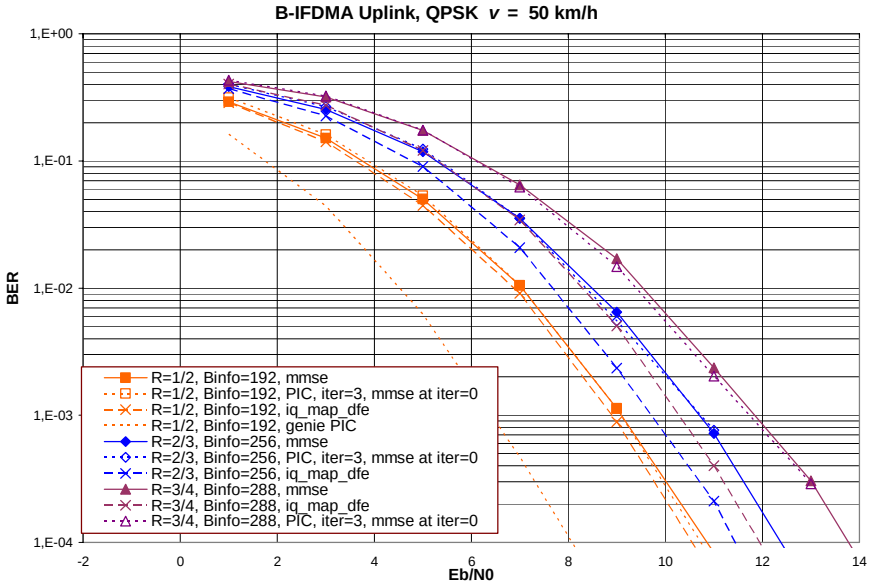

Figure A2.17: BER performance of B-IFDMA

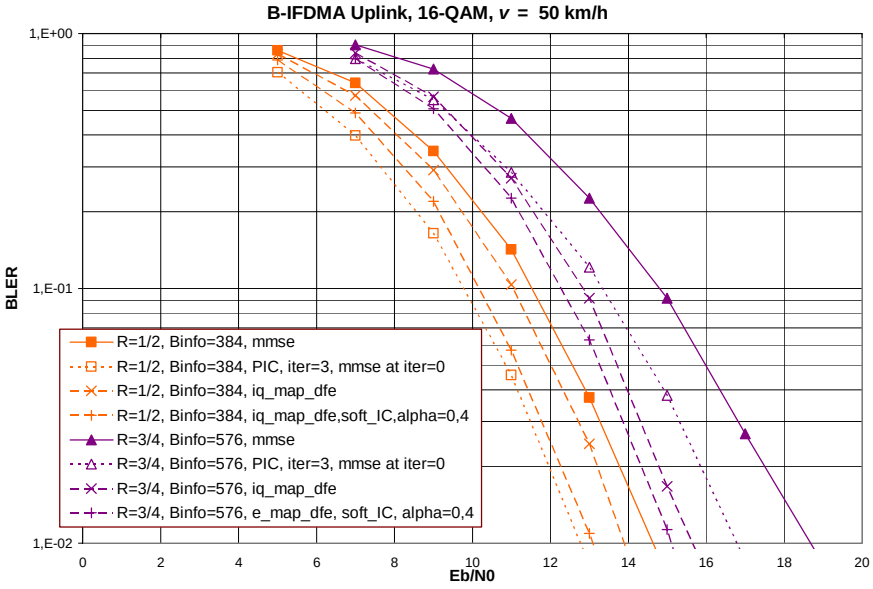

***F*igure A.2.18: BLER performance of B-IFDMA with 16-QAM**.

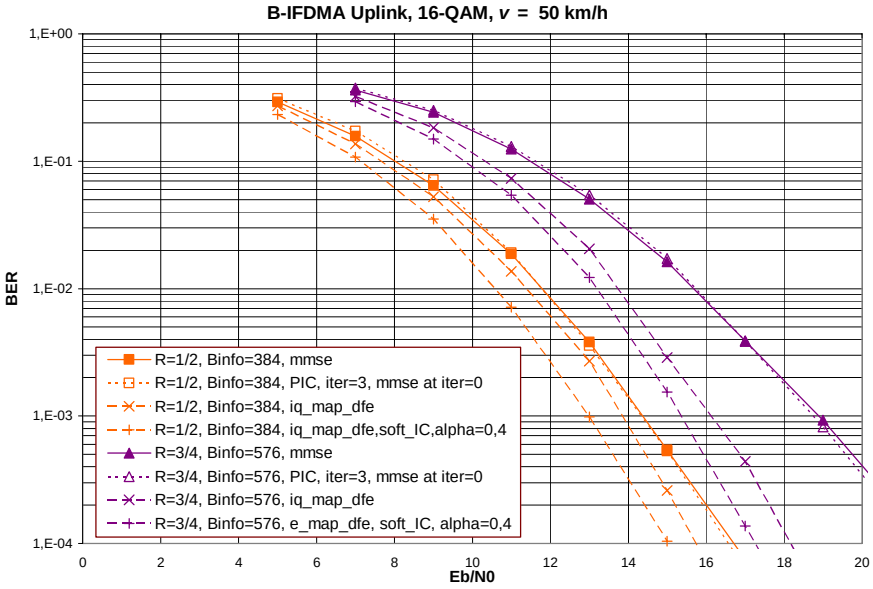

Figure A.2.19: BER performance of B-IFDMA with 16-QAM.

A.2.2.2 Channel coding over two frames

To improve the B-IFDMA performance, we intend to increase the information size of channel coding. We aim to collect some time diversity when the mobile moves with a speed of 50 km/h. So one coded block is distributed into two frames. The number of information bits in a coded block is double. For R=1/2, we have the information size equal to 384 bits instead of 192 bits. For comparison purpose, we have increased the mobile speed to 100 km/h to see how the performance evolves. Also for comparison, we have considered the case where we have also doubled the coded block size, but we use two lots in a same frame. So each user spreads his coded and modulated symbols into 16 chunks and occupies two lots of 4 subcarriers x 3 OFDM symbols in each chunk. This configuration allows to provide the performance reference without time diversity. Figure A.2.20 shows the obtained BLER performance for the code rate equal to R=1/2 and for the three above configurations. As iterative PIC has good BLER performance for this code rate, in our simulation, we have considered the iterative PIC and of course the basic MMSE. From the figure, we can observe that for the basic MMSE detector, the double frames improves 0.5 dB as

compared to the double lots in one frame; and that we can obtain another 0.2 dB of gain if the mobile speed increases to 100 km/h. For the PIC detector, a gain more than 1 dB is obtained for all the three configurations. The iterative PIC requires SNR of 5, 4.6 and 5.4 dB for the cases of two frames, two frames with v=100km/h and two lots in one frame, respectively. The BER performance is given in the Figure A.2.21. We observe some small gain of the iterative PIC detector as compared to the MMSE detector. The gain obtained by the iterative PIC detector comes from that the channel decoder is more powerful in the presence of time diversity in coded bits.

As the information size is double compared to the baseline assumption above, we would study the influence of the channel coding type on the performance. Normally, Turbo code works better with larger information size. In Figures A.2.22 and A.2.23, we illustrate the BLER and the BER performance of B-IFDMA with Turbo and convolutional codes with R=1/2 for both and for QPSK and 16-QAM. As looking on the BLER performance, the turbo code gives a gain of about 0.7 dB for QPSK and for the three configurations and a gain of 0.8, 1.0 or 1.2 dB for 16-QAM and for the configurations of two lots in one frame, two frames or two frames with v=100 km/h, respectively. The increase of gain from QPSK to 16-QAM should be caused by the increase of the information size. However for the BER performance, the gain remains to less than 0.5 dB whatever the modulation and the code block configuration.

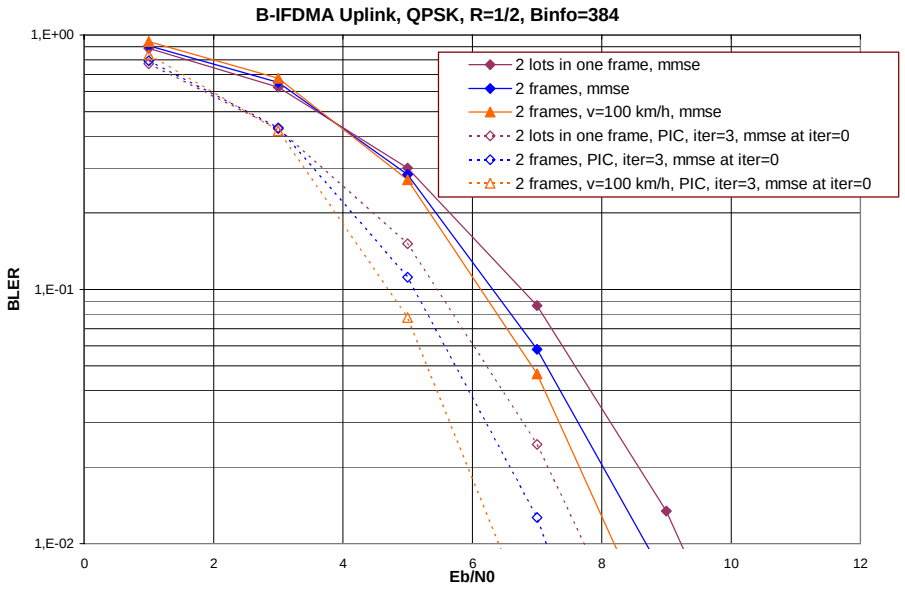

Figure A.2.20: BLER Performance improvement by increasing the coded block size.

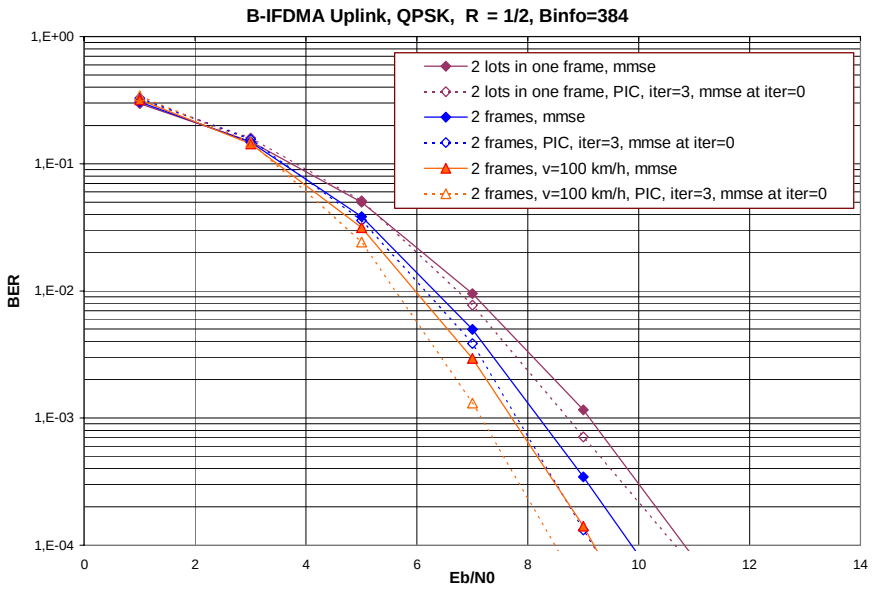

Figure A.2.21: BER Performance improvement by increasing the coded block size.

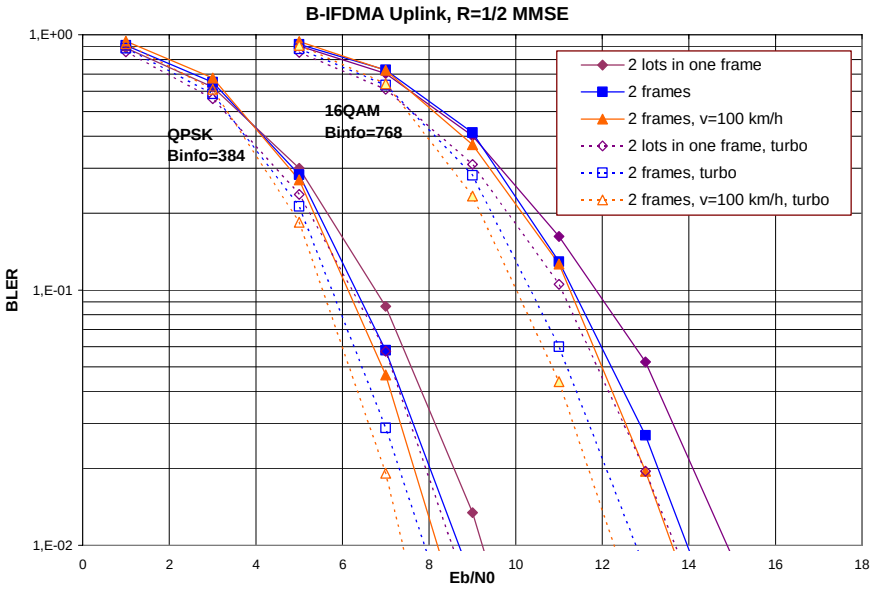

Figure A.2.22: Turbo code and convolutional code comparison on the BLER performance.

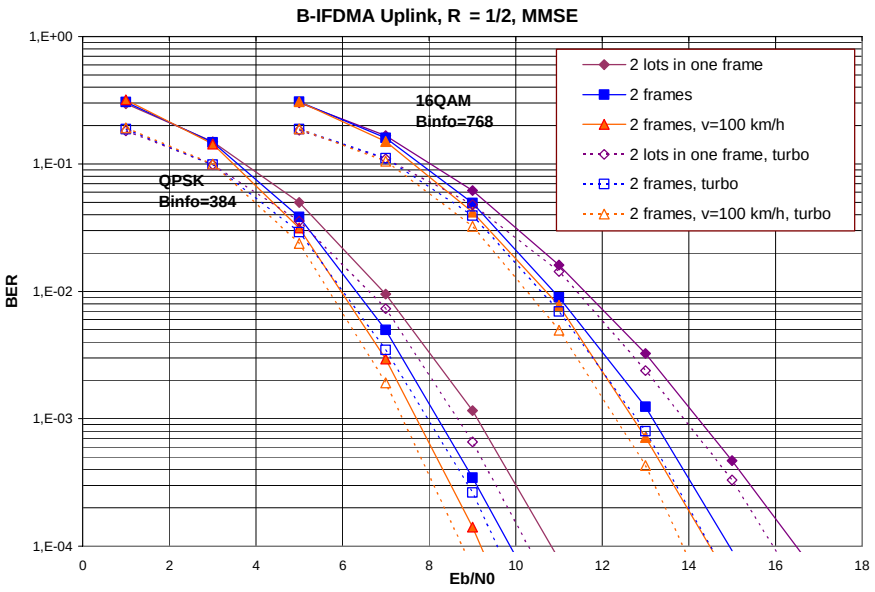

Figure A.2.23: Turbo code and convolutional code comparison on the BER performance

A.2.2.3 IFDMA size increase

The small gain of the previous section due to the information size increasing, the time domain diversity and the turbo code availability encourages us to double the IFDMA size. We will maintain the coded bits inside one frame to not increase the coding delay and to have some more diversity come from the frequency domain. So with the IFDMA size equal to 32, we have the information size equal to 384 bits and 786 bits for R=1/2 and for QPSK and 16-QAM respectively; and the size increases to 576 bits and 1152 bits for R=3/4. When the chunk distance equal to 4, the B-IFDMA signal is spread onto 128 chunks or 1054 subcarriers. When the chunk distance equal to 2, the B-IFDMA signal is spread onto 512 subcarriers. Recall that in the baseline concept, as IFDMA size equal to 16 and chunk distance equal to 4, the B-IFDMA signal is spread onto 512 subcarriers. The Figures A.2.24 and A.2.25 show the BLER and BER curves for the coding rate R=1/2 and for the MMSE and the IQ-MAP-DFE with α=0.4 and soft IC detectors. For comparison purpose, the curves of the two frames structure of the previous section are reported also. From these figures, we can see that for IFDMA size equal to 32, the case of chunk distance equal to 2 provide a little better performance than the case of chunk distance equal to 4: about 0.2 dB of gain. As the second case has little more frequency diversity than the first case, we should expect an inverse situation appears. We could explain this by the counter point of the intersymbol interference. As compared to the two frames basic B-IFDMA, the B-IFDMA with IFDMA size equal to 32 and chunk distance equal to 2 provides almost the same performance. From detector point of view, the IQ-MAP-DFE with α=0.4 and soft IC outperforms the MMSE; the gain becomes significant for 16-QAM: about 1.5 dB. The Figures A.2.26 and A.2.27 show the BLER and BER curves for the coding rate R=3/4. The advantage of the chunk distance equal to 2 over equal 4 is conserved, but with smaller gain: about 0.1 dB. The B-IFDMA with IFDMA size equal to 32 and chunk distance equal to 2 outperforms a little the two frames basic B-IFDMA. The IQ-MAP-DFE with α=0.4 and soft IC provides 1.5 dB and 2.5 dB gain for QPSK and 16-QAM modulations respectively.

To conclude this section, we can confirm that if we need to double the information size in a code block, we can use a B-IFDMA with the IFDMA size equal to 32 instead to use two system frames.

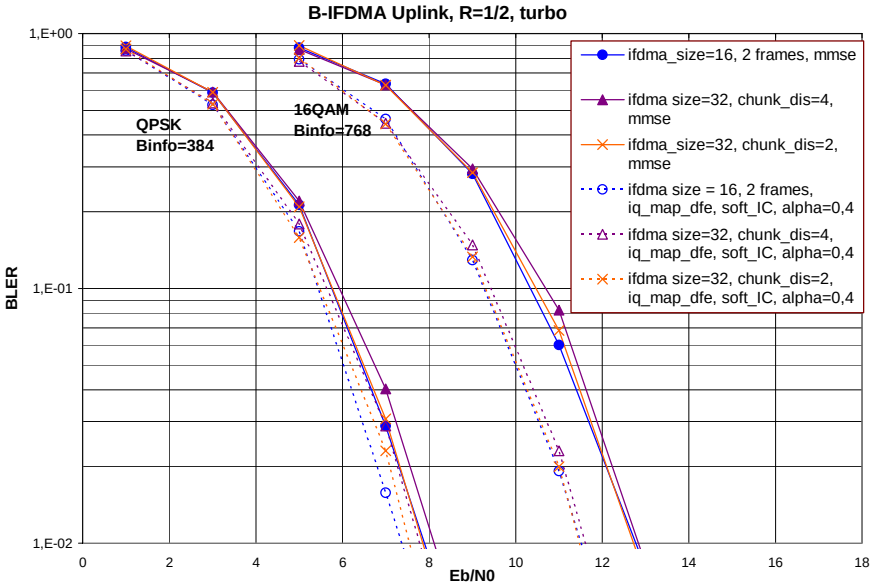

*Fi*gure A.2.24: BLER performance for the IFDMA size equal to 32 and R=1/2.

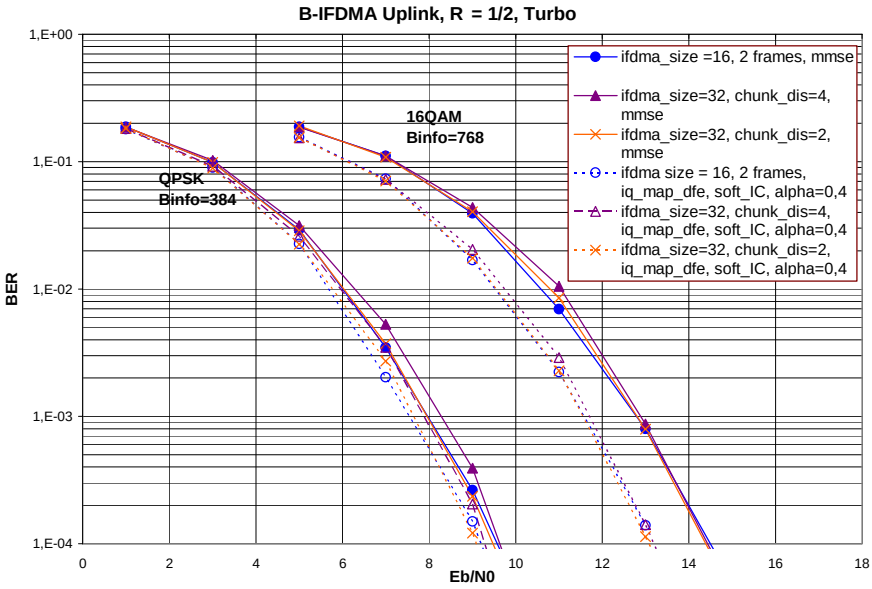

Figure A.2.25: BER performance for the IFDMA size equal to 32 and R=1/2.

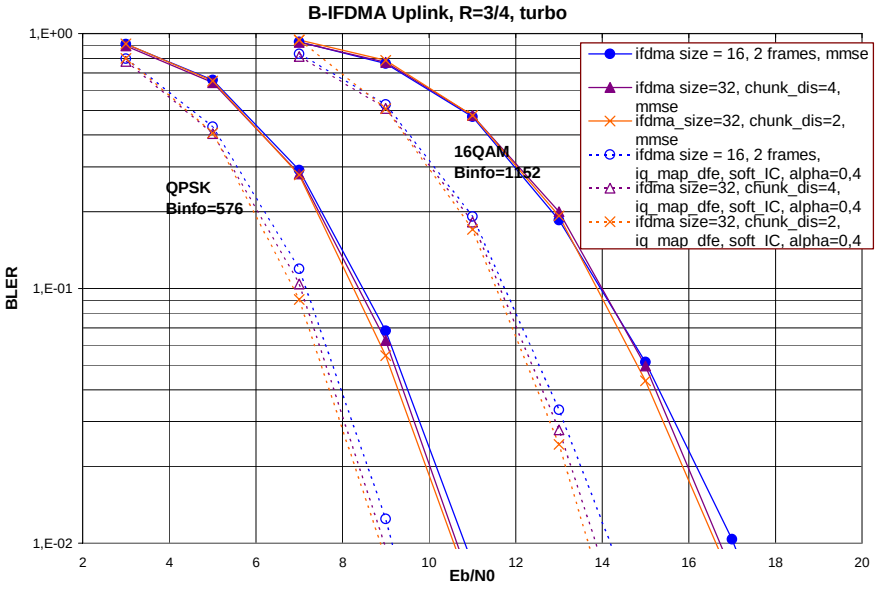

Figure A.2.26: BLER performance for the IFDMA size equal to 32 and R=3/4.

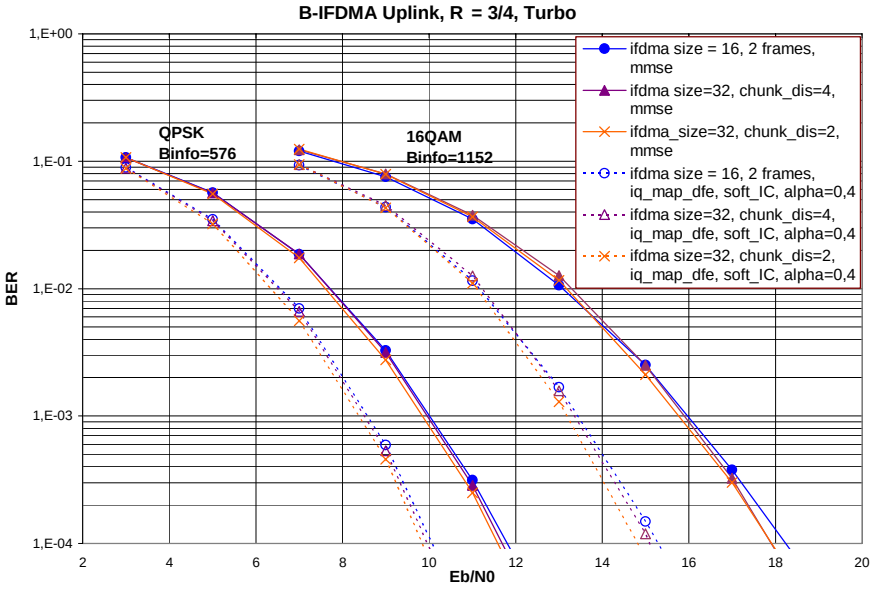

Figure A.2.27: BER performance for the IFDMA size equal to 32 and R=3/4.

A.2.2.4 Receive Diversity

As channel gains in different subcarriers (chips) of IFDMA cause the intersymbol interference (ISI), which leads to important performance loss as compared to the performance limit obtained by the fictitious genie PIC, we try to decrease the subcarrier gain difference. One way is to introduce the receive diversity; so channel gain at each subcarrier is an average of the all gains of the receive antennas at this subcarrier. In addition, as the SNR in a mobile system corresponds to the signal to interference ratio, which is measured antenna per antenna. So the multi receive antennas power gain can be considered as system gain, which means that we do not need to shift $10\log(N_R)$ dB of receive power gain if the BLER and BER performance are given as function of "Eb/N0 per antenna". The Figure A.2.28 shows the BLER performance versus the Eb/N0 per antenna for two receive antennas, for the MMSE, iterative PIC and IQ-MAP-DFE detectors and for QPSK modulation. The MMSE detector requires Eb/N0 per antenna of 1.1, 2.4 and 2.9 dB for code rate R equal to 1/2, 2/3 and 3/4 , respectively. The iterative PIC detector requires Eb/N0 per antenna of 0.5, 1.3 and 2.0 dB for code rate R equal to 1/2, 2/3 and 3/4 , respectively. The

performance of IQ-MAP-DFE is between those of MMSE and iterative PIC. In Figure A.2.29, we give the BER performance of B-IFDMA with two receive antennas. We can note that at R=3/4, the IQ-MAP-DFE detector outperforms the iterative PIC detector; that at R=2/3, the two detectors have the same performance; and that at R=1/2, the iterative PIC detector outperforms the IQ-MAP-DFE detector.

We have considered the 16-QAM modulation and applied the turbo code to this modulation because the information size is more important than QPSK. Figure A.2.30 and Figure A.2.31 give the BLER and BER performance respectively. For comparison purpose, the performance of the convolutional code is reported in the figures; and the single receive antenna configuration is also considered. As concerning the BLER performance and as compared to the convolutional code, turbo code gives a gain of less than 0.5 dB for R=1/2 and almost no gain for R=3/4. For the BER performance, turbo code gives almost no gain for R=1/2 and for R=1/3 a gain depending on the BER value: 1.6 dB for $N_R = 1$ and 0.8 dB for $N_R = 2$ at BER=10^{-3}, and 3.6 dB for $N_R = 1$ and 2.5 dB for $N_R = 2$ at BER=10^{-1}.

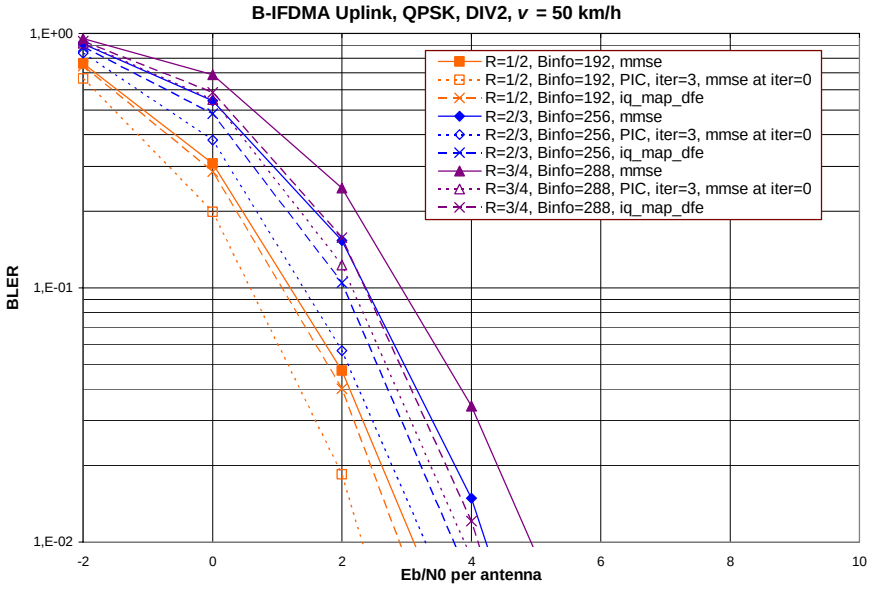

Figure A.2.28: BLER performance of B-IFDMA with two receive antenna and for different detection techniques.

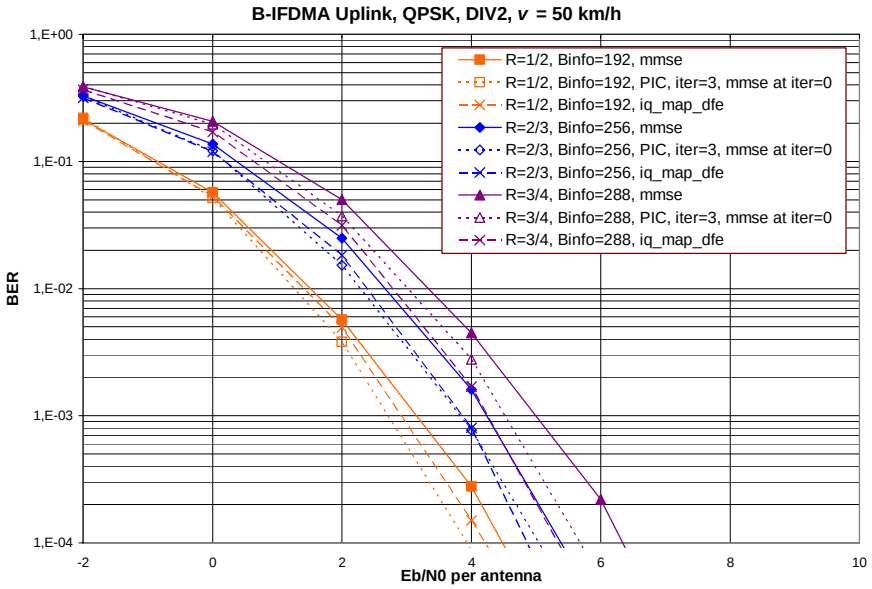

Figure A.2.29: BER performance of B-IFDMA with two receive antenna and for different detection techniques.

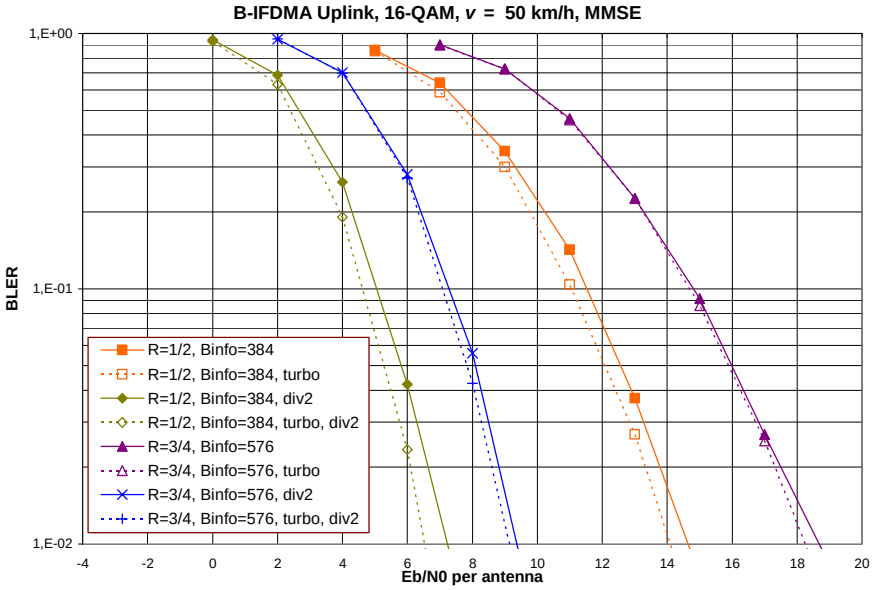

Figure A.2.30: Comparison between Turbo and convolutional codes on the BLER performance.

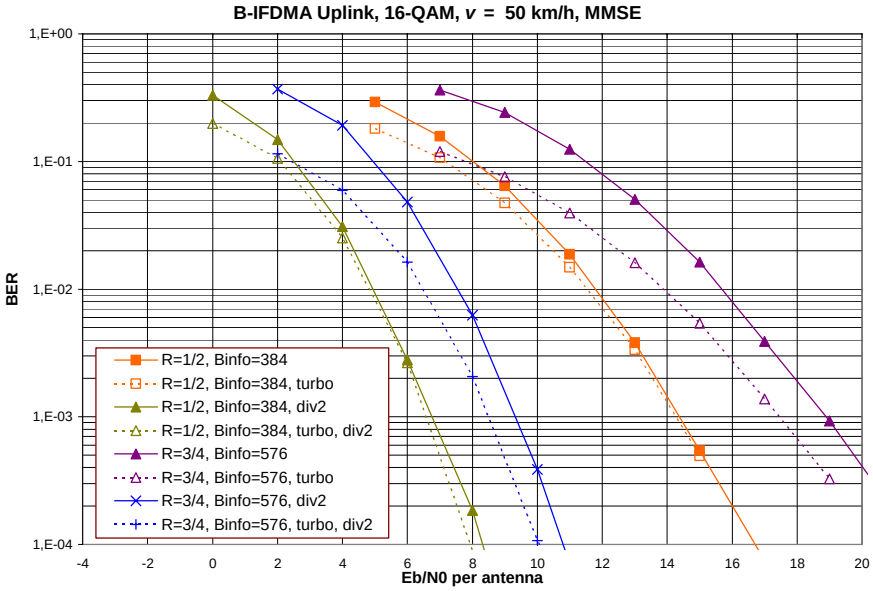

Figure A.2.31: Comparison between Turbo and convolutional codes on the BER performance.

A.2.2.4 Conclusions

We have evaluated partially the link level performance of the B-IFDMA and find that the obtained performance is not enough good: the iterative PIC requires 5.5 dB of Eb/N0 for a BLER of 10% for a code rate of 1/2, QPSK modulation and convolutional code. And we have proposed two ideas to improve the performance. The first one is the multi frames structure. Another corresponds to the multi receive antennas. For the first one, we have considered the two frames structure. We note that as the iterative PIC works better with time diversity in the coded bits and that this detector provide a BLER equal to 10% for Eb/N0 equal to 5 dB and for R=1/2. We have examined an alternative of the two frames structure: the B-IFDMA with double IFDMA size; and we have concluded that the alternative can substitute the initial two frames structure without performance loss. For the receive diversity, we have given the B-IFDMA performance with two receive antennas and show that for a BLER equal to 10% the required Eb/N0 per

antenna is only 0.5 dB with iterative PIC detector and R=1/2. In our study, we have note that the IQ-MAP-DFE outperforms the iterative PIC in most cases for high code rate; the IQ-MAP-DFE with α=0.4 and soft-IC outperforms all the other detectors on the BER performance and can approach to the iterative PIC at low code rate and outperforms all the other detector at high code rate on the BLER performance; and that the BER performance of the iterative PIC is almost the same of the MMSE for the baseline concept. However the BER performance of the IQ-MAP-DFE outperforms the MMSE for the same case. The Turbo code as compared to the convolutional code has non significant gain on the BLER performance. However for the double frames structure, Turbo code gives a gain of about 1 dB or about 0.7 dB at BLER=10^{-1} for R=1/2 and for 16-QAM and QPSK respectively.

A.2.3 Link to System Interface for Hybrid-ARQ

A.2.3.1 The WINNER MIESM Link to System Interface

We recall rapidly the standard WINNER MIESM Link to System (L2S) interface, under the following simplifying assumptions:

- For a given transmission, if the packet occupies several chunks, the same modulation is used over all the allocated chunks (even in the frequency adaptive case)
- The modulation type is considered constant for all retransmissions

The first assumption gives suboptimal performances. The penalty is however less important in the configurations in which the chunks allocated to a given users have similar SNIR (which is the aim of some frequency adaptive schedulers), since in this case the modulation will more likely be the same over all the allocated chunks.

The second simplifying assumption is dictated by the sake of feasibility in the building of a complex system-level simulator. Moreover, this approximation, even if it is suboptimal, makes some sense in case of HARQ: in fact HARQ is supposed to be used when the varying channel conditions, bad channel or SNR estimation or unpredictable interference produce an erroneous choice in the Link Adaptation (LA) algorithm. In these conditions the task of adapting the modulation format will probably lead to minor performance improvements due to imperfect channel prediction. Hence it makes sense to fix the modulation format at the initial transmission and try to recover performance by decreasing the coding rate (IR) or increasing diversity (CC).

The L2S interface specified in WINNER works as follows: given a received packet

1) Calculate the SINR values for all or a subset (according to SINR sampling period in time and frequency[10]) of resource elements covered by the codeword of interest. The SINR are stored in a vector of length, say, P: [SINR_1,… , SINR_P]. The SINR derivation has to include power allocation, (spatial) pre- and post-processing as well as the instantaneous channel and interference characteristics.
2) Compute effective SINR according to

$$\mathrm{SINR}_{\mathrm{eff,dB}} = 10\log 10\left[\beta \cdot I_M^{-1}\left(\frac{1}{P}\sum_{p=1}^{P} I_M\left(\frac{\mathrm{SINR}_p}{\beta}\right)\right)\right] \qquad \text{(A.2.16)}$$

where

β	is an optimization parameter to be derived from link level simulations
M	is an identifier of the modulation alphabet applied to all element of the packet
I_M	is the mutual information associated with the modulation alphabet M as a function of S(I)NR.

[10] The sampling period parameter N_{sT} and N_{sF} depend on the channel coherence time and bandwidth, respectively. Good accuracy has been obtained using 2 samples per λ/2, every 4th subcarrier.

3) Map $SINR_{eff,dB}$ to PER by using the AWGN curve (which we will call AWGN LUT in the following) corresponding to the given MCS. This mapping is generally specific to code rate, code type, codeword length and modulation type. The parameter β can be tuned to achieve a "good" fit, but, as a first approximation, it can be fixed to 1.0 (which was shown to give an acceptable approximation).

A.2.3.2 Extension of the WINNER MIESM L2S Interface for HARQ

We propose two extensions of the WINNER MIESM L2S interface in case of HARQ, according to the selected strategy: Chase Combining (CC) or Incremental Redundancy (IR).

We first introduce some general notation. Consider a given HARQ process, and suppose that transmission NT has been received[11]. The receiver has to store all the SINR of previous received packets (and the current one), whose sizes are P_1, P_2, …, P_{NT}, and are in general not equal, depending on the number of chunks each RTU has been assigned to. A maximum number of transmissions (including the initial one) NT_{max} is fixed.

We define the SINR vector of the generic transmission NT as $[SINR_{1,NT},\dots, SINR_{PNT,NT}]$.

Chase Combining

In case of Chase Combining, the same RTU is retransmitted and then combined at the receiver (CC exploits the so called diversity combining gain). Hence $P_1 = P_2 = \dots = P_n = P$ for all retransmissions. This is true due to our simplifying assumption which assumes constant modulation for all the retransmissions (indeed same MCS for all RTU). The WINNER proposal in this case is basically to add up the SINR of the different transmissions, obtain the effective SINR and to check the PER in the AWGN LUT corresponding to the MCS of the initial transmission.

The MIESM L2S interface works as follows:

1) Let us suppose that the NTth transmission (including the first one) arrives at the receiver and that the SINR of all the previous (and current) packets are available, and have same size P (the one of the initial transmission). The SINR of the different retransmissions corresponding to the same symbol should be combined as described in the next step. Anyway, in order to simulate a different interleaving for each retransmission, the entries of each SINR vector (except the one corresponding to the initial transmission) can be independently and randomly permutated.
2) Compute effective SINR according to

$$\mathrm{SINR}_{\mathrm{eff,dB}} = 10\log 10\left[\beta \cdot I_M^{-1}\left(\frac{1}{P}\sum_{p=1}^{P} I_M\left(\frac{\sum_{n=1}^{NT}\mathrm{SINR}_{p,n}}{\beta}\right)\right)\right] \qquad \text{(A.2.17)}$$

where

β is an optimization parameter to be derived from link level simulations

M is an identifier of the modulation alphabet applied to all element of the packet, for all transmissions

I_M is the mutual information associated with the modulation alphabet M as a function of S(I)NR.

3) Map $SINR_{eff,dB}$ to PER by using the AWGN LUT corresponding to the MCS of the initial transmission. This mapping is generally specific to code rate, code type, code word length and modulation type, but not on the transmission number. The parameter β can be tuned to achieve a "good" fit.

Few remarks:

- In general, a different calibration factor should be used for each transmission; however a common simplifying assumption is to use the same calibration factor corresponding to the MCS

[11] The counting is done including the initial transmission, so n = 1 is the initial transmission, n = 2 is the first retransmission and in general the nth transmission is equivalent to the (n-1)th retransmission.

of the initial transmission. The diversity combining mechanism is (as a first approximation at least) well modelled by the sum of the SINRs.

- The optional random permutation of the SINR vectors models the use of a random interleaver or the fact that, for each retransmission, a different interleaver is used before mapping to the sub-carriers as well as possible different constellation rearrangement patterns.

Incremental Redundancy

When Incremental Redundancy is used, different redundancy versions (RVs) are sent: RV*1*, RV*2* …, RVNT_{max}, where NT_{max} is the maximum number of transmissions. We suppose that no repeated bit is sent during all the retransmissions. Moreover, the size P_n (in complex symbols) of RV*n* can in general depend on *n*.

The MIESM L2S interface works as follows:

1) Let us suppose that at the receiver side we received the *NT*th transmission (including the first one), and that the SINR of all the previous (and current) transmissions are hence available, and with size P_n.
2) Compute effective SINR according to

$$\mathrm{SINR}_{\mathrm{eff,dB}} = 10\log 10\left[\beta_{NT}\cdot I_M^{-1}\left(\frac{1}{\sum_{n=1}^{NT}P_n}\sum_{n=1}^{NT}\sum_{p=1}^{P_n} I_M\left(\frac{\mathrm{SINR}_{p,n}}{\beta_{NT}}\right)\right)\right] \qquad \text{(A.2.18)}$$

where

β_{NT} is an optimization parameter to be derived from link level simulations, function of the retransmission number

M is an identifier of the modulation alphabet applied to all element of the packet, for all transmissions

I_M is the mutual information associated with the modulation alphabet M as a function of S(I)NR.

3) Map $\mathrm{SINR}_{\mathrm{eff,dB}}$ to PER by using the AWGN LUT corresponding to the equivalent code of retransmission *NT*. This mapping is generally specific to the MCS, transmission number, code rate, code type, code word length and modulation type. The parameters β_n with $n = 1, \ldots, NT_{max}$ can be tuned to achieve a "good" fit for each transmission.

The equivalent code at transmission *NT* we talk about is the code whose codewords are obtained by concatenating (after demodulation and proper order rearrangement) the bits received over the first *NT* transmissions. In case of Rate Compatible codes, by supposing that at transmission *NT*, the rate of the code is R_{NT}, the AWGN LUT of transmission *NT* is the one of the code with rate R_{NT} combined with the modulation format corresponding to the selected MCS. In this perspective, Equation (A.2.18) is a simple extension of the initial MIESM L2S interface in the sense that at each retransmission we simply consider the corresponding equivalent code, i.e. its AWGN LUT, after having calculated the average mutual information over all the received complex symbols of all the transmissions.

Extension to RVs with repeated bits

Let us suppose that the implemented IR strategy uses NT_{max} different RVs as above with possibly different packet sizes, but now we allow for some repeated bits (systematic or parity bits) inside each RVs. One example of such strategy could be the one in which at each retransmission systematic bits are always sent with some new parity bits (sometimes in the literature this strategy is called HARQ type III).

One possible way to manage this case could be to make a sort of combining for the repeated bits. However this strategy can not be easily implemented, because the L2S interface can only use the SINR of the complex symbols *before* the soft-demodulator, while in the real communication chain the repeated bits are combined *after* the soft demodulator, at bit level (and not at complex symbol level). Moreover, the interleaver is allowed to map repeated bits and not-repeated ones in a single complex symbol. Then, special care should be taken to calculate the correct SINR of the repeated bits, which should be combined, and the SINR of the newly sent bits, which should not be combined.

To avoid all these complications, we propose to take into account the effect of the repeated bits in the AWGN LUT of the different retransmissions. The equivalent code associated to the transmission *NT* is composed by all the bits sent only one time during the retransmissions plus a set of bits which are repeated one or more times. Its AWGN LUT is generated calculating the residual PER over the AWGN channel after *NT* transmissions (always sending *NT* RVs). In this way, the same L2S interface can be used, by using the proper AWGN LUT at each transmission. Obviously the optimal calibration factor of the case of IR without repeated bits can be different to the one with repeated bits even for the same MCS and transmission number, since the AWGN LUT as well as the corresponding equivalent code change.

Remark: Chase Combining can be considered as an IR in which at each retransmission the RV have only repeated bits. In general, for transmission *NT*, the AWGN LUT of a repetition-*NT* code superimposed to the code of the initial transmission should be used, with the proper calibration factor. In AWGN channel this corresponds to a shift of $10\log_{10}(NT)$ dB to the left of the LUT of the initial transmission. Hence, this could be an alternative model for CC, but we do not use it in our study (we use the one previously specified, which adds up the SINR).

Extension to IR with repeated RVs

Consider the case in which the system allows NT_{max} transmissions at maximum, but the available RVs are only $N_r < NT_{max}$, so that at the N_r+1 transmission the RV*1* is send again and so on. There could be some repeated RVs. In fact, the MIESM L2S interface above can be used, by defining the good equivalent codes, by obtaining their AWGN LUT and their corresponding optimal calibration factors.

Anyway a further simplification of the L2S interface could be to combine the SINR of the repeated RVs, so that we need to calculate only N_r AWGN LUT, instead of $NT_{ma3.2.}$ Let S_n with $n = 1, \ldots, N_r$ be the set of retransmission number in which RV*n* has been sent. For example, let $N_r = 2$ so that we have only RV*1* and RV*2*, and let $NT_{max} = 6$ so that the IR strategy is {RV*1*, RV*2*, RV*1*, RV*2*, RV*1*, RV*2*}: if the current transmission number $NT = 3$ we have $S_1 = \{1,3\}$ and $S_1 = \{2\}$.

If $NT \le N_r$, use the L2S MIESM interface.

If $N_r < NT \le NT_{max}$, the procedure is as follows (actually only points 2) and 3) are affected)

1) Let us suppose that the *NT*th transmission (including the first one), $N_r < NT \le NT_{max}$, arrives at the receiver side and that the SINR of all the previous (and current) transmission are available. For each vector of SINR, with size P_n, (except the one corresponding to the initial transmission) possibly draw an independent random permutation and permute the entries of the vector.

2) Compute effective SINR according to

$$\mathrm{SINR}_{\mathrm{eff,dB}} = 10\log 10\left[\beta_{N_r}\cdot I_M^{-1}\left(\frac{1}{\sum_{n=1}^{N_r}P_n}\sum_{n=1}^{N_r}\sum_{p=1}^{P_n}I_M\left(\frac{\sum_{k\in S_n}\mathrm{SINR}_{p,k}}{\beta_{N_r}}\right)\right)\right] \qquad \text{(A.2.19)}$$

where

β_{Nr} is the optimization parameter to be derived from link level simulations associated to transmission number N_r

M is an identifier of the modulation alphabet applied to all element of the packet, for all transmissions

I_M is the mutual information associated with the modulation alphabet M as a function of S(I)NR.

3) Map $\mathrm{SINR}_{\mathrm{eff,dB}}$ to PER by using the AWGN LUT corresponding to the equivalent code of retransmission N_r for all the transmission $NT > N_r$. This mapping is generally specific to the MCS, transmission number, code rate, code type, code word length and modulation type. The parameters β_{Nr} is tuned only once, since for transmissions $NT > N_r$ only the effect of combining is simulated by adding up the SINRs.

As stated in the procedure above, only the first N_r AWGN LUTs are needed. In fact, for all $NT > N_r$, the LUT of the equivalent code corresponding to transmission N_r is always used, because the RVs are simply repeated and their contributions are modeled by adding up their SINRs as it happens for Chase Combining (diversity combining). This is naturally only a simplification, in order to simulate less LUTs. For the random permutation, see comment in the Chase combining section. We currently have no precise quantification of the degradation given by this approximation.

A.2.3.3 Calibration Results

We consider here the MIESM L2S interface for IR introduced in Section, and we calibrate it in two cases: MCS 1 is a 16-QAM with rate ¾, block size is 1440 information bits, and MCS 2 is a 64-QAM with rate ¾, block size is 2160 information bits. For both MCSs, RV*1* is obtained by letting the information bits be coded by a duo-binary turbo mother coder (rate ½) and by puncturing opportunely a part of the parity bits (we do not enter in the details here). For both MCSs, RV*2* is composed by the parity bits which were not sent in RV*1*, by the other part (already sent) of the parity bits and by a part of the systematic bits (already sent) in order to obtain a packet which have the same length of the corresponding RV*1* packet. We consider, hence, the case with different RVs but with repeated bits inside them. We have $P_1 = P_2 = 480$ and $NT_{max} = 2$.

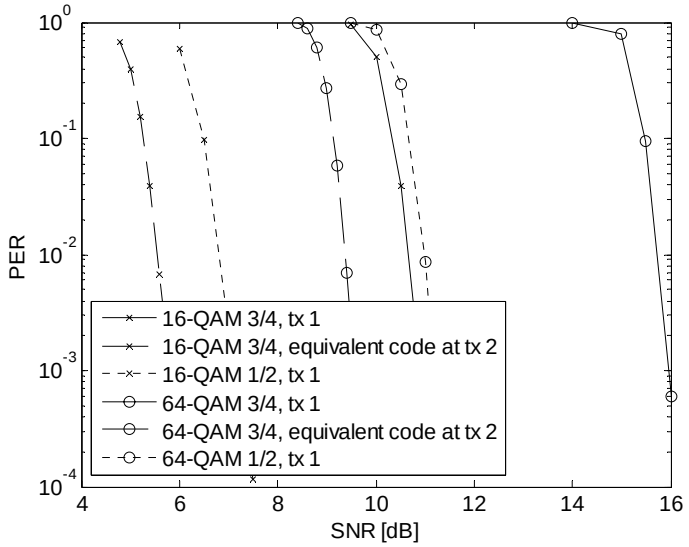

Figure A.2.32: LUTs used for the MIESM L2S interface with IR (dashed lines); LUTs of the initial transmissions (solid lines); LUTs of MCS with the same rate of the IR equivalent code but without repeated bits (dotted lines).

In Figure A.2.32 the AWGN LUTs used in the calibration process are plotted. The solid lines are the PER curves of MCS 1 and 2 at the initial transmission. The dashed lines are the LUTs of the equivalent codes associated to MCS 1 and 2 after 2 transmissions (the initial one and the first retransmission). We recall that the equivalent code is obtained by concatenating all the RV*1* with their associated RV*2*: so, all the parity bits of the mother code ½ are sent, plus some repeated parity and systematic bits. By comparison we plotted also the LUTs (dotted lines) of a 16-QAM and 64-QAM with rate ½ (size is 960 and 1440 information bits), without repeated bits. As seen in the figure, the equivalent codes at transmission 2 have a gain of about 2 dB with respect to the codes at rate ½ because of their repeated bits[12].

We run some PHY level simulation under Typical Urban (TU) channel with 6 taps, and a generic OFDMA system with PHY level parameters similar to 3GPP LTE. We recall that useful insights about

[12] The equivalent codes and the codes with rate 1/2 without repeated bits in Figure have not the same size in information bits. However, even if we consider longer codes for the case rate 1/2, in order to have the same size of in information bits, the dotted lines will shift only of at maximum 0.5 dB.

the calibration factors and the L2S models can be obtained independently of the channel model and the PHY level parameters, as long as the receivers are of the same type.

We have calibrated the MIESM L2S interface by using different MSE criteria over the log10(PER). By comparison we provide also the calibration results obtained with an EESM L2S interface for IR, which operates as the MIESM one only changing the mutual information function to the exponential function. The results are reported in Table A.2.9: different intervals of PER are considered for calibration (all the points outside the given PER interval were not taken into account in the calibration process).

Table A.2.9: Calibration results for initial transmission and IR with two transmissions. Different intervals of PER were taken into consideration.

		Optimal β		MSE on $\log_{10}$(PER)	
PER interval	Method	1st tx	2nd tx	1st tx	2nd tx
MCS: 64-QAM rate ¾					
[10^-2, 0.95]	MI	0.935	0.8	0.040	0.040
	EESNR	25.34	9.2	0.127	0.061
[10^-3, 0.95]	MI	0.96	0.8	0.062	0.057
	EESNR	26.225	9.45	0.219	0.098
[10^-2, 0.6]	MI	0.935	0.8	0.050	0.052
	EESNR	25.505	9.25	0.153	0.077
[10^-3, 0.6]	MI	0.96	0.8	0.074	0.071
	EESNR	26.37	9.45	0.252	0.117
[10^-3, 0.3]	MI	0.965	0.8	0.083	0.086
	EESNR	26.545	9.5	0.277	0.130
[3*10^-4, 0.3]	MI	0.965	0.8	0.084	0.097
	EESNR	26.695	9.6	0.286	0.135
MCS: 16-QAM rate ¾					
[10^-2, 0.95]	MI	1.06	1.2	0.015	0.033
	EESNR	7.52	4.55	0.045	0.036
[10^-3, 0.95]	MI	1.08	1.25	0.028	0.055
	EESNR	7.665	4.75	0.065	0.071
[10^-2, 0.6]	MI	1.06	1.2	0.018	0.036
	EESNR	7.525	4.55	0.054	0.038
[10^-3, 0.6]	MI	1.08	1.25	0.033	0.058
	EESNR	7.67	4.75	0.075	0.075
[10^-3, 0.3]	MI	1.08	1.3	0.038	0.067
	EESNR	7.685	4.8	0.085	0.078
[3*10^-4, 0.3]	MI	1.09	1.3	0.047	0.074
	EESNR	7.74	4.8	0.111	0.084

Precision over optimal calibration factor: 0.005 for intial tx; 0.05, for tx 2

Results show that the optimal value of the calibration factor of the MIESM L2S interface for IR is around 0.8 and 1.3, respectively for the 64-QAM ad the 16-QAM case, rate ¾. The corresponding initial transmissions were optimally calibrated by a calibration factor of respectively 0.94 and 1.08.

For the EESM L2S interface, the optimal calibration factor for the initial transmission is about 26 and 7.6 respectively for the 64-QAM and 16-QAM case, rate ¾. For the IR with two transmissions the optimal values are respectively about 9.5 and 4.7.

We can conclude (at least for this case), that for two transmissions, the optimal calibration factor is less sensible to the transmission number in the case of MIESM than in case of EESM. Moreover, as we can see in Table A.2.9, the MSE with optimal calibration is lower for MIESM than for EESM. For these reasons the MIESM L2S interface is still preferred for IR too.

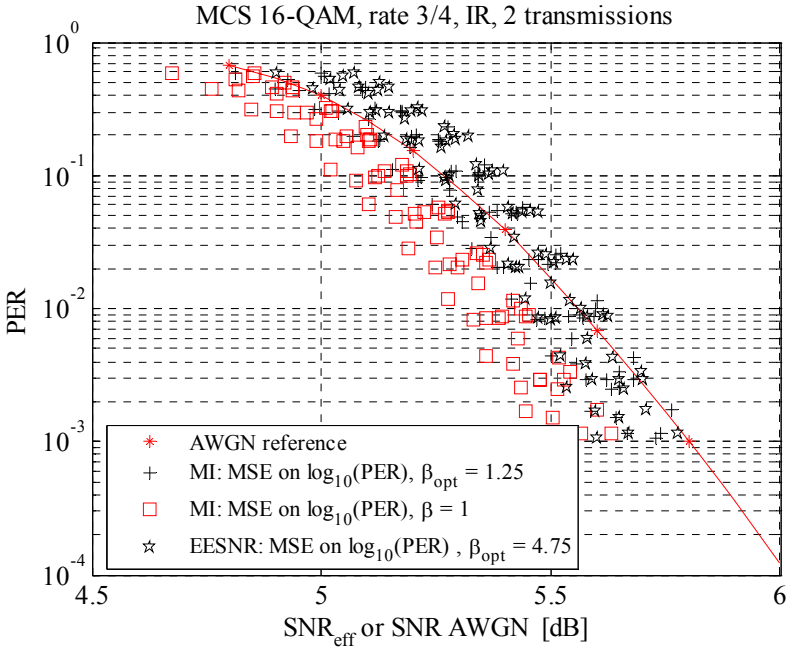

Figure A.2.33: Calibration for 16-QAM rate ¾, IR with 2 transmissions. As seen, beta = 1 is suboptimal (underestimation of the PER), but the estimated PER are in average only about 0.3 dB apart. PER points used for calibration are in between 1e-3 and 0.6.

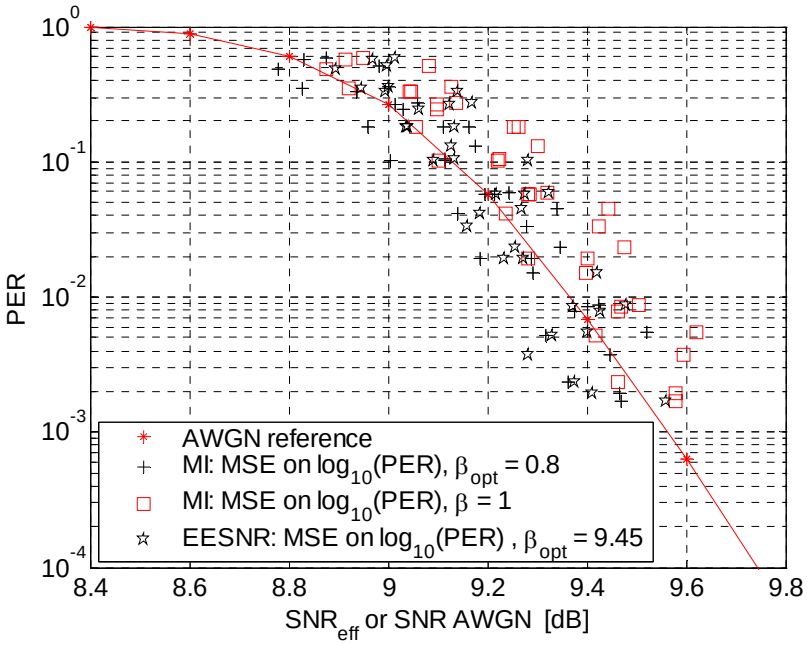

Figure A.2.34: Calibration for 64-QAM rate ¾, IR with 2 transmissions. As seen, beta = 1 is suboptimal (underestimation of the PER), but the estimated PER are in average only about 0.1 dB apart. PER points used for calibration are in between 1e-3 and 0.6.

- In Figure A.2.33 and Figure A.2.34 we give and example of calibrated points for IR with 2 transmissions: the MIESM L2S interface seems to give acceptably accurate results. Moreover, red squares are the predictions given by a sub-optimally calibrated L2S interface with calibration factor equal to 1.

A.2.3.4 Proposed Approximations in the L2S for HARQ

Since the sensitivity of the calibration factor with respect to the transmission number is not enormous, we propose to set the calibration factor equal to 1.0. This value corresponds to no calibration at all, which speeds up the evaluation of the system performance, since the long calibration procedure is skipped. To estimate the impact on the approximation performance in the two study cases, in Figure A.2.33 and Figure A.2.34 the predictions given by the MIESM L2S interface with optimal and approximated calibration factor are shown. As it can be appreciated in the figures, the maximal shift of the predicted point is about 0.3 dB. This shift obviously impacts on the performance at system-level (spectral efficiency and delay).

It is very difficult to estimate the impact of setting the calibration factor equal to 1 on the system-level performance. In fact, the absolute value of the degradation in dB of the PER predictions for a generic MCS with respect of the case of optimal calibration is not simply predictable. Nor we are able to say if the PER will be over-estimated or under-estimated. However, some remark can still be drawn. The system-level performance heavily depends on the set of MCS chosen for the system. The approximation will influence in different way the performance according to the MCS set using for the simulation. We can reasonably say that for few, well-spaced MCSs the performance shift due to the approximation will impact performance to smaller extent than in case of a denser set of MCSs over the same SNR interval of interest. Hence, if sub-optimal calibration factor equal to 1 is used with MIESM L2S interface for IR, our suggestion to limit the performance impact of this approximation is to run simulations with a sparse MCS set (some dB in between each AWGN LUT of the MCS set).

A.2.4 Performance of Adaptive TDMA/OFDMA in Wide Area with Hybrid-ARQ

A.2.4.1 Simulator constraints and assumptions

Simulations compliant with the WINNER baseline [WIN2D6137] were carried out in order to investigate the impact of different HARQ strategies, using LDPC FEC coding and the above L2S for HARQ, on

system level performance in the presence of inter-cell interference. To better identify the influence of HARQ, we simulated the system in the simple configuration of one antenna at the BS and 2 antennas at the UT (receive diversity only).

We simulated a half-duplex system (FDD WA).

Table A.2.10: Deviated simulation parameters.

Deviated parameter	
Signal bandwidth	40 MHz (instead of 45 MHz)
Number of chunks	128 (instead of 144)
Number of antenna at BS	1
Type of array at the UT	Linear array of 2 antennas with separation of half wavelength
Segmentation of the information	According to the selected MCS as in Table A.2.10.

Deviation from the baseline: we considered a linear array at UT with a separation between the antennas of half wavelength (no cross-polarized antennas at UT were simulated).

As in the baseline, we assumed one RTU per slot per user composed by one FEC block. The size of the packet is not fixed to 360 and 1200 information bits, but it depends on the selected MCS. The MCS set is reported in Table A.2.12. The information payload per MCS was calculated according to the constraint that each modulated packet should occupy 16 chunks independently of the selected MCS. We considered 80 over 96 useful complex symbols per chunk as fixed in [WIN2D6137] so that each packet has 16 × 80 = 1280 complex data symbols. The number of information bits was calculated for each MCS in order to occupy as many as possible of these 1280 complex symbols and at the same time to satisfy the constraint that the information block size should be a multiple of 48 for LDPC. This particular choice on the size of the packets gives in fact a maximum of 8 active users per slot over the whole signal bandwidth of 40 MHz, and it was in part dictated by constraints on simulation time (more users corresponds to longer simulations).

Table A.2.11: MCS set with information payload for LDPC.

MCS	**1**	**2**	**3**	**4**	**5**	**6**	**7**	**8**	**9**	**10**
Mod.	BPSK		QPSK			16-QAM			64-QAM	
R	1/2	2/3	1/2	2/3	3/4	1/2	2/3	3/4	2/3	3/4
Info bits LDPC	624	816	1248	1680	1920	2544	3408	3840	5088	5760

The AWGN LUTs of the PER curves for LDPC codes are derived from the ones available in [Bon04]. For a given MCS in Table A.2.11, we have chosen the LUT of [Bon04] corresponding to the code whose length was closest to that of the given MCS. For sizes greater than the ones available in [Bon04], we selected the LUT in [Bon04] with the largest size, since the PER curves seem to converge to a limit curve.

Assumptions made for retransmissions and the HARQ process they are assigned to:

- Each retransmission occupies the same number of chunks as a first transmission (i.e. 16 chunks).
- Each retransmission is prioritized, in the sense that a given HARQ process cannot send a new packet if there is a pending retransmission.
- When the HARQ process is scheduled and a retransmission is pending, the retransmission is sent using the same modulation format of the first transmission, independently on the actual channel status (this is a simplifying assumption)

Since the retransmission (RV*2*) occupies the same number of chunks than the first transmission (RV*1*), it is clear that the first retransmission RV*2* contains some newly sent parity bits, but in general also some repeated systematic and parity bits coming from the initial transmission. For this reason, when the

maximum number of transmissions (including the initial one) was fixed to 2, so that the IR strategy is {RV*1*, RV*2*}, we adopted the L2S for HARQ interface Equation (A.2.18) with the proper LUTs. When the selected IR strategy admitted more than 2 total transmissions, then there could be some repeated redundancy versions. In this case we used the L2S interface for HARQ in Equation (A.2.19) even if we did not run specific link-level simulation to investigate the dependency of the optimal calibration factor with respect to the transmission number. For all cases we used L2S for HARQ models without calibration (i.e. calibration factor equal to 1.0).

A.2.4.2 Performance results

In Figure A.2.35 we present some measures related to the user throughput and their dependence on the maximum number of retransmission of a CC protocol with LDPC FEC coding. The system was simulated with UT at 50 km/h and frequency adaptive Score Based scheduling. One transmit antenna was considered at the BS and 2 at the UT to take into account the benefits of receive diversity (1x2 rxDiv).

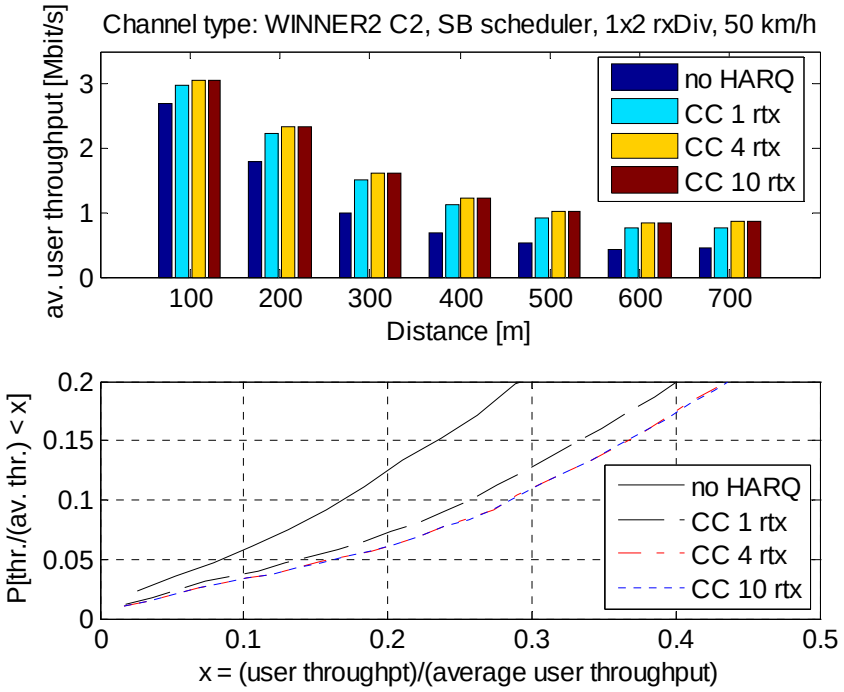

Figure A.2.35: Average user throughput versus distance (top) and cdf of user throughput normalized versus average user throughput (bottom), frequency adaptive mode (WA) with SB scheduler, LDPC codes, Chase Combining, 1x2 rxDiv at 50 km/h.

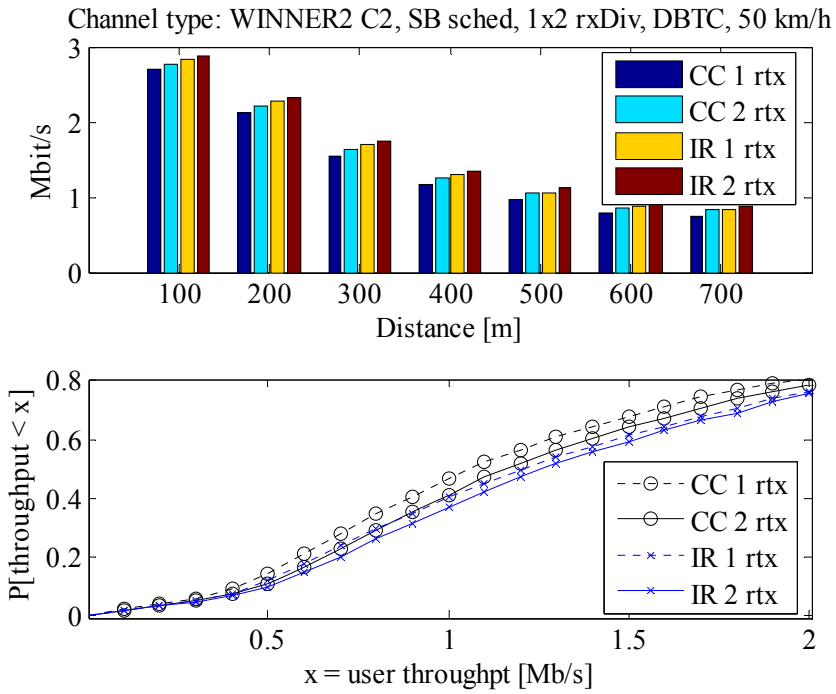

Figure A.2.36: Average user throughput versus distance (top) and cdf of user throughput normalized versus average user throughput (bottom), frequency adaptive mode (WA) with SB scheduler, DBTC codes, Chase Combining versus Incremental Redundancy, 1x2 rxDiv at 50 km/h.

As it can been seen, while there is a great gain to introduce an CC protocol instead of no HARQ protection, the gain between 1 retransmission (i.e. 2 transmissions including the initial one) and 4 retransmissions at maximum is very limited. Further increment of the retransmission number yields no gain at all. This is true both at the border and at the center of the cell, also in term of user throughput cdf. This behaviour is probably to be attributed to the short delays of the WINNER system. In the previous simulation, the delay between the channel measure at UT and the use by the scheduler at BS was set to one frame (about 0.69 ms), the minimum proposed by the WINNER baseline. Inter-cell interference was taken into account in these simulations and it was simulated like Gaussian interference (no detailed frequency-selective interference channel was simulated). We suppose that the UT is able to perfectly measure the SINR (interference plus noise) and to report it to the BS. Under these ideal hypotheses and short delay, even if the UT is at vehicular speed, two retransmissions are sufficient to completely recover the uncertainty introduced by the mobile speed. Note that no channel predictor is implemented in the simulator.